MOLECULAR REGULATION OF BACTERIAL STRESS RESPONSES AND PYOCIN PRODUCTION

By

CHRISTOPHER WILLIAM HAMM

Bachelor of Arts in Biological Sciences
Oklahoma State University
Stillwater, Ok
2018

Submitted to the Faculty of the
Graduate College of the
Oklahoma State University
in partial fulfillment of
the requirements for
the Degree of
DOCTOR OF PHILOSOPHY
May, 2023

MOLECULAR REGULATION OF BACTERIAL STRESS RESPONSES AND PYOCIN PRODUCTION

Dissertation Approved:

Dr. Matthew T. Cabeen
Dissertation Adviser

Dr. Robert Burnap

Dr. Erika Lutter

Dr. Jeff Hadwiger

Dr. Patricia Canaan

ACKNOWLEDGEMENTS

I would like to start by thanking my mentor and advisor Dr. Matthew T. Cabeen who accepted me into his lab as an undergraduate researcher and allowed me to continue as a graduate student. Dr. Cabeen was a wonderful mentor who encouraged me to think critically and analyze problems, helping me develop as a scientist and learn to develop and design my own experiments. Thank you for always being there for me, and for all the wonderful advice you have given me over the years. I will miss all the lab outings, lab pizza night at the Cabeens, and gym sessions at the Colvin. I have greatly enjoyed being in your lab and will miss you and all the other wonderful people working in the lab.

Thank you to all my committee members, Dr. Robert Burnap, Dr. Jeff Hadwiger, Dr. Erika Lutter, and Dr. Patricia Canaan. Thank you for your support and feedback during both classes and committee meetings. Your ideas and the discussions during meetings as well as teaching was invaluable and helped me develop both a strong foundation as well as strong research projects. Thank you to my past lab members Adam Bronson, Nina Baggett, Sarah Winburn, as well as multiple others who made spending time in lab fun and enjoyable. Thank you to Rabindra Khadka, Somalisa Pan, and Dr. Simon Underhill for listening to my ramblings in lab and being there to help bounce ideas off. All of you helped me stay sane in lab and I will miss spending the majority of my waking hours with you all in lab.

Thank you to my parents for always being there and supporting me throughout my Ph.D., I am grateful you have been so encouraging throughout my entire life and have always been there to help me or just listen whenever I need it. Thank you to my sister and brother-in-law Andrea and Matt Stallings, you have both been a blessing and always having a place for me to spend the holidays or weekends off. Thank you both for helping me and being there for me no matter what. A special thank you to Noelie Bircher for supporting me and being with me through the most difficult years of my Ph.D. You helped me stay sane and were always a bright light on the difficult days. Thank you for encouraging me to have a life outside of work and teaching me how to have a healthier work/life balance. I love you and look forward to spending the rest of our lives together, and seeing where our journey takes us next.

Thank you to the many people in the department who have been a help and have been supportive over the last 5 years. I have been blessed to be surrounded by so many amazing people and will miss my OSU family.

Thank you all

Name: CHRISTOPHER WILLIAM HAMM

Date of Degree: MAY, 2023

Title of Study: MOLECULAR REGULATION OF BACTERIAL STRESS

RESPONSES AND PYOCIN PRODUCTION

Major Field: MICROBIOLOGY, CELL & MOLECULAR BIOLOGY

Abstract:

Bacteria have a variety of systems to sense stress and respond ensuring the survival of cells. *Bacillus subtilis* uses stressosomes—large cytoplasmic multiprotein complexes—to sense environmental stressors and trigger the general stress response through activation of the alternative sigma factor σ^B. Stressosomes are comprised of 40 RsbR proteins made up of four paralogous (RsbRA, RsbRB, RsbRC, and RsbRD) putative stress sensors. Previous work uncovered differences in the timing and magnitude of the RsbR paralogs' σ^B response profiles to the same stressor. In chapter 1, we use microfluidic-coupled microscopy to investigate the σ^B responses mediated by each paralog and how they differ in the presence of different environmental stressors. Wild-type and RsbRA-only cells activate σ^B with a characteristic transient response irrespective of the stressor, modulating the magnitude of the response. Other individual RsbR paralogs show distinct timing and magnitude of responses to stressors, implying RsbR proteins can distinguish among stressors. In Chapter 2 we explore how these differences in σ^B activation affect the fitness of cells by conducting competition experiments under stress conditions. Our data suggests that the dynamics of the σ^B responses, which are impacted by the single RsbR paralogs, is capable of affecting fitness of cells.

Pyocins are bacteriophage tail-like complexes released via cell lysis and kill other strains of *P. aeruginosa*, thought to aid in the elimination of competition for resources within a niche. The production of pyocins in *xerC* mutant strains occurs through a previously unknown non-canonical pathway. Normally the production of pyocins and resulting cell death is kept off by the transcriptional repressor PrtR, which undergoes autocleavage allowing pyocin production to occur only when RecA binds to damaged DNA. In chapter 3 we investigate the genetic regulation of pyocins via PrtR which appears to have previously unappreciated targets. In a *recA* and *xerC* double deletion, pyocins are still produced despite the trigger (RecA) for cleaving the repressor (PrtR) being absent, suggesting the *xerC* deletion is bypassing the PrtR repressor. Surprisingly, replacement of PrtR with a non-cleavable version still allows pyocin expression but somehow blocks production of functional pyocins, suggesting other previously unknown targets of PrtR.

TABLE OF CONTENTS

Chapter Page

Chapter Page

Chapter Page

LIST OF TABLES

Table Page

LIST OF FIGURES

Figure Page

Figure Page

Figure Page

CHAPTER I

BACILLUS SUBTILIS STRESSOSOME SENSOR PROTEIN SEQUENCES GOVERN THE ABILITY TO DISTINGUISH AMONG ENVIRONMENTAL STRESSORS AND ELICIT DIFFERENT σ^B RESPONSE PROFILES

Note: The following chapter is largely published in the ASM journal mBio, with published work located at https://doi.org/10.1128/mbio.02001-22.

1.1 Abstract

Bacteria use a variety of systems to sense stress and mount an appropriate response to ensure fitness and survival. *Bacillus subtilis* uses stressosomes—cytoplasmic multiprotein complexes—to sense environmental stressors and enact the general stress response by activating the alternative sigma factor σ^B. Each stressosome includes 40 RsbR proteins, representing four paralogous (RsbRA, RsbRB, RsbRC, and RsbRD) putative stress sensors. Population-level analyses suggested that the RsbR paralogs are largely redundant, while our prior work using microfluidics-coupled fluorescence microscopy uncovered differences among the RsbR paralogs' σ^B response profiles with respect to timing and intensity when facing an identical stressor. Here, we use a similar approach to address the question of whether the σ^B responses mediated by each paralog differ in the presence of different environmental stressors: can they distinguish among stressors? Wild-type cells (with all four paralogs) and RsbRA-only cells activate σ^B with characteristic transient response timing irrespective of stressor but show various response magnitudes. However, cells with other individual RsbR paralogs show distinct timing and magnitude in their responses to ethanol, salt, oxidative, and acid stress, implying that RsbR proteins can distinguish among stressors. Experiments with hybrid fusion proteins comprising the N-terminal half of one paralog and the C-terminal half of another argue that the N-terminal identity influences response magnitude and that determinants in both halves of RsbRA

are important for its stereotypical transient σ^B response timing.

1.2 Introduction

Bacteria must be able to sense and respond appropriately to stressful environments to survive and grow. Bacterial responses to stress can be mediated by many different mechanisms that connect environmental sensing to gene expression, but one common mechanism employs alternative sigma factors, such as the σ^S general stress response, the σ^{38} stationary-phase and osmotic shock factor, or the σ^{32} heat shock factor of Escherichia coli [1]–[4]. In Bacillus subtilis, as well as other related Gram-positive organisms, the general stress response (GSR) is mediated by σ^B, which activates hundreds of genes [5]–[10]. σ^B activates gene expression in response to energy depletion and during the stationary phase of growth, and it responds to a range of environmental stressors, such as high and low temperatures, salt, ethanol, pH changes, and oxidative and osmotic stress [7], [11]–[15]. The characteristic σ^B transcriptional response to environmental stress in wild-type cells is transient: fast-onset, detectable in minutes, peaking within approximately 30 min, and subsiding thereafter [16]–[19].

To ensure a fast response, alternative sigma factors are present within cells but prevented from binding RNA polymerase until activating conditions are met. Under unstressed conditions, σ^B is held inactive by the anti-sigma factor RsbW [20]. Activation is achieved when the anti-anti-sigma factor RsbV is dephosphorylated and preferentially bound by RsbW, freeing σ^B [21]. RsbV can be dephosphorylated by either of two analogous proteins in response to starvation or environmental stressors. The energy stress response is mediated by RsbQ, which activates the RsbV-phosphatase RsbP; meanwhile, the environmental stress pathway is mediated by RsbT, which activates the RsbV-phosphatase RsbU [13], [14], [19], [22]. While the pathway between RsbP or RsbU and the activation of σ^B is well characterized, the initial steps of stress sensing and transduction are less well understood. RsbU requires activation through binding to RsbT, which is typically sequestered by RsbR proteins and RsbS in a protein complex known as the stressosome [9], [18], [23]. When stress is sensed by the stressosome, RsbT, which also has kinase activity, triggers its own

release in association with phosphorylation of RsbR at Thr residues 171 and 205 and RsbS at Ser residue 59 [24]. Mutation of the phosphorylated Ser residue to Ala in RsbS or mutational inactivation of RsbT kinase activity abrogates σ^B activation in Listeria monocytogenes [25] and B. subtilis [18], [26]. Released RsbT activates RsbU, resulting in σ^B release from RsbW and subsequent activation of the GSR. The system is reset by RsbX, a phosphatase that dephosphorylates RsbR and RsbS, presumably allowing the stressosome to recapture RsbT and discontinuing activation of σ^B [27]–[29]. The signal for RsbT to phosphorylate RsbR and RsbS and trigger its release from the stressosome is thought to be mediated by stress sensing by RsbR via a process that remains unknown.

Relatively few species appear to use stressosome complexes to respond to stress. The stressosome is best known in *B. subtilis* and *Listeria monocytogenes*, but similar complexes have been discovered in *Vibrio vulnificus* and *Moorella thermoacetica* [25], [30], [31]. In B. subtilis, the stressosome complex, which is composed of RsbR and RsbS proteins and can additionally sequester RsbT, is responsible for sensing and responding to environmental stress by activating σ^B as described above (Figure 1.1A) [18], [32]. The stressosome itself is a large, 1.8-megadalton pseudoicosahedral structure with a core comprising 20 RsbR dimers, each bound to an RsbS protein (Figure 1.1B) [17], [32]. The RsbRS core can sequester up to 20 RsbT proteins (Figure 1.1B) that are released upon sensing of stress [9], [33]. There are thought to be 10 to 20 of these large stressosome complexes within the cytoplasm of each B. subtilis cell (Figure 1.1A) [32]. The stressosome appears to be the sensory component of the σ^B activation pathway, yet how it senses stress remains a mystery.

The N-terminal half of RsbR is thought to be a sensing domain, as it extends out into the cytoplasm as a “turret” from the stressosome core [32]. Wild-type cells encode four RsbR paralogs, termed RsbRA, RsbRB, RsbRC, and RsbRD (Figure 1.1C), that are thought to be present in the stressosome and whose genes are scattered around the chromosome. A fifth paralog known as YtvA is known to sense blue light using a light-oxygen-voltage (LOV) domain in its N-terminal half, but YtvA is unable to form stressosomes on its own in

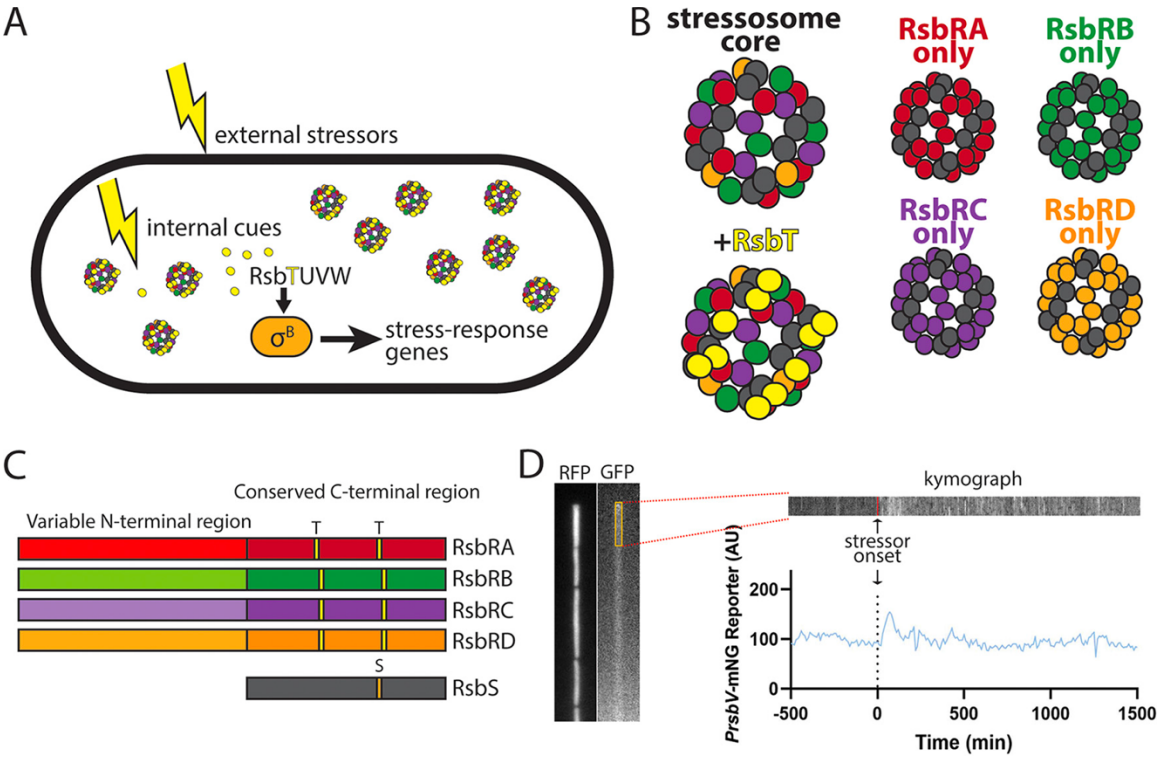

Figure 1.1 Schematic of stressosomes within cytoplasm, stressosome construction and paralogs, as well as lineage tracking. **A)** Schematic of Bacillus subtilis cell containing stressosomes within the cytoplasm sensing stress and triggering the activation of σ^B. Once activated, σ^B turns on gene expression of the general stress response, including the PrsbV-mNeonGreen reporter that we used to detect when σ^B is active. **B)** Schematics of the stressosome complex in the wild type and stressosomes formed by single RsbR paralogs. Stressosomes are comprised of 20 RsbS proteins (gray) and 20 RsbR dimers (RsbRA in red, RsbRB in green, RsbRC in purple, and RsbRD in orange). All strains in this study contained the ΔytvA deletion of the blue light sensor to prevent activation by fluorescence imaging. **C)** Diagram of RsbR paralogs compared to one another, as well as RsbS, with their phosphorylation sites highlighted. RsbR paralogs and RsbS share a conserved C-terminal sulfate transporter and anti-sigma factor antagonist (STAS) domain, which makes up the core of the stressosome. **D)** Image of a single cell lineage in a channel in the microfluidic device. The red fluorescent protein (RFP) image shows the cell boundaries, whereas the green fluorescent protein (GFP) image reports on σ^B activity. The yellow box is a 5 × 50-pixel region of interest (ROI) drawn in ImageJ for analysis, from which we obtained a kymograph depicting that ROI over time. The ROI was also used to obtain the mean GFP fluorescence value to plot over time for graph generation. Data curation and analysis were manually performed for each individual cell lineage.

vivo, instead forming a heterotetramer with an RsbRA dimer [34]–[37]. RsbRA, RsbRB, RsbRC, RsbRD, and YtvA share a conserved C-terminal sulfate transporter and anti-sigma factor antagonist (STAS) region with RsbS and have a non-heme globin variable N-terminal region thought to be the sensing domain [30], [32], [38]. The presence of the sensory LOV domain in the N-terminal half of YtvA bolsters the idea that the N-terminal halves of the other RsbR paralogs also serve sensory functions. Within wild-type cells, the levels of RsbRA, RsbRB, and RsbRC appear to be comparable, while RsbRD is present at very low levels, rising only to 30% of the level of RsbRA during stressful conditions [38].

It is possible to delete all but one paralog, and stressosomes comprised of only one type of RsbR protein will form (Figure 1.1B), allowing study of individual RsbR paralogs [16], [38], [39]. Even stressosomes comprised of only RsbRD, which is present at 20% of the levels of the other single-RsbR proteins, are still able to prevent σ^B activation in the absence of stress [38], suggesting that all available RsbT is sequestered and further implying that wild-type cells harbor excess RsbT-sequestering capacity. B. subtilis strains containing single-RsbR paralogs maintain a σ^B response to environmental stressors [18], but our previous work using microfluidics coupled to fluorescence microscopy showed that individual RsbR paralogs each show a distinct σ^B response profile when subjected to the same ethanol stressor [16].

A long-standing question in the field asks why species like B. subtilis and L. monocytogenes encode multiple RsbR paralogs. Given that the GSR responds to a diversity of environmental stressors, one attractive hypothesis is that having multiple RsbRs broadens the sensory capacity of the stressosome, with different paralogs "specializing" in sensing different types of stress. Supporting this idea, in L. monocytogenes, the stressosome is used for sensing both environmental and nutritional stress, and in B. subtilis, RsbRC and RsbRD can sense nutritional stress in the absence of RsbRA and RsbRB [39]. On the other hand, the demonstrated ability of single-RsbR strains to respond to a given stress [16], [18] raise the nonexclusive possibility that RsbRs respond to a common intracellular signal triggered by multiple environmental stressors. If all the RsbR paralogs respond to a common signal, then each paralog may merely modulate the strength and timing of the response rather than distinguishing among different stressors.

We previously examined the responses of wild-type and single-RsbR strains to a single environmental stressor (ethanol) using microfluidics coupled to fluorescence microscopy. That experimental approach allowed the visualization of single-cell σ^B responses to introduced stressors over long periods of time under uniform conditions [16], [40]. We revealed previously unappreciated differences in the σ^B response profiles of individual RsbR paralogs, with each paralog showing different response dynamics [16]. However, it has been unknown whether wild-type or single-RsbR strains can distinguish among

different environmental stressors by enacting different σ^B response profiles. It is also unknown whether the response profile of a particular RsbR paralog is governed by its N-terminal variable region, its C-terminal conserved region, or a combination of both.

Here, we extended our microfluidics-based approach to investigate whether and how wild-type and single-RsbR B. subtills strains modulate their σ^B responses to different stressors. We challenged cells with a panel of four stressors: ethanol, sodium chloride, hydrogen peroxide, and mild acidification. We first validated our experimental approach by comparison with our previous results [16]. We then found that whereas wild-type and RsbRA-only cells vary only in the magnitude of their response to different stressors, showing a characteristic transient response, other single-RsbR strains vary their responses to different stressors not only in magnitude but also in timing (shape of the response), suggesting that RsbR paralogs can indeed distinguish among different stressors. We also use a set of strains bearing RsbR hybrid fusion proteins to probe the effects of different N- and C-terminal regions on the σ^B response profile enacted by a particular RsbR sequence. Our results suggest that the N-terminal sequence exerts an effect on the magnitude of the response and that the characteristically transient response of RsbRA (which mimics the wild-type response) requires both halves of RsbRA.

1.3 Materials and Methods

1.3.1 Strains and growth conditions

The bacterial strains used in this study are listed in Table 1.1 and in the S1 Text. *B. subtilis* strains were routinely grown in LB Lennox broth (10 g/liter tryptone, 5 g/liter yeast extract, 5 g/liter NaCl) or on Lennox agar plates fortified with 1.5% Bacto agar at 37°C. When appropriate, antibiotics (MLS: 0.5 μg/mL erythromycin and 2.5 μg/mL lincomycin; 100 μg/mL carbenicillin) were added to select for markers. All strains used for microfluidic analysis contained the hag_{A233V} point mutation to render cells immotile, thereby preventing cell loss from side channels without interfering with motility regulation [41]. Markerless replacement of *rsbR* genes with hybrid versions was performed using the pMiniMAD

vector (a gift of Daniel Kearns) for allelic replacement. Details of strain construction are given in the Supplemental Information, Text S1.

1.3.2 Microfluidic apparatus setup and media

We used polydimethyl siloxane (PDMS) microfluidic devices. One version was dimensionally identical to that previously described [41], while a second was very similar to the previously described version [41], with shallow surrounding channels. A third version was dimensionally similar but lacked the shallow surrounding channels and had a shorter central cell-confining channel. We used this version when challenging cells with salt stress, as salt-treated cells tended to fill the shallow side channels (Fig S2). We speculate that NaCl treatment may cause cells to contract slightly or become more flexible [42]. The second and third versions were custom fabricated by ConScience AB (Mölndal, Sweden). Cured devices (10:1 Sylgard 184) cast on a silicon master (with SU-8 features) were punched with a 0.75-mm biopsy specimen punch to create holes to connect the fluidics using 21-gauge blunt needles. The devices were bonded to isopropyl alcohol-cleaned glass coverslips by oxygen-plasma treatment at ~200 mTorr O_2 for 15 s at 30 W and baked at 65°C for at least 1 h before use. The devices were passivated with growth medium containing 1 mg/mL bovine serum albumin (BSA) before cell loading. The cells were grown in shaking culture to stationary phase (optical density at 600 nm [OD_{600}] = ~4 to 5), filtered through a 5-μm filter to remove cell chains, concentrated by centrifugation at 5,000 × *g* for 10 min, and loaded into the device using gel-loading tips. The cells were then spun into the side channels of the device in a custom-designed microcentrifuge adaptor at 6,000 × *g* for 10 min. The fluidics were then connected to the device and run at 35 μL/min for approximately 20 min to flush out excess cells before being run at 1.5 μL/min for imaging. Imaging was not initiated until the cells in the device had resumed uniform exponential growth.

The media used for fluidics always contained 0.1 mg/mL BSA as a passivation agent to limit cell adhesion to the device during flow. The fluidics were fed by 20-mL syringes in six-channel syringe pumps (New Era Pump Systems, Farmingdale, NY) that were connected by 21-gauge blunt needles to Tygon flexible tubing with an inner diameter (ID)

Strain or plasmid	Relevant genotype or description	Source or reference
MTC1761	3610 *hag*$_{A233V}$ Δ*ytvA* Δ*rsbRB* Δ*rsbRC* Δ*rsbRD amyE*::*DG364*-P$_{hyperspank}$-*mNeptune*(Cm^R) *ywrK*::*DG1730-P$_{rsbV}$-mNeonGreen* (Spc^R)	16
MTC1763	3610 *hag*$_{A233V}$ Δ*ytvA* Δ*rsbRA* Δ*rsbRC* Δ*rsbRD amyE*::*DG364-P$_{hyperspank}$-mNeptune*(Cm^R) *ywrK*::*DG1730-P$_{rsbV}$-mNeonGreen* (Spc^R)	16
MTC1765	3610 *hag*$_{A233V}$ Δ*ytvA* Δ*rsbRA* Δ*rsbRB* Δ*rsbRD amyE*::*DG364-P$_{hyperspank}$-mNeptune*(Cm^R) *ywrK*::*DG1730-P$_{rsbV}$-mNeonGreen* (Spc^R)	16
MTC1767	3610 *hag*$_{A233V}$ Δ*ytvA* Δ*rsbRA* Δ*rsbRB* Δ*rsbRC amyE*::*DG364-P$_{hyperspank}$-mNeptune*(Cm^R) *ywrK*::*DG1730-P$_{rsbV}$-mNeonGreen* (Spc^R)	16
MTC1801	3610 *hag*$_{A233V}$ Δ*ytvA amyE*::*DG364-P$_{hyperspank}$-mNeptune* (Cm^R) *ywrK*::*DG1730-P$_{rsbV}$-mNeonGreen* (Spc^R)	16
MTC2540	3610 *hag*$_{A223V}$ Δ*ytvA* Δ*rsbRB* Δ*rsbRC* Δ*rsbRD rsbRA*::*rsbRC/A amyE*::*DG364-P$_{hyperspank}$-mNeptune* (Cm^R) *ywrK*::*DG1730-P$_{rsbV}$-mNeonGreen* (Spc^R); RsbRC/A hybrid as only source of RsbR within the cell	This study
MTC2541	3610 *hag*$_{A223V}$ Δ*ytvA* Δ*rsbRA* Δ*rsbRB* Δ*rsbRD rsbRC*::*rsbRA/C amyE*::*DG364-P$_{hyperspank}$-mNeptune* (Cm^R) *ywrK*::*DG1730-P$_{rsbV}$-mNeonGreen* (Spc^R); RsbRA/C hybrid as only source of RsbR within the cell	This study
MTC2542	3610 *hag*$_{A223V}$ Δ*ytvA* Δ*rsbRA* Δ*rsbRC* Δ*rsbRD rsbRB*::*rsbRC/B amyE*::*DG364-P$_{hyperspank}$-mNeptune* (Cm^R) *ywrK*::*DG1730-P$_{rsbV}$-mNeonGreen* (Spc^R); RsbRC/B hybrid as only source of RsbR within the cell	This study
MTC2543	3610 *hag*$_{A223V}$ Δ*ytvA* Δ*rsbRA* Δ*rsbRB* Δ*rsbRD rsbRC*::*rsbRB/C amyE*::*DG364-P$_{hyperspank}$-mNeptune* (Cm^R) *ywrK*::*DG1730-P$_{rsbV}$mNeonGreen* (Spc^R); RsbRB/C hybrid as only source of RsbR within the cell	This study
MTC2544	3610 *hag*$_{A223V}$ Δ*ytvA* Δ*rsbRB* Δ*rsbRC* Δ*rsbRD rsbRA*::*rsbRD/A amyE*::*DG364-P$_{hyperspank}$-mNeptune* (Cm^R) *ywrK*::*DG1730-P$_{rsbV}$-mNeonGreen* (Spc^R); RsbRD/A hybrid as only source of RsbR within the cell	This study
MTC2545	3610 *hag*$_{A223V}$ Δ*ytvA* Δ*rsbRA* Δ*rsbRB* Δ*rsbRC rsbRD*::*rsbRA/D amyE*::*DG364-P$_{hyperspank}$-mNeptune* (Cm^R) *ywrK*::*DG1730-P$_{rsbV}$-mNeonGreen* (Spc^R); RsbRA/D hybrid as only source of RsbR within the cell	This study
MTC2546	3610 *hag*$_{A223V}$ Δ*ytvA* Δ*rsbRB* Δ*rsbRC* Δ*rsbRD rsbRA*::*rsbRB/A amyE*::*DG364-P$_{hyperspank}$-mNeptune* (Cm^R) *ywrK*::*DG1730-P$_{rsbV}$-mNeonGreen* (Spc^R); RsbRB/A hybrid as only source of RsbR within the cell	This study
MTC2547	3610 *hag*$_{A223V}$ Δ*ytvA* Δ*rsbRA* Δ*rsbRC* Δ*rsbRD rsbRB*::*rsbRA/B amyE*::*DG364-P$_{hyperspank}$-mNeptune* (Cm^R) *ywrK*::*DG1730-P$_{rsbV}$-mNeonGreen* (Spc^R); RsbRA/B hybrid as only source of RsbR within the cell	This study

Table 1.1 A list of strains used in this study.

of 0.02 in. To permit medium switches, two banks of syringes were used: one for the one for the prestress phase containing plain medium and the other for the stress phase containing the stressor. Each pair of syringes (minus and plus stressor) was joined with a polypropylene 1.6-mm-ID Y connector with 200-series barbs; 2-cm lengths of flexible silicone tubing (0.04-in. ID, 0.085-in. outer diameter) were used to connect the Tygon lines to the two input branches of the Y connector. The lengths of silicone tubing facilitated the placement of small binder clips to one or the other branch to make pinch valves. A 1-cm

length of silicone tubing was used to connect a 10-cm length of Tygon tubing to the output of the Y connector. The output Tygon tubing was directly connected to a bent 21-gauge blunt needle that was then connected to the PDMS device, and a similarly constructed needle-tube combination was used to carry the outflow of the device to a waste beaker.

The environmental stressors used in this study included ethanol, salt, oxidative, and acid stress. We used lower concentrations of the stressors in the microfluidic platform than in previous reports testing the same stressors in culture flasks. We attribute this difference to the fact that in a closed (flask) culture, a defined and finite amount of stressor may be neutralized over time, whereas the microfluidic system is constantly replenished with respect to stressor. For ethanol stress, we added 2% EtOH to LB + 0.1 mg/mL BSA; the prestress medium was LB + 0.1 mg/mL BSA alone. For oxidative stress, we used 0.005% H_2O_2 added to LB + 0.1 mg/mL BSA. For acid stress, we used LB at a pH of 6.25 + 0.1 mg/mL BSA, and the prestress medium was LB at pH 6.5 + 0.1 mg/mL BSA. pH was adjusted by adding HCl or NaOH as needed to LB. Because LB Lennox medium already contains NaCl, we used a salt-free formulation of LB termed LBK because of its potassium phosphate (10 g/liter tryptone, 5 g/liter yeast extract, 21 mM K2HPO4, 11 mM KH2PO4) + 0.1 mg/mL BSA as the prestress medium and for salt stress added 500 mM NaCl to LBK + 0.1 mg/mL BSA.

Every strain and medium combination in this study was tested in at least two separate experiments (either completely separate lanes in a microfluidic device or separate microfluidic devices). If we suspected that reporter activity might be spurious (due to cell clogs or medium-flow stoppage), we repeated the experiment additional times to obtain consistent results. The lineages plotted in figures are representative and in some cases are taken from multiple experiments.

1.3.3 Medium Switching

The experiments were always initiated in stressor-free medium, and this initial growth phase typically lasted approximately 10 to 12 h before the switch. In the initial phase, pinch

valves were closed on the stressor-containing branch of the fluidics, and the corresponding syringe pump was paused. At the switch, the syringe pump with stressor-free medium was paused, the binder clips were carefully moved to the stressor-free branch of the Y connectors, and the other (stressor-containing) syringe pump was activated (at 2.5 μL/min). Tests with marker beads and dyes indicated that the second medium took approximately 50 min to reach the cells in the device. The switch apparatus was housed within a temperature-controlled microscope enclosure during imaging (see below).

1.3.4 Automated Imaging

Imaging was performed with a Nikon Eclipse Ti inverted microscope equipped with a Photometrics Prime 95B sCMOS camera, a 100× Plan Apo oil objective (NA 1.45, Nikon), an automated stage (Nikon), a Lumencor SOLA SE II 365 Light Engine fluorescent illumination system, and an OKO temperature-controlled enclosure in which the temperature was maintained at approximately 37°C during imaging. Image acquisition was performed using NIS-Elements AR 5.11.03 64-bit. Filter cubes for GFP and mCherry were used to image mNeonGreen and mNeptune, respectively. mNeonGreen (used for σ^B reporters) was imaged at approximately 33% illumination power with 200-ms exposures, and mNeptune (used for cell visualization) was imaged with at approximately 33% power with 400-ms exposures. The images were captured at 10-min intervals. Phase-contrast images were occasionally also captured.

1.3.5 Lineage Tracking and Curation

Lineage tracking and curation of the average mNeonGreen average intensity in mother cells was used to generate σ^B reporter traces. Lineages were manually filtered to retain only lineages that were tracked for >150 continuous frames. Images of cells were then stabilized to eliminate any movement or shifts during the time lapse by using the ImageJ plugin "Template Matching and Slice Alignment." Because spontaneous cell death events and other anomalies (e.g., overcrowding of side channels) were associated with spurious peaks in reporter intensity, the full filtered set of lineages was then manually curated to remove

spurious events. The mean mNeonGreen fluorescence value was then determined for each lineage by drawing a region of interest (ROI) box slightly smaller than the size of a cell in ImageJ and using the ImageJ plugin "Time Series Analyzer." The position of the ROI, which otherwise remained static at each time point, was manually reviewed, and corrected when necessary to ensure that the ROI contained the mother cell of each lineage for the duration of the experiment. The mean pixel intensity in the mNeonGreen channel in the ROI of the cell at each 10-min interval was collected and then corrected by subtraction of the average background adjacent to the cell to eliminate any fluctuations during the time lapse. To facilitate comparison between strains, as well as to correct for variations in imaging parameters among experiments (such as exposure and illumination intensity), we normalized the prestress value to 100 AU. To do so, the average fluorescence value of each lineage prior to stressor onset (average of the first 50 frames) was obtained; 100 was divided by this average value to obtain a normalization constant. The normalization constant was then applied at every time point for that lineage. This process was independently repeated for each lineage. The curated and corrected lineage sets were used to plot average traces and overlaid single-lineage (single-cell) traces.

The mean GFP values for all tracked lineages, both the raw background-corrected values and the normalized values, are available in Excel spreadsheets on Dryad at https://doi.org/10.5061/dryad.2ngf1vhs1.
All supplementary movies and their legends are available on Dryad at https://doi.org/10.5061/dryad.2ngf1vhs1.

1.4 Results

1.4.1 Consistency between analytical pipelines for microfluidics-coupled fluorescence microscopy

A key approach in our previous work [16] permitting us to detect subtle differences among the RsbR paralogs was microfluidics-coupled fluorescence microscopy. Unlike in bulk studies, the microfluidic environment in which cells are growing is both uniform and

controllable, and σ^B responses are observed in single cells, allowing us to distinguish among different single-cell behaviors that might give rise to similar ensemble behaviors. However, as the present study was performed using different microfluidic devices, different imaging equipment, and a different analysis method in a different laboratory, we first sought to ensure that data from our present setup was comparable to our previously published data. As we had done previously, we used a PrsbV-mNeonGreen fluorescent reporter to detect σ^B-directed GSR activity. We equilibrated cells in the microfluidic device under constant flow in the absence of stressor while imaging every 10 min for >500 min prior to adding a stressor. After switching cells to stressor-containing medium, we continued growing cells under constant stressed conditions while imaging at 10-min intervals for >1,500 min. Fluorescence quantification was performed using manual curation in ImageJ by drawing a region of interest (ROI) slightly smaller than the size of an individual cell and measuring the average pixel value within the ROI (Figure 1.1D). We then subtracted the average background value from several measurements of unoccupied areas of the device and plotted fluorescence over time (Figure 1.1D) to obtain individual cell traces.

We compared our present imaging and analysis workflow to our previous work by using 2% ethanol as a stressor and assessing a wild-type strain and strains containing only RsbRA, RsbRB, RsbRC, or RsbRD. We observed a transient, synchronous response by wild-type cells that was very similar to the response we previously observed (Figure 1.2A and 1.2B) [16]. Cells containing only RsbRA exhibited a similar response to wild-type cells, while cells containing only RsbRC showed a slower-onset repeated response that was stochastic across individual cells, again matching our previous work (Figure 1.2A and 1.2B). Again, consistent with our previous observations, RsbRB-only cells showed a RsbRC-like response but weaker in magnitude (Figure 1.2A and 1.2B). We did notice a modest difference from our previous results [16] in the RsbRD-only response, which here lacked an initial response spike before an RsbRC-like repeated response (Figure 1.2). After repeating this experiment several times, we are convinced of the accuracy of the result presented here. We conclude that our present experimental approach yields

comparable results to our previous work despite minor technical and methodological differences, demonstrating the utility and consistency of the approach.

1.4.2 The wild-type σ^B response to four environmental stressors differs in magnitude but not timing

We next approached the longstanding question of whether having multiple RsbR paralogs abets cells' ability to sense a range of environmental stressors. Do cells with wild-type stressosomes (i.e., containing all four RsbR paralogs) differentiate among different stressors by altering the timing or magnitude of their σ^B responses? To answer this question, we assembled a panel of four well-known environmental stressors: ethanol, salt (NaCl), pH, and oxidative stress (thermal stress is also a well-known environmental stressor, but we limited our analysis to stressors that we could add to the medium) [7], [8], [11], [25], [31], [41], [43]–[46]. Previous studies analyzing the wild-type B. subtilis response to different environmental stressors showed the typical transient response irrespective of stressor [8], [11], [16], [47]. However, as these studies were performed in bulk cultures, typically using β-galactosidase assays to assess the σ^B response at the population level, we hypothesized that our microfluidic approach might detect subtle differences among the responses to different stressors that manifest at the single-cell level.

One experimental design consideration was that microfluidic growth can change the tolerance of cells to stressors relative to batch growth. When a stressor is added to a closed culture, the concentration of that stressor may decline as it reacts with cell components, is metabolized, or is otherwise detoxified by the bacterial cells. In contrast, in a microfluidic device, fresh medium with a set concentration of stressor is continuously replenished, so that the stressor concentration never appreciably declines. We attribute to this difference our informal observations that stressors or antibiotics are lethal at lower concentrations in the microfluidic platform than in bulk culture [16]. Hence, we found that we often had to lower the concentration or magnitude of a stressor relative to previous reports. Our initial tests showed that previously reported stressors, such as pH shift from 6.5 to 5.5 or challenge with 1 M NaCl as previously used [7], [11], [43], caused widespread cell lysis or death,

with very few survivors that continued to grow and divide at a normal rate under the stress condition. Hence, we used empirically determined sublethal concentrations of stressors that stimulated the σ^B response without broadly killing cells. Guided by the literature and pilot studies, we used 2% ethanol, 500 mM NaCl, 0.005% H_2O_2, and acid stress from pH 6.5 to 6.25 as our stressors. We challenged wild-type cells with each stressor and used our current analysis method to assess their σ^B response profiles.

Wild-type cells always responded with the same characteristic σ^B response profile, irrespective of which stressor we used (Figure 1.3; Figure S2 and S7; Movies S1 to S4 at https://doi.org/10.5061/dryad.2ngf1vhs1). Individual cells synchronously activated σ^B upon introduction of the stressor (Figure S2; Figure S2 through S6 show separate graphs for single cells of each strain and condition), and the response was transient, peaking roughly 30 min after exposure and then declining toward the baseline nonactivated state despite continued exposure to the stressor (Figure 1.3). However, we observed stressor-specific differences in the response magnitude. Acid and oxidative stress elicited a relatively weak response compared to ethanol and NaCl, with NaCl eliciting the strongest response (Figure 1.3B). Moreover, only ethanol- and NaCl-challenged cells showed a weak but prolonged response after the initial response peak, not quite returning to the prestress baseline (Figure 1.3B). Previous research has shown that the magnitude of the response can be affected by the concentration of the stressor used [7], [16], [47], [48]. Because environmental stressors may stress cells in different ways, stressor concentrations are not directly comparable. Our initial testing suggested that at least for some stressors, H_2O_2 for instance, greater stressor concentrations cause cell death rather than eliciting a stronger σ^B response. However, none of the stressor concentrations used in this work substantially affected cell growth, arguing in favor of the stressors having a comparable effect on cells. Collectively, our results suggest that cells with wild-type stressosomes display a stereotypical transient and synchronous σ^B response pattern irrespective of stressor identity but that different stressors provoke different response magnitudes.

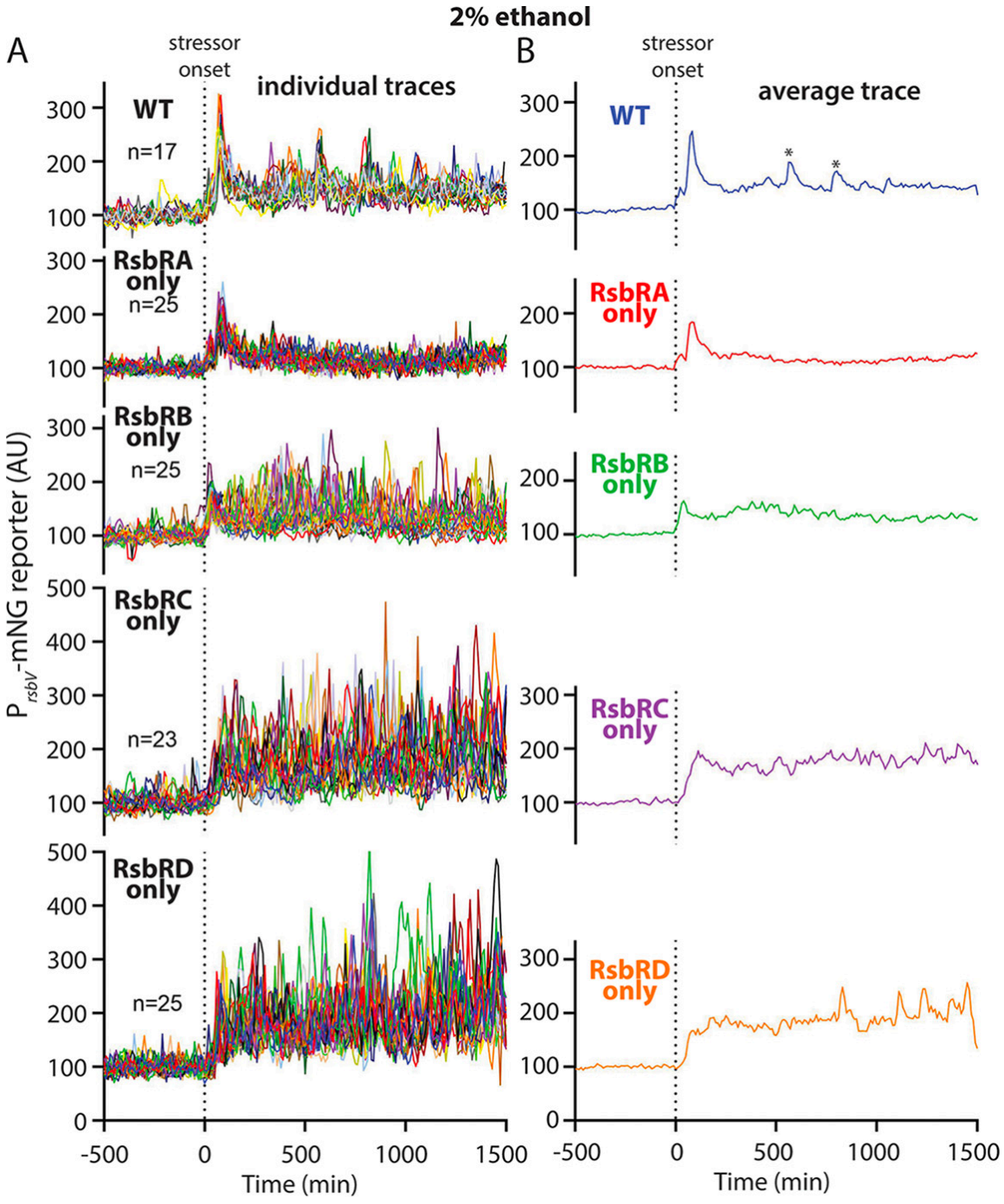

Figure 1.2 Individual-lineage tracking and average traces of the wild-type strain as well as individual RsbR paralogs **A)** Individual-lineage intensity traces of a stress-responsive P_{rsbV}-mNeonGreen reporter in a wild-type (WT) strain (MTC1801) and strains containing only RsbRA (MTC1761), RsbRB (MTC1763), RsbRC (MTC1765), and RsbRD (MTC1767) before and after the addition (indicated by vertical dotted line) of 2% ethanol. **B)** Average intensity of the P_{rsbV}-mNeonGreen reporter corresponding to the single-cell traces from panel A. Asterisks in the EtOH trace denote peaks that were present in only some lineages corresponding to the same experimental replicate and hence are considered artifactual.

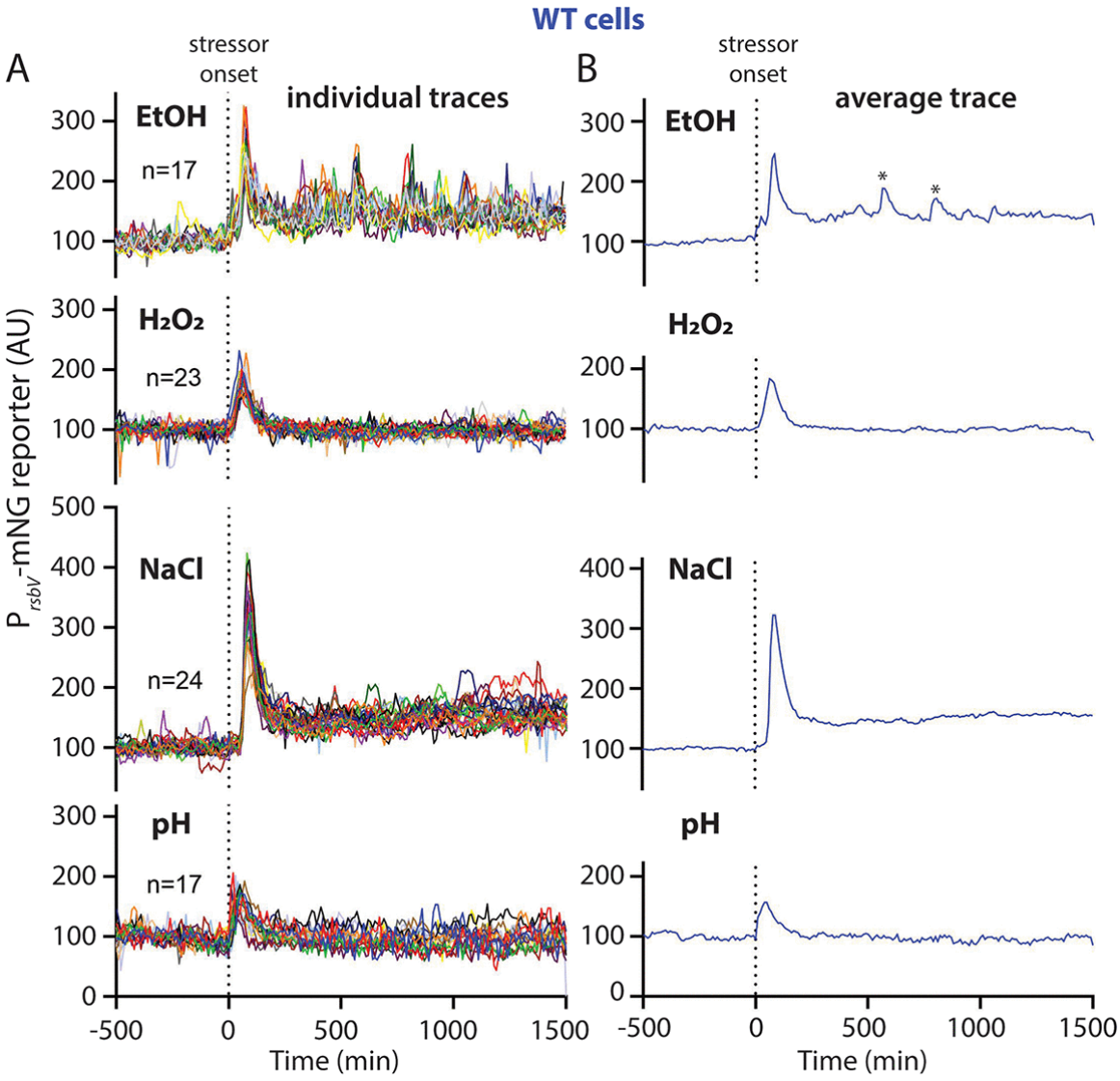

Figure 1.3. Individual-lineage tracking, and average traces of the wild-type strain subjected to four different stressors. **A)** Individual-lineage intensity traces of a stress-responsive P_{rsbV}-mNeonGreen reporter in a wild-type strain (MTC1801) before and after the addition (indicated by vertical dotted line) of the indicated stressors. The stressors were 2% ethanol, 0.005% H_2O_2 500 mM NaCl, and pH shift from 6.5 to 6.25. **B)** Average intensity of the P_{rsbV}-mNeonGreen reporter corresponding to the single-cell traces from panel A. Asterisks in the EtOH trace denote peaks that were present in only some lineages corresponding to the same experimental replicate (see also Figure S2) and hence are considered artifactual.

1.4.3 The RsbRA-only response closely resembles the wild-type response

Our experimental approach, here (Figure 1.2) and in previous work [16], revealed distinct σ^B response profiles for cells bearing stressosomes containing each individual RsbR paralog in isolation. Hence, we asked whether the σ^B response profiles of such single-RsbR

strains change depending on stressor. We began by examining RsbRA-only cells, whose response profile closely matched the wild-type profile in our present work (Figure 1.2) and in previous research, suggesting that RsbRA dominates the response in wild-type cells [16]. We thus hypothesized that the RsbRA-only response might closely match the wild-type response across our panel of four stressors.

Indeed, our results revealed that the RsbRA-only response pattern largely resembles the wild type (Figure 1.4; Figures S3 and S7; Movies S5 to S8 at https://doi.org/10.5061/dryad.2ngf1vhs1). We observed the same stereotypical synchronous, transient response regardless of stressor identity, and the response magnitudes were also similar to the wild type (compare Figure 1.3 and 1.4; Figure S7). As in the wild type, NaCl stress provoked the strongest response, whereas pH induced the weakest response (Figure 1.4B and 1.3B). One modest difference between wild-type and RsbRA-only cells was that H_2O_2 stress elicited a stronger response in the RA-only cells, with some individual cells peaking more than twice as high as in the wild type (Figure 1.3A and 1.4A). Meanwhile, the response to 2% ethanol was slightly weaker in RsbRA-only cells. These data continue to support a model in which the RsbRA-type response largely dominates in wild-type cells containing all four RsbR paralogs. They also suggest the possibility that RsbRA is particularly sensitive to oxidative stress and that the presence of other RsbR paralogs has a moderating influence on the σ^B response to hydrogen peroxide.

1.4.4 The RsbRB-only response differs according to stressor and is insensitive to oxidative stress

We next expanded our analysis to the remaining RsbR paralogs. Unlike wild-type and RsbRA-only cells, with their characteristically synchronous and transient response, our present (Figure 1.2) and previous work [16] shows that ethanol stress elicits, to various degrees, repeated activation of σ^B in cells bearing one of the other RsbR paralogs. For example, in ethanol, RsbRB-only cells show a repeated response that is dissimilar to the pattern generated by RsbRA-only cells (Figure 1.2A and 1.2B). While RsbRA-only cells responded comparably to different stressors, the responses differing mainly by magnitude,

we asked whether cells bearing other RsbR paralogs would modulate their response timing based on stressor identity.

Interestingly, we observed that RsbRB-only cells distinguish among different stressors with respect to the timing of the subsequent σ^B response patterns. In ethanol, as in our previous work [16], we observed a sustained response (Figure 1.5B) manifesting at the single-cell level as stochastic, repeated response peaks (Figure 1.5A; Movie S9 at https://doi.org/10.5061/dryad.2ngf1vhs1). We saw a qualitatively similar but stronger response in NaCl stress (Figure 1.5A and 1.5B; Figure S4 and S7; Movie S11 at https://doi.org/10.5061/dryad.2ngf1vhs1), with a sustained response that set RsbRB apart from the RsbRA and wild-type responses. Oxidative stress elicited a very weak, barely detectible repeated response compared to RsbRA-only or the wild type (compare Figure 1.3B, 1.4B, and 1.5B; Movie S10 at https://doi.org/10.5061/dryad.2ngf1vhs1). RsbRB-only cells may still sense H_2O_2 but less sensitively; however, in our initial testing, the fast transition to lethality as H_2O_2 concentrations rise precluded our testing higher concentrations. RsbRB-only cells displayed a sharper and stronger response to acid stress than either wild-type or RsbRA-only cells (Figure 1.5B; Movie S12 at https://doi.org/10.5061/dryad.2ngf1vhs1). The acid stress response was synchronous and transient, distinguishing it from the ethanol or NaCl response of RsbRB-only cells. These results suggest that the RsbRB protein differs from RsbRA in that RsbRB can elicit different σ^B response patterns according to the identity of the environmental stressor, at least among the tested stressors.

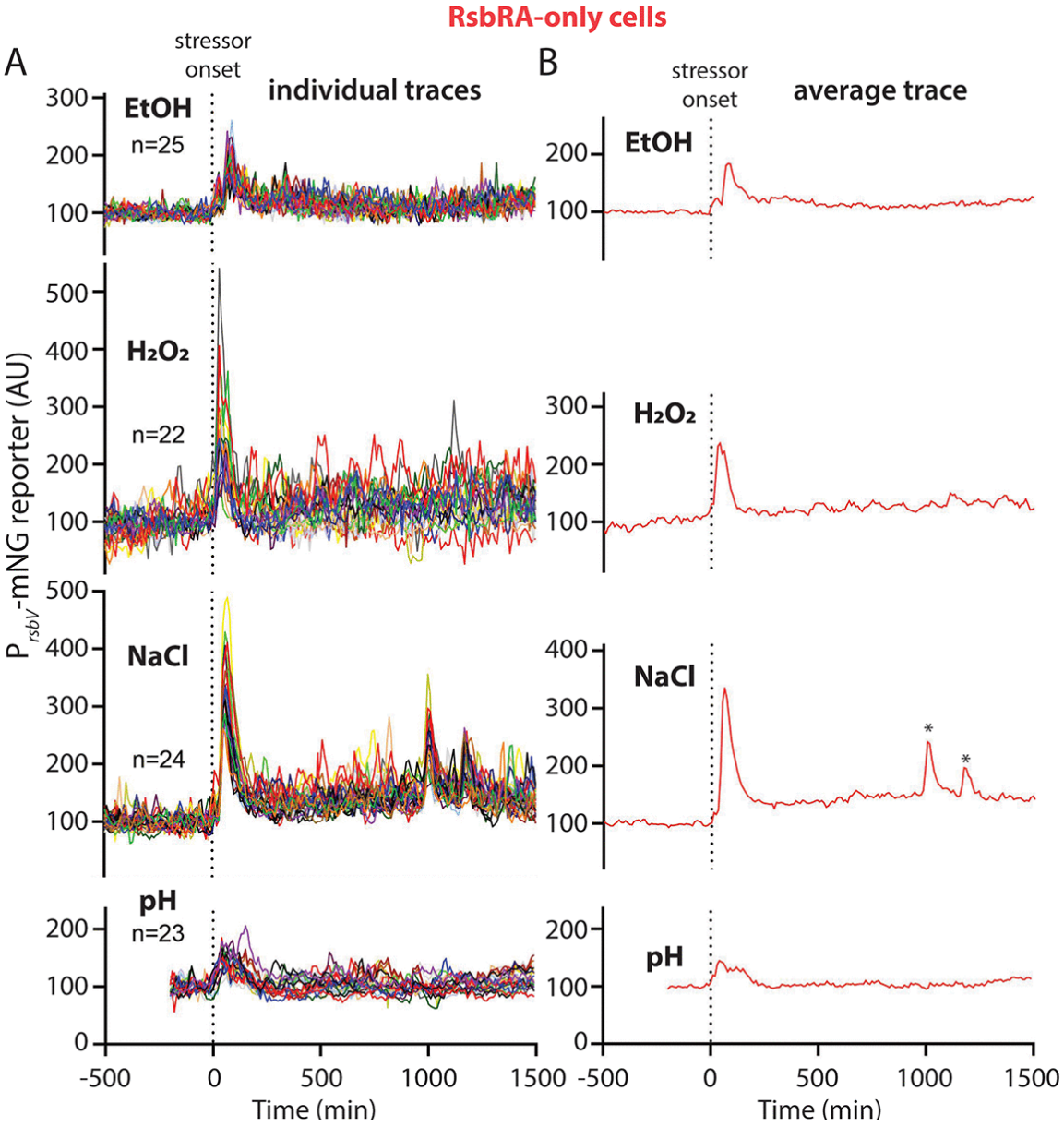

Figure 1.4. Individual-lineage tracking, and average traces of the RsbRA-only strain subjected to four different stressors. **A)** Individual-lineage intensity traces of a stress-responsive P_{rsbV}-mNeonGreen reporter in an RsbRA-only strain (MTC1761) before and after the addition (indicated by vertical dotted line) of the indicated stressors. The stressors were 2% ethanol, 0.005% H_2O_2, 500 mM NaCl, and pH shift from 6.5 to 6.25. **B)** Average intensity of the P_{rsbV}-mNeonGreen reporter corresponding to the single-cell traces from panel A. Asterisks in the NaCl trace denote peaks that were present in only some lineages corresponding to the same experimental replicate (see also Figure S3) and hence are considered artifactual.

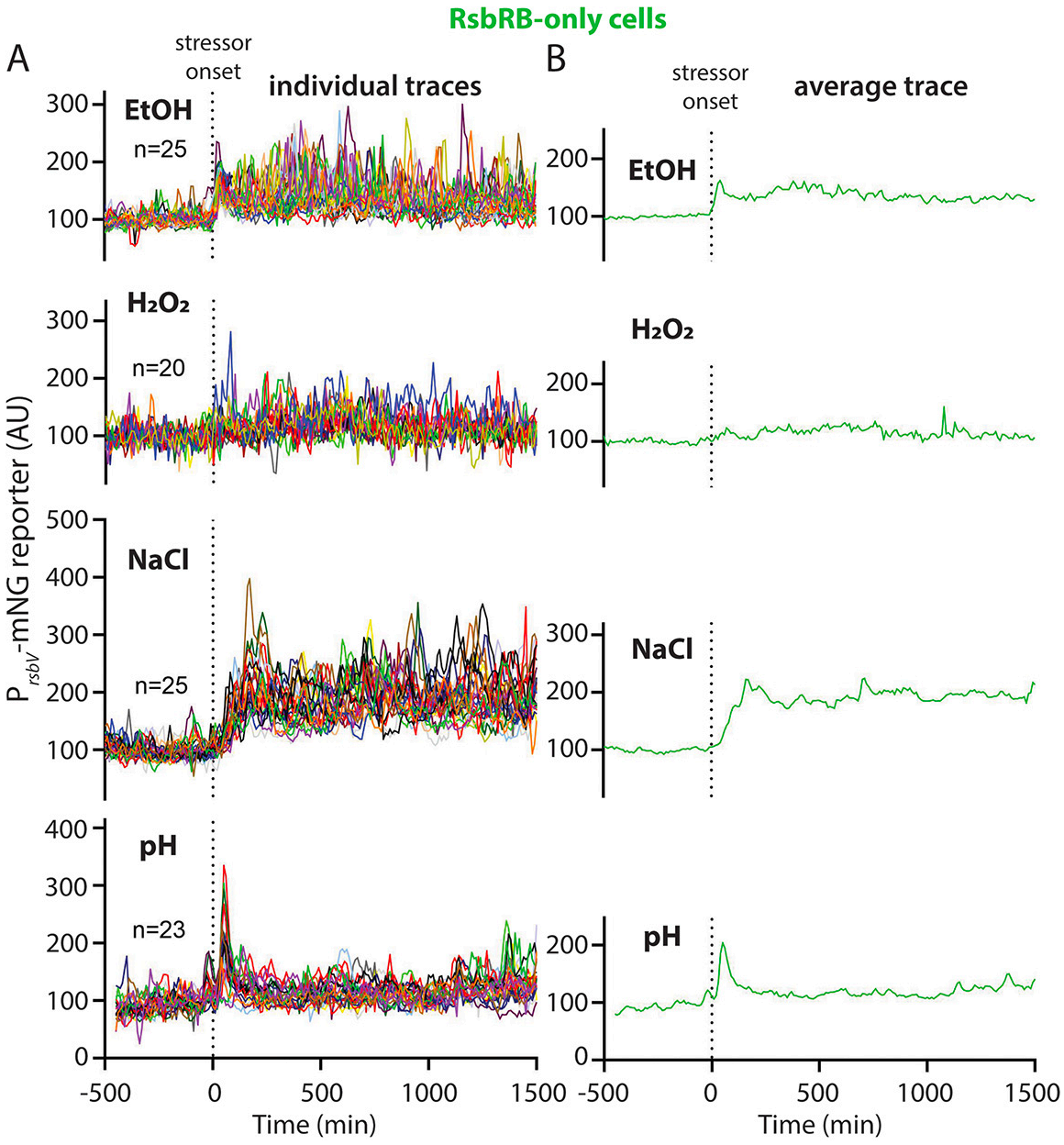

Figure 1.5. Individual-lineage tracking, and average traces of the RsbRB-only strain subjected to four different stressors. **A)** Individual-lineage intensity traces of a stress-responsive P_{rsbV}-mNeonGreen reporter in an RsbRB-only strain (MTC1763) before and after the addition (indicated by vertical dotted line) of the indicated stressors. The stressors were 2% ethanol, 0.005% H_2O_2, 500 mM NaCl, and pH shift from 6.5 to 6.25. **B)** Average intensity of the P_{rsbV}-mNeonGreen reporter corresponding to the single-cell traces from panel A. Representative individual traces are shown in Figure S4.

1.4.5 The RsbRC-only response is characterized by repetition and insensitivity to oxidative stress

Having uncovered evidence that RsbRB-only cells can differentiate between stressors, we next tested RsbRC-only cells. RsbRC-only cells were originally characterized in ethanol as resembling RsbRB-only cells but with a greater response magnitude (Figure 1.2B) [16]. Namely, a sustained average response after stressor onset was composed at the single-cell level of stochastic, repeated σ^B activation events (Figure 1.2A and 1.6A; Figure S8; Movie S13 at https://doi.org/10.5061/dryad.2ngf1vhs1). We observed here that this pattern was largely preserved in other stressors; for example, NaCl and acid stress both resulted in repeated responses among single cells throughout the duration of stress exposure (Figure 1.6A; Figure S5 and S7; Movies S14 and S16 at https://doi.org/10.5061/dryad.2ngf1vhs1). However, both NaCl and acid stress elicited initial synchronous peaks, unlike the more gradual, asychronous response to ethanol (Figure 1.6A). Overall, despite some similarities, RsbRC exhibited several differences from RsbRB across our panel of stressors. RsbRB-only cells respond more quickly and synchronously to ethanol than RsbRC, which takes longer to respond but then maintains a higher average response (Figure 1.5 and 1.6). The patterns are reversed in NaCl stress, with which RsbRC-only cells show the faster and more synchronous response and RsbRB-only cells respond more slowly but mount a higher average sustained response (Figure 1.5 and 1.6). Both RsbRC-only and RsbRB-only cells showed weak responses to oxidative stress, with RsbRC mediating a slightly stronger, transient response (Figure 1.5 and 1.6). The patterns displayed by RsbRC-only cells strengthen the evidence that stressor identity can affect the σ^B responses mediated by different RsbR paralogs.

1.4.6 The RsbRD-only response largely resembles the RsbRC-only response

Within wild-type cells containing all four RsbR paralogs, RsbRA, RsbRB, and RsbRC are expressed at similar levels during growth, while RsbRD is reportedly present at a much lower level [38]. RsbRD levels rise only mildly during stressed conditions [38], leaving RsbRD as a minority player among the RsbR paralogs in the stressosome. In response to

ethanol, cells containing only RsbRD looked similar to cells containing only RsbRC, but with a slightly weaker initial response that modestly increased in magnitude over the duration of exposure (Figure 1.7A and 1.7B; Figure S6 and S7; Movie S17 at https://doi.org/10.5061/dryad.2ngf1vhs1). Like RsbRC-only cells, RsbRD-only cells also showed a very weak, synchronous, and transient response to oxidative stress and a stronger but still synchronous and largely transient response to acid stress (Figure 1.7A and 1.7B; Movies S18 and S20 at https://doi.org/10.5061/dryad.2ngf1vhs1). We observed a similar response to NaCl stress between RsbRD and RsbRC, with a stochastically repeated response following an initial synchronous response to the introduction of stress, although RsbRC-only cells exhibited a sharper and more synchronous initial peak (Figure 1.6 and 1.7; Movie S19 at https://doi.org/10.5061/dryad.2ngf1vhs1). Our results show that RsbRD-only cells are similar to RsbRC-only cells in their response patterns and magnitude, and that the responses of both of these paralogs are distinct from those mediated by RsbRB. Collectively, our findings indicate that while the wild-type and RsbRA-only responses have a stereotypical response shape that varies only in magnitude among different stressors, the, RsbRB-, RsbRC-, and RsbRD-only responses appear to distinguish among different stressors in terms of their consequent σ^B response profiles.

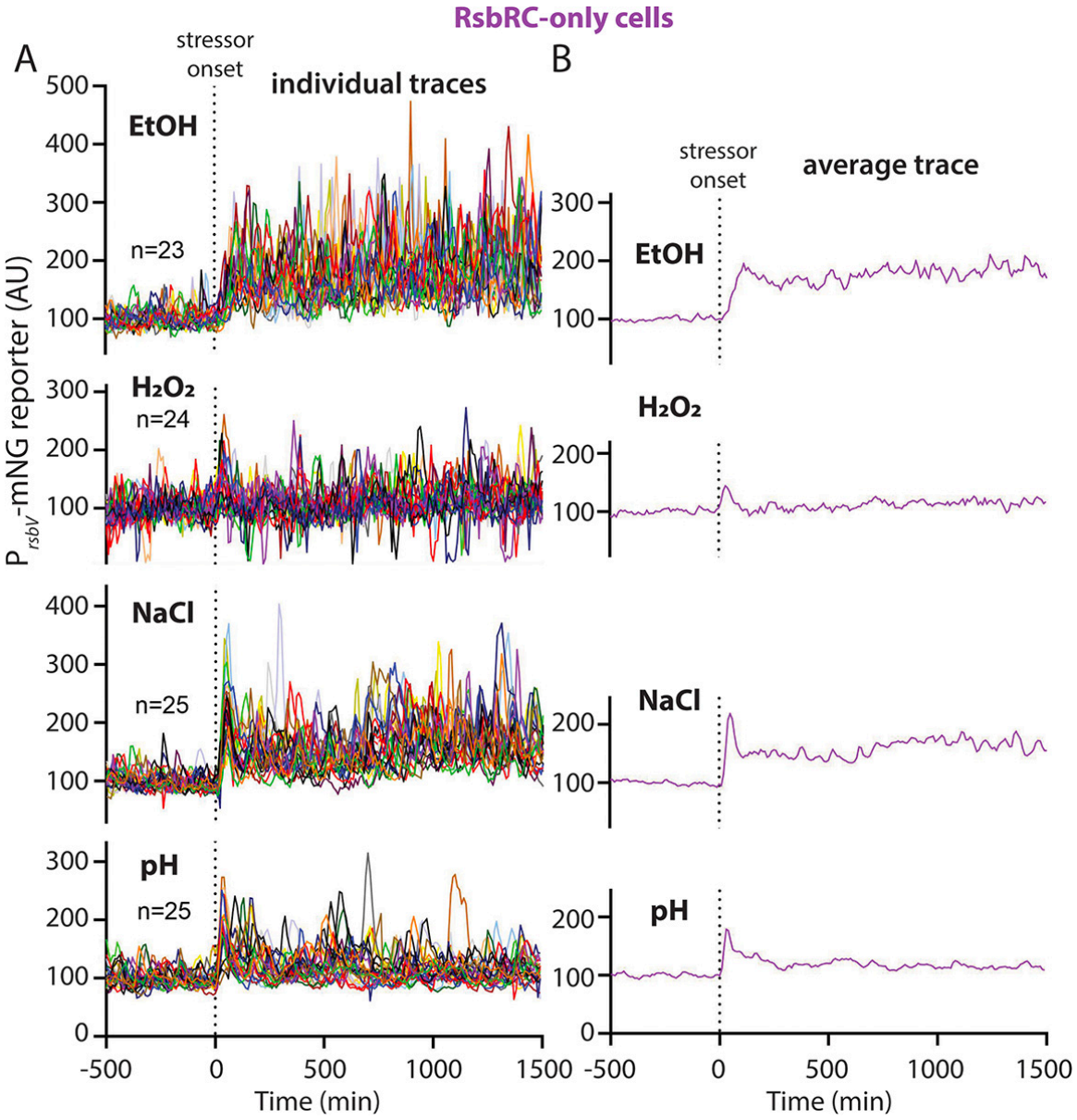

Figure 1.6. Individual-lineage tracking, and average traces of the RsbRC-only strain subjected to four different stressors. **A)** Individual-lineage intensity traces of a stress-responsive P_{rsbV}-mNeonGreen reporter in a an RsbRC-only strain (MTC1765) before and after the addition (indicated by vertical dotted line) of the indicated stressors. The stressors were 2% ethanol, 0.005% H_2O_2, 500 mM NaCl, and pH shift from 6.5 to 6.25. **B)** Average intensity of the P_{rsbV}-mNeonGreen reporter corresponding to the single-cell traces from panel A. Representative individual traces are shown in Figure S5.

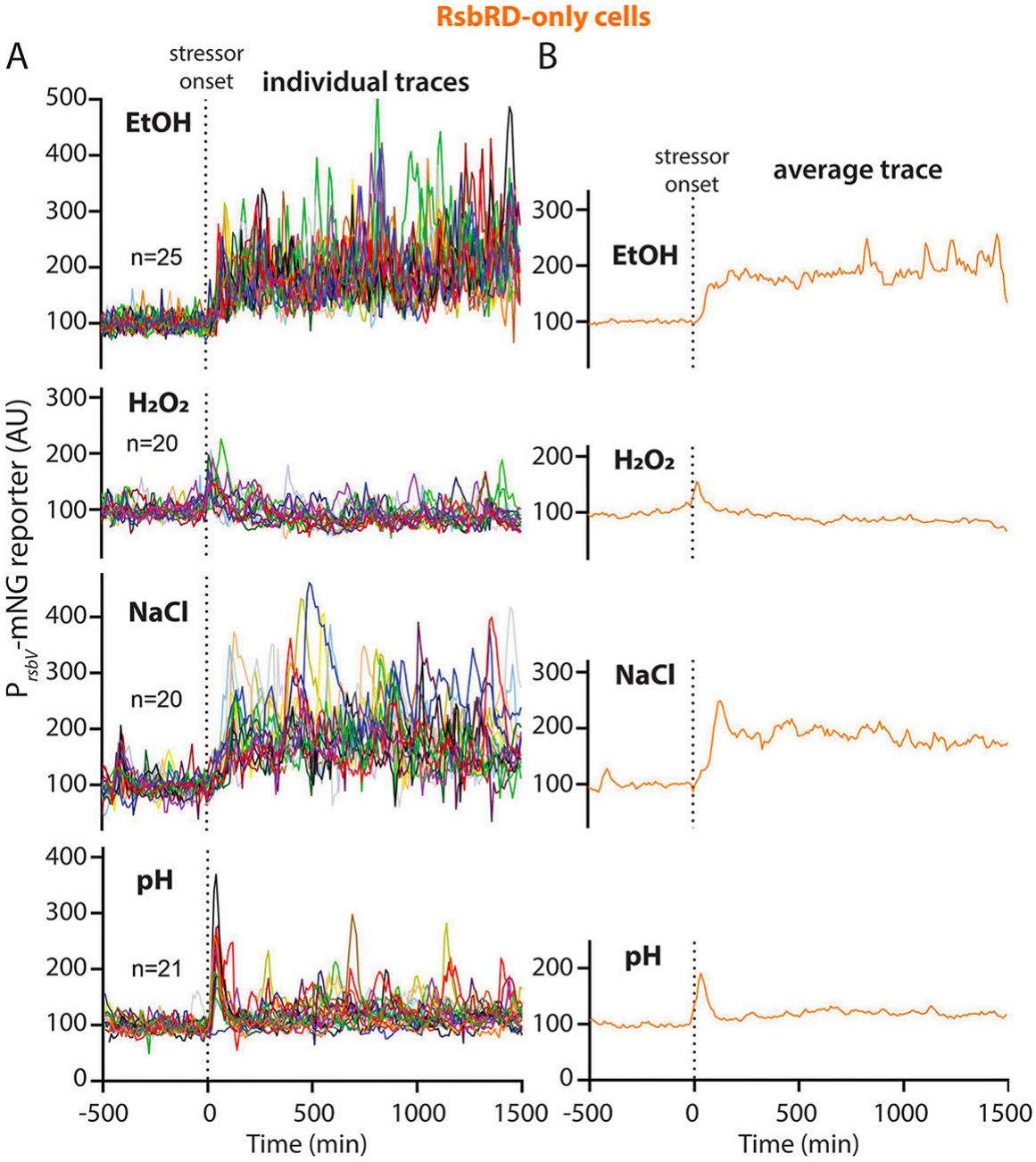

Figure 1.7. Individual-lineage tracking, and average traces of the RsbRD-only strain subjected to four different stressors. **A)** Individual-lineage intensity traces of a stress-responsive P_{rsbV}-mNeonGreen reporter in an RsbRD-only strain (MTC1767) before and after the addition (indicated by vertical dotted line) of the indicated stressors. The stressors were 2% ethanol, 0.005% H_2O_2, 500 mM NaCl, and pH shift from 6.5 to 6.25. **B)** Average intensity of the P_{rsbV}-mNeonGreen reporter corresponding to the single-cell traces from panel A. Representative individual traces are shown in Fig. S6

1.4.7 The N-terminal region of RsbR paralogs influences response magnitude in hybrid fusions

Except for RsbRA, we observed that each individual RsbR paralog showed σ^B response profiles that differed from paralog to paralog and from stressor to stressor. The RsbR paralogs are characterized by a largely conserved C-terminal domain and an N-terminal domain that varies among the paralogs (Figure 1.1C and 1.8A). Therefore, we hypothesized that the observed differences among the RsbR paralogs in their response profiles is due to the differences in their primary sequences. As an initial test of this hypothesis, we investigated which region of RsbR is responsible for mediating the response profile. Our strategy was to engineer hybrid proteins composed of the variable region of one paralog and the conserved region of another. For example, a hybrid with the variable domain of RsbRC and the conserved region of RsbRA, joined at the STAS domain linker, was termed an RsbRC/A hybrid (Figure 1.8A) [49]. We inserted by markerless allelic replacement each hybrid-encoding gene at the locus of the C terminus (i.e., the rsbRC/A gene would be at the rsbRA locus) as the only source of RsbR in the cell. We constructed several hybrid combinations to learn whether any trends in response pattern were associated with particular variable or conserved sequences. For the sake of simplicity, we limited this initial analysis to 2% ethanol stress.

First, we observed that none of the hybrids perfectly mimicked the response of one of the constituent paralogs. Instead, nearly all the responses showed a repeated pattern of various magnitudes when challenged with ethanol. The response profiles of the eight hybrids we tested bifurcated into two rough classifications, with some initial responses being "weak" (below the dashed horizontal line in Figure 1.8B) and others being "strong" (above the dashed horizontal line in Figure 1.8B). We noted that the weak, sometimes barely detectable responses were observed when the hybrid contained the variable region of either RsbRB or RsbRD (Figure 1.8D and 1.8F; Movies S24, S25, and S27 at https://doi.org/10.5061/dryad.2ngf1vhs1). Nonetheless, the RsbRB/C and RsbRD/A hybrids showed a weak but repeated response throughout the duration of stress exposure.

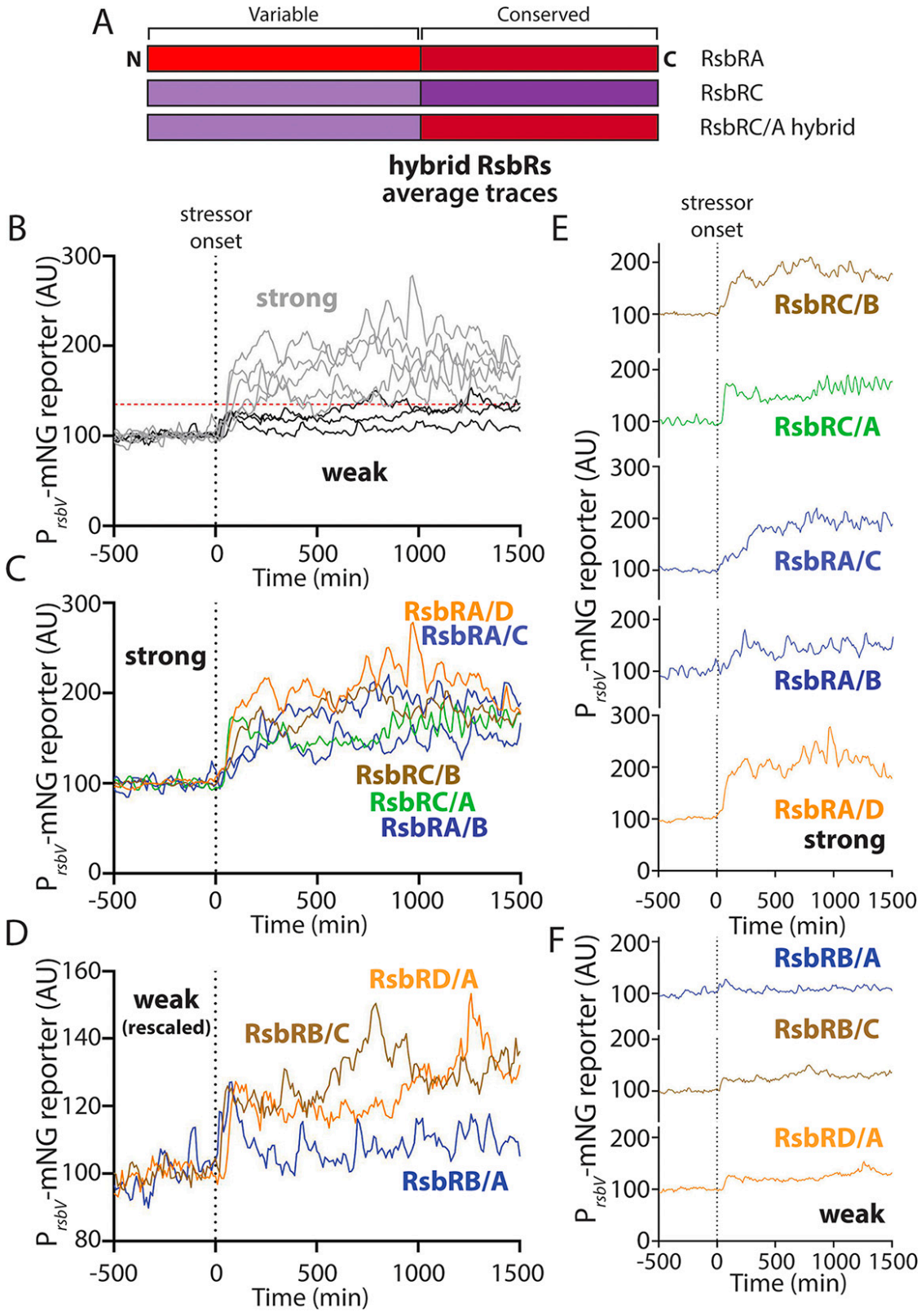

Figure 1.8 Schematic of hybrid strain construction and individual traces of hybris strains subjected to ethanol stress. **A)** Schematic illustrating the domain architecture of two different RsbR paralogs (RsbRA and RsbRC are shown as examples) and a hybrid between them, comprising the N-terminal variable domain or RsbRC

and the C-terminal conserved domain of RsbRA. The schematic also illustrates the nomenclature of the example RsbRC/A hybrid. **B)** Average traces of P_{rsbV}-mNeonGreen reporter in hybrid strains (see strain table for complete genotypes and accession numbers) before and after addition (indicated by the vertical dotted line) of 2% ethanol. High average responses (gray lines) and low average responses (black) were distinguished, with the horizontal dotted line at 135 AU as a visual guide for "strong" and "weak" responses. **C)** Individual average traces of P_{rsbV}-mNeonGreen reporter in the indicated hybrid strains with a strong response (A or C in the N terminus) before and after addition of 2% ethanol. **D)** Individual average traces of P_{rsbV}-mNeonGreen reporter in the indicated hybrid strains with a weak response (B or D in the N terminus) before and after addition of 2% ethanol. **E)** Traces of strong-response strains (as in panel B) displayed individually. (F) Traces of weak-response strains (as in panel C) displayed individually.

Conversely, RsbRB/A was the only tested hybrid that showed a transient response, with a weak response peak (Figure 1.8B, 1.8D, and 1.8F; Movie S27 at https://doi.org/10.5061/dryad.2ngf1vhs1). While the variable regions of RsbRB and RsbRD corresponded with weak responses, the variable regions of RsbRA and RsbRC were associated with stronger responses, all of which were sustained rather than transient (Figure 1.8C and 1.8E; Movies S21 to S23, S26, and S28 at https://doi.org/10.5061/dryad.2ngf1vhs1). However, the speed of the response onset varied among the hybrids. The RsbRC/A and RsbRA/D hybrids both showed a fast onset (steep slope in Figure 1.8C and 1.8E), whereas a slower onset was observed for RsbRC/B, RsbRA/C, and RsbRA/B (shallower slope in Figure 1.8C and 1.8E). This pattern suggests that the RsbRA and RsbRD C-terminal regions mediate a faster onset, whereas the RsbRB and RsbRC C-terminal regions mediate a slower onset to ethanol stress. In sum, these data suggest that the downstream σ^B response profile mediated by a given RsbR protein is not solely dependent upon the variable N-terminal region traditionally thought to be the sensing domain. Instead, it appears that both halves of the protein contribute to the timing and magnitude of the stress response. RsbRA is an exemplar of this principle, as its characteristic strong, synchronous, and transient response to ethanol was not recapitulated in any of the RsbRA-containing hybrids we constructed, suggesting that both halves of RsbRA are needed for its typical response. Further testing is warranted to determine which specific residues or regions within the RsbR paralogs allow for sensing stress and govern the resulting response profiles, not only in ethanol but across different environmental stressors.

1.5 Discussion

Our findings in this work highlight differences among the RsbR paralogs with respect to their σ^B response profiles when challenged with different environmental stressors. We also confirm the utility of microfluidics-coupled fluorescence microscopy for distinguishing different stress-response patterns with single-cell resolution. Collectively, our results indicate that wild-type cells do not substantially change the timing of their σ^B responses according to stressor—the response is always transient across stressors—but responses do show different magnitudes. What is clear from our work is that different RsbR paralogs elicit responses to different stressors that can depart from the wild-type response to a given stressor and, additionally, differ among the paralogs. Taking the response to NaCl as an example, wild-type and RsbRA-only cells display a sharp, strong, and transient response, whereas RsbRB-only cells show a slower-onset but sustained response. RsbRC-only cells show an initial spike but then maintain a higher sustained response level, while RsbRD-only cells show a response that largely mimics the RsbRB response. In contrast, H_2O_2 always elicited a fast and transient response, but the magnitude of the response varied from virtually undetectable (RsbRB) to intermediate (RsbRC, RsbRD) to strong (wild type, RsbRA). Hence, when considered in isolation, different RsbR paralogs can elicit different σ^B response patterns to different stressors. While the available evidence points to these differences being due to the identity of the RsbR paralog(s) in the cell, we also acknowledge the possibility of alternative models. For instance, RsbRA, RsbRB, and RsbRC are produced in roughly equal amounts, and RsbRD is produced more weakly in wild-type cells [38]. As we produced each paralog from its native locus, we assume that our results are not affected by differences in their actual cellular levels, but we cannot rule out the formal possibility that the observed σ^B response patterns may be affected by the abundance of a particular RsbR paralog. Similarly, although our previous work using ethanol revealed qualitatively similar response patterns for each RsbR paralog that varied only in amplitude according to stressor concentration [16], we did not test here the possibility that other stressors may elicit different σ^B response patterns according to stressor concentration.

An important implication of RsbR paralog- and stressor-specific σ^B response patterns is that there may be multiple proximate signals within cells that can lead to stressosome activation and RsbT release. Presumably, the different response patterns—strong or weak, transient, or repeated—are a product of how a given stress stimulus interacts with components of the stressosome to govern the kinetics of RsbT release and recapture. The relative roles of different molecular players in this process remain to be determined. For instance, consider the contrast between a slower-onset, sustained response composed of repeated activation events in individual cells, such as that observed for RsbRB in NaCl (Figure 1.5) or RsbRC in ethanol (Figure 1.6), and the transient response of RsbRA to NaCl (Figure 1.4). Do the kinetics of RsbR/RsbS dephosphorylation by RsbX differ among RsbR paralogs, and does this process make an important contribution to the overall response pattern? Do different stimuli differ in their ability to elicit RsbR/RsbS phosphorylation by RsbT and the subsequent RsbT release? What is responsible for the apparently stochastic (Figure 1.2 and 1.5-1.7; Figure S8) repetition of σ^B activation in many cases? Such stochastic activation resembles a pattern previously seen with energy (mycophenolic acid) stress and recapitulated with induced expression of constitutively active RsbTU [50]. We never observed long durations of σ^B activity at the single-cell level. Might sustained release of RsbT in single-RsbR strains (i.e., other than RsbRA) result in stochastic pulsing? These remain key questions for a molecular-level understanding of stressosome activation.

Having examined the responses of each RsbR paralog in isolation, an important outstanding question is how different RsbR paralogs interact when simultaneously present in stressosomes. The close similarity between the σ^B responses of wild-type and RsbRA-only cells across multiple stressors support our earlier suggestion [16] that RsbRA dominates the wild-type response, enforcing a transient pattern. Because the stressosome governs the σ^B response pattern by sequestering and releasing RsbT, one hypothetical way that RsbRA could enforce a transient response is by recapturing the RsbT molecules released upon stress onset, but with RsbRA in a refractory state that is resistant to subsequent activation and RsbT release. Because there appears to be an approximately 10-fold excess of RsbR proteins over RsbT [38], all cellular RsbT could in principle be bound by RsbRA in stressosomes, even in the presence of other RsbR paralogs. If most of the

initially released RsbT molecules were recaptured on refractory RsbRA proteins, subsequent σ^B responses would be suppressed, even if other RsbR paralogs were in a state that would normally release RsbT. Such a scenario would explain why the distinct σ^B responses of other RsbR paralogs are unmasked when analyzed in isolation (Figure 1.5 to 1.7). We previously speculated that other RsbR paralogs might dominate in stressors other than ethanol [16], but our present work argues that RsbRA dominates across different types of stressors. An important test of this model will be to analyze cells with pairs of RsbR paralogs to learn whether the presence of RsbRA is sufficient to mask the distinctive responses of a second RsbR paralog. It will also be interesting to learn whether one non-RsbRA paralog can dominate over another. For example, would cells containing both RsbRC and RsbRB respond more strongly (like RsbRC) or more weakly (like RsbRB) to H_2O_2?

Our initial analyses using hybrid fusion proteins lead us to conclude that the characteristically transient σ^B responses of RsbRA are the exception, not the rule, among the RsbR paralogs. In nearly every fusion combination we tested, we observed responses that more closely resembled a sustained (repeated in single cells) response than a transient, RsbRA-type response. From these data, it appears that both the N- and C-terminal halves of RsbRA are important for achieving a transient response. The fusion results also suggested that both halves of an RsbR protein influence the resulting response profile, with the variable (N-terminal) regions of RsbRA and RsbRC associated with stronger responses and the conserved (C-terminal) regions of RsbRA and RsbRD associated with a faster response onset. While it is a possibility that different cellular levels of the hybrid proteins affect the σ^B response profile, the observation that the σ^B reporter remains off in the absence of stress argues that the hybrid proteins are stable enough to form stressosomes and sequester RsbT in the absence of stressors. The next frontier in this line of inquiry is to identify key residues or regions within the N- or C-terminal halves of different paralogs that are responsible for their distinct σ^B profiles.

How do the distinct responses of RsbRB, RsbRC, and RsbRD contribute to the overall wild-type response, given how similar the RsbRA-only responses are to the wild type? One

possibility is that the other (non-RsbRA) paralogs make a minor contribution to the overall response; for instance, they may abet the wild-type response to acid stress, which was weaker in RsbRA-only cells than in the wild type but was relatively strong in RsbRB-, RsbRC-, and RsbRD-only cells. It is perhaps more likely that the different paralogs play more prominent roles in natural conditions, in contrast to the highly controlled conditions of the laboratory. We engineered strains to produce only single-RsbR paralogs to probe the response capabilities of each, and we thus far have considered individual stressors under exponential-phase growth conditions. In nature, stationary-phase or slow-growing cells likely encounter multiple stressors simultaneously, and perhaps under such conditions, each RsbR paralog has an important function in conditioning the σ^B response for optimal survival. A fuller understanding of the role of each RsbR paralog will require us to examine simultaneous and sequential stressor combinations and different growth phases. In any case, our results underscore the idea that the stressosome represents a flexible, robust stress-response system that can distinguish among stressors and produce many different response profiles.

1.6 Technical Issues

The microfluidic process is a very technical procedure and tabulated below are many of the various ways over the years I have found to completely ruin an experiment and subsequently your day. Please use caution in future experiments to ensure you avoid any of these potential pitfalls.

Failure to properly mix PDMS prior to pouring chip, results in an unevenly cured polymer
Failure to vacuum all bubbles out of PDMS after pouring and prior to curing
Failure to ensure all bubbles are popped in the PDMS, so one interferes with light path
Someone turning the oven too high, chip then cures and is brittle and cracks, leaking media
Someone turning oven too high and petri plate melts around the glass bonded chip, resulting in breakage of the glass chip, despite your best efforts to melt the plastic with a heated paper clip very carefully
Someone turning the oven too low, causing chip to not bond, and come apart when media is flowed through the channels

Failure to ensure all specks of dust are free of chip, resulting in a blockage during media flow
A small chunk of PDMS you cannot see inside the wells you punch coming loose, blocking media flow, and killing all your cells
Punching the chip and hitting the little border right next to the channels, resulting in media flowing around the chip, instead of to the cells
PDMS not punching though all the way because the biopsy punches become too dull
Contamination in the media at the syringes
Contamination in the lines of plumbing
Contamination in the Y-junction for media switching
Contamination of the chip even though your plasma cleaned the chip
After autoclaving all plumbing to ensure it is not contaminated, it is now soft and pliable, becoming loose and leaking media everywhere
Plumbing cracking after autoclaving, leaking media
BSA contamination, resulting in failure to passivate the chip and random bacterial contamination
Loss of focus on the microscope over the course of your multi-day experiment
PFS failure, resulting in loss of focus once again
Objective on microscope becoming stuck somehow, jumping and shattering your glass chip spilling media and small shards everywhere
Automated fluorescence filter failing to call the appropriate fluorescence cube only at some random times
Oil on objective drying up, ruining focus
Air bubble in the oil on the objective, scatters light and thus ruins your images
Random drift of your chip by microns, despite the chip being taped to the slide insert
Microsoft updates on windows computers in the middle of the night over your multi-day timelapse
Oklahoma State University disabling our ability to pause Microsoft updates, so it continues to update in the middle of the night during long time-lapses
NIS-elements crashing during timelapse
Not having enough storage to save your 100+ gb file at the end of the experiment
Syringe pump power failure due to a blackout
Syringe pump power failure due to its power cord being a little frayed and a light breeze nudged it loose for a second
Accidently bumping the withdrawal button on the syringe pump instead of the push because it is in a small room
Forgetting to turn off the non-stress syringe pump bank after switching over to the stressed media, resulting in a pressure buildup and eventual media spill when the plumbing blows from a pressure buildup
Someone turning on the lights in the scope room, and leaving on the lights during a fluorescence time-lapse
A large clump of cells building up and blocking flow for just bit, before being pushed out, causing a transient blockage in media flow.
Yet many more problems not listed here

Table 1.2 A list of the many ways I have experienced failure during microfluidic time-lapse fluorescence microscopy.

1.7 Acknowledgements

This research was supported by National Institutes of Health grant No. R35GM138018 (M.T.C.).

We thank members of the Cabeen lab and R. Burnap for helpful discussions.

C.W.H. and M.T.C. conceived the study, performed the experimental work, analyzed data, and wrote the paper. D.R.B. analyzed the data.

1.8 Figures and Data

All supplementary data for this work, as well as movies can be found and accessed on mBio where this work was published: https://journals.asm.org/doi/full/10.1128/mbio.02001-22

CHAPTER II

DIFFERENT σ^B RESPONSE PROFILES OF THE STRESS SENSING PARALOGS WITHIN THE STRESSOSOME OF BACILLUS SUBTILIS EFFECTS THE FITNESS OF CELLS TO VARIOUS ENVIRONMENTAL STRESSORS

Note: The following data and experiments was performed in collaboration with several undergraduate researchers in our lab, including Sydney Bush, Shelby Sanders, Jake Osborne, Nick Frey, Nick Boyne, Madeline Toews, and Sarah Winburn M.S.

2.1 Abstract

Bacillus subtilis uses large cytoplasmic protein complexes known as stressosomes to sense environmental stressors and trigger the general stress response through activation of σ^B. Recent work with microfluidic microscopy observing single cells showed that all four putative stress sensing paralogs within the stressosome (RsbRA, RsbRB, RsbRC and RsbRD) are each individually capable of modulating their response to environmental stressors effecting the timing and magnitude of σ^B activation. Wild-type cells (containing all four paralogs) and RsbRA have timing in their responses irrespective of the stressor used, differing only in magnitude. Here in this work, we wanted to test if the differences in response profile in individual cells conveyed any fitness advantage at the population level of cells exposed to stressors. We show that when cells containing stressosomes comprised of individual RsbR paralogs were subjected to 2% ethanol as a stress, no fitness advantage was seen. However, when 4% ethanol was used, we saw that RsbRA-only cells and wild-type cells were more fit than cells containing other single RsbR paralogs, and that RsbRD-only cells did not survive well in ethanol. In contrast to ethanol, when cells were subjected to 1M NaCl as a stressor, RsbRD-only cells now outcompeted all other strains, while

RsbRA-only and wild-type cells were less fit than all other individual paralogs. Even if more than one RsbR paralog was present in the stressosome such as a stressosome comprised of RsbRA and RsbRD, the presence of RsbRA was detrimental to fitness when subjected to salt stress. In fact, when a ΔRsbRA strain was constructed containing all other RsbR paralogs within the stressosome but lacking RsbRA, cells showed an advantage over wild-type when subjected to salt stress, while the wild-type survived better than ΔRsbRA strain when grown in the presence of ethanol. This, along with the previous findings of similar responses from RsbRA-only and wild-type cells suggests that the presence of RsbRA within the stressosome may be able to dominate and override the other RsbR paralog response profiles. These findings suggest that individual RsbR paralogs response timing and magnitude can affect the fitness of cells via activation of the general stress response.

2.2 Rationale

Bacillus subtilis has to respond to a variety of stressors in in the environment rapidly to survive, and cells respond quickly with the general response mediated by σ^B [51], [52]. Activation of σ^B aides in managing stressors such as heat, cold, ethanol shock, acid shock and salt shock, and results in a non-specific resistance to future stressors [5]–[10], [53], [54]. While it is known more than 200 plus genes are regulated by σ^B, the mechanism by which RsbR paralogs modulate the activation of σ^B remains unknown. Why *B. subtilis* encodes four RsbR paralogs has been an enduring mystery, and until recently they were thought to be largely redundant. Our work in the previous chapter shows that while the individual RsbR paralogs are able to alter both the timing and magnitude of σ^B mediated general stress response based on the environmental stressor present during exponential phase growth [16], [55]. For instance, RsbRA responds quickly and transiently to both ethanol and salt stressors, while RsbRC and RsbRD individual cells show repeated activation of σ^B. The wild-type cells exhibit similar σ^B activation as RsbRA to ethanol, acid, and salt shock, as well as hydrogen peroxide, suggesting the transient activation may be the most advantageous response, since this is the predominant response pattern exhibited by the stressosome. It remains unknown at present how the RsbR homologs may impact

σ^B responses in natural environments, as wild-type cells contain all four paralogs respond in a stereotypical way (with a rapid, transient σ^B response) under our laboratory conditions. As the principal difference among strains encoding different individual RsbR paralogs appears to be the σ^B response profile, we asked whether differences in σ^B response profile correspond with any functional consequences for the cell. As σ^B is part of a stress-response system, we reasoned that one important consequence might be the relative fitness—growth rate—of strains that are exposed to environmental stressors. Here, we compete wild-type and single-RsbR strains in pairwise co-cultures in the presence of environmental stressors that activate the GSR. We find that wild-type and single-RsbR strains exhibit hierarchies of fitness that are different in different stressors, such that the most fit strain in one stressor is the least fit in another. Our data collectively suggest that the fitness of each strain is impacted by the dynamics of its σ^B response profile.

2.3 Materials and Methods

2.3.1 Strains and growth conditions

The bacterial strains used in this study are listed in Table 2.1. *B. subtilis* strains were routinely grown in LB Lennox broth (10 g/liter tryptone, 5 g/liter yeast extract, 5 g/liter NaCl) or on Lennox agar plates fortified with 1.5% Bacto agar at 37°C. When appropriate, antibiotics (MLS: 0.5 μg/mL erythromycin and 2.5 μg/mL lincomycin; 100 μg/mL carbenicillin) were added to select for markers. Markerless replacement of *rsbR* genes with hybrid versions was performed using the pMiniMAD vector (a gift of Daniel Kearns) for allelic replacement. Details of strain construction are given in the Supplemental Information, Text S1.

2.3.2 Competition growth and stress experiments

Strains were grown overnight, and back diluted 1,000x in 3 mL of LB, and grown until in exponential phase growth for 2-3 hours. OD600 was monitored and strains were back diluted again to equal OD for approximately an approximately equal number of cells. Both strains for competition were inoculated into a 25 mL flask of LB and placed in a shaking

incubator at 37°C for 1 minute to allow cell cultures to mix before a sample was taken for plating, and stressor added. Samples were taken and diluted for plating (samples diluted in order to get a countable number of cells on a LB plate) every 3 hours for 9 hours total. Ethanol was added to its final concentration (2% or 4%) from a 100% ethanol stock to swirled cultures (to dissipate the concentrated stressor immediately). NaCl was added to cultures at a 1:1 ratio from a 2 M sterile NaCl stock in water. Samples (typically 100 µl) were taken and serially diluted for plating (on plain LB agar or LB agar with appropriate antibiotics) every 3 hours for 9 hours total. The OD_{600} was monitored, and cultures were diluted to ensure that cultures remained in exponential phase, defined here as $OD_{600} < 0.5$. Plates were grown overnight at 37°C and images were taken in appropriate fluorescence channels (RFP or GFP) and colonies were counted as described in Hamm, et al 2021 [56]. Typically, three plates were spread at each dilution for CFU counting at each time point to reduce any bias in plating. When multiple plates and/or serial dilutions yielded well-countable colonies for both strains, the colony numbers were averaged. Osmolyte five-minute stress testing was performed in a similar manor, with % surviving being calculated after brief exposure to osmolytes. Osmolytes used KCl, KH_2PO_4, sucrose, NaH_2PO_4, Na-citrate, with 0.5M, 1M, or 1.5M NaCl as stressor.

2.3.3 Strain construction

The markerless gene replacement in the strains below were added in succession using the pminiMAD vector (gift of Daniel Kearns) or pHyperspank. A vector propagated in E. coli and containing the desired gene was directly transformed into PY79 via competence {Wilson, 1968 #1148} and selected on MLS (0.5 µg/ml erythromycin and 2.5 µg/ml lincomycin) or chloramphenicol plates as needed. A phage SPP1 lysate was prepared from that intermediate strain, and the recipient strain was phage-transduced with the PY79 strain containing the desired chromosomally integrated pminiMAD vector and again selected on MLS or Chlor. Five to 10 transductants were then inoculated into liquid LB and kept in exponential phase at approximately 25°C for several hours to permit plasmid excision before being repeatedly diluted and grown in liquid LB at 37°C (restrictive for plasmid replication) to promote loss of excised plasmid in the case of pminiMAD. The cells were

then plated, and single colonies were screened for the successful replacement by colony PCR, restreaked for single colonies, patched on plain LB and LB/MLS plates to verify plasmid loss, restreaked, verified by PCR and stored at -80°C. Fluorescent markers were added in the same way as above but were selected on chloramphenicol antibiotic plates and screened for gain of fluorescence with the integrative pHyperspank. Detailed strain construction and is listed in supplemental text S2.

2.3.4 Microfluidic microscopy and data curation

Was performed as describes in chapter 1 [55]. All plumbing was designed and set up according to [55], with the media being used for microfluidics as LB and LB + 2% ethanol or LBK and LBK + 500 mM NaCl. Media switching was performed as indicated above [55].

2.3.5 Automated imaging

Imaging was performed with a Nikon Eclipse Ti inverted microscope equipped with a Photometrics Prime 95B sCMOS camera, a 100× Plan Apo oil objective (NA 1.45, Nikon), an automated stage (Nikon), a Lumencor SOLA SE II 365 Light Engine fluorescent illumination system, and an OKO temperature-controlled enclosure in which the temperature was maintained at approximately 37°C during imaging. Image acquisition was performed using NIS-Elements AR 5.11.03 64-bit. mNeonGreen (used for σ^B reporters) was imaged at approximately 33% illumination power with 200-ms exposures, and phase contrast was used for cell visualization. The images were captured at 10-min intervals. Cell lineages were manually curated, tracked, and plotted as in our previous work [55].

Strain or plasmid	Relevant genotype or description	Source or reference
CSS 408	3610 Δ*ytvA amyE*::pHyperspank-mKate2 (Cm^R)	This study

CSS 409	3610 Δ*ytvA* Δ*rsbRB* Δ*rsbRC* Δ*rsbRD amyE*::pHyperspank-mKate2 (Cm^R)	This study
CSS 410	3610 Δ*ytvA* Δ*rsbRA* Δ*rsbRC* Δ*rsbRD amyE*::pHyperspank-mKate2 (Cm^R)	This study
CSS 411	3610 Δ*ytvA* Δ*rsbRA* Δ*rsbRB* Δ*rsbRD amyE*::pHyperspank-mKate2 (Cm^R)	This study
CSS 412	3610 Δ*ytvA* Δ*rsbRA* Δ*rsbRB* Δ*rsbRC amyE*::pHyperspank-mKate2 (Cm^R)	This study
CSS 414	3610 Δ*ytvA amyE*::pHyperspank-GFP (Cm^R)	This study
CSS 415	3610 Δ*ytvA* Δ*rsbRB* Δ*rsbRC* Δ*rsbRD amyE*::pHyperspank-GFP (Cm^R)	This study
CSS 416	3610 Δ*ytvA* Δ*rsbRA* Δ*rsbRC* Δ*rsbRD amyE*::pHyperspank-GFP (Cm^R)	This study
CSS 417	3610 Δ*ytvA* Δ*rsbRA* Δ*rsbRB* Δ*rsbRD amyE*::pHyperspank-GFP (Cm^R)	This study
CSS 418	3610 Δ*ytvA* Δ*rsbRA* Δ*rsbRB* Δ*rsbRC amyE*::pHyperspank-GFP (Cm^R)	This study
MTC 1973	3610 hag_{A223V} Δ*ytvA* Δ*rsbRA amyE*::*DG364-*$P_{hyperspank}$*-mNeptune* (Cm^R) *ywrK*::*DG1730-*P_{rsbV}*-mNeonGreen* (Spc^R); Stressosome containing all RsbR paralogs except RsbRA	This study
MTC 2540	3610 *hagA223V ΔytvA ΔrsbRB ΔrsbRC ΔrsbRD rsbRA::rsbRC/A amyE::DG364-*$P_{hyperspank}$*-mNeptune (CmR) ywrK::DG1730-*P_{rsbV}*-mNeonGreen* (SpcR); RsbRC/A hybrid as only source of RsbR within the cell	[55]
MTC 2541	3610 *hagA223V ΔytvA ΔrsbRA ΔrsbRB ΔrsbRD rsbRA::rsbRA/C amyE::DG364-*$P_{hyperspank}$*-mNeptune (CmR) ywrK::DG1730-*P_{rsbV}*-mNeonGreen* (SpcR); RsbRC/A hybrid as only source of RsbR within the cell	[55]
MTC 2542	3610 *hagA223V ΔytvA ΔrsbRA ΔrsbRC ΔrsbRD rsbRA::rsbRC/B amyE::DG364-*$P_{hyperspank}$*-mNeptune (CmR) ywrK::DG1730-*P_{rsbV}*-mNeonGreen* (SpcR); RsbRC/A hybrid as only source of RsbR within the cell	[55]
MTC 2543	3610 *hagA223V ΔytvA ΔrsbRA ΔrsbRB ΔrsbRD rsbRA::rsbRB/C amyE::DG364-*$P_{hyperspank}$*-mNeptune (CmR) ywrK::DG1730-*P_{rsbV}*-mNeonGreen* (SpcR); RsbRC/A hybrid as only source of RsbR within the cell	[55]
MTC 2544	3610 *hagA223V ΔytvA ΔrsbRB ΔrsbRC ΔrsbRD rsbRA::rsbRD/A amyE::DG364-*$P_{hyperspank}$*-mNeptune (CmR) ywrK::DG1730-*P_{rsbV}*-mNeonGreen* (SpcR); RsbRC/A hybrid as only source of RsbR within the cell	[55]
MTC 2545	3610 *hagA223V ΔytvA ΔrsbRA ΔrsbRB ΔrsbRC rsbRA::rsbRA/D amyE::DG364-*$P_{hyperspank}$*-mNeptune (CmR) ywrK::DG1730-*P_{rsbV}*-mNeonGreen* (SpcR); RsbRC/A hybrid as only source of RsbR within the cell	[55]
MTC 2546	3610 *hagA223V ΔytvA ΔrsbRB ΔrsbRC ΔrsbRD rsbRA::rsbRB/A amyE::DG364-*$P_{hyperspank}$*-mNeptune (CmR) ywrK::DG1730-*P_{rsbV}*-*	[55]

	mNeonGreen (SpcR); RsbRC/A hybrid as only source of RsbR within the cell	
MTC 2547	3610 *hagA223V ΔytvA ΔrsbRA ΔrsbRC ΔrsbRD rsbRA::rsbRA/B amyE::DG364-P$_{hyperspank}$-mNeptune (CmR) ywrK::DG1730-P$_{rsbV}$-mNeonGreen* (SpcR); RsbRC/A hybrid as only source of RsbR within the cell	[55]

Table 2.1 A list of strains used in this study.

2.4 Results

2.4.1 A differential fluorescence assay to measure competitive advantage

Given that strains containing single RsbR proteins showed different response profiles to an identical stressor [16], we asked whether strains containing different single RsbR paralogs might show different fitness when challenged with particular environmental stressors. To determine relative fitness, we used competitive co-cultures of strain pairs growing in stressor-containing media. In each co-culture, we aimed to inoculate equal numbers of each strain into a stressor-containing medium, taking periodic samples to monitor the relative strain populations over a period of nine hours. To circumvent any changes in fitness due to cells entering stationary phase, we maintained the co-cultures in exponential phase (defined here as $OD_{600} < 0.5$) via dilution with fresh (stressor-containing) medium. To distinguish the co-cultured strains from one another, we labeled each strain with cytoplasmic green or red fluorescent protein under the control of a constitutive promoter. Dilutions of the co-culture were spread on solid media, and the number of colony-forming units (CFU) with each fluorescent color were enumerated in photographs taken under fluorescence illumination (Figure 2.1) [56]. We elected to use a CFU-based method rather than other potential methods, such as relative DNA abundance, flow cytometry, or fluorescence microscopy, because of the stringency of CFU counts, which exclusively consider living cells of each strain.

2.4.2 Single-RsbR strains display no inherent fitness advantage against one another

The standard model for σ^B activation implies that under non-stress conditions, σ^B is inactive, making it unlikely that the cellular complement of RsbR proteins would impact

fitness in the absence of a stressor. To test this hypothesis, we co-cultured single-RsbR strains in exponential phase, in the absence of stress, for 9 hours, sampling the co-culture for relative population analysis every 3 hours. In the absence of stress, and after 9 h of co-culture, no single-RsbR strain moved more than 2% in either direction from the initial population fractions (Fig 2.2), implying that the single-RsbR strains we used do not have any inherent fitness advantage or disadvantage over one another, regardless of fluorophore used. Importantly, these data also provide a reasonable estimate of the error in our experimental setup. As no strain pair was outside a 48:52 to 52:48 boundary after 9 hours of stress-free co-culture, we subsequently considered only shifts outside this margin as constituting a competitive advantage under stress conditions.

2.4.3 Competition in 2% ethanol reveals no salient fitness differences

Because we had previously detected different σ^B activation kinetics in different single-RsbR strains challenged with 2% ethanol, we first co-cultured strain pairs in LB medium containing 2% ethanol. We plated cells just before stressor addition and then maintained the co-cultures in exponential phase under stress conditions for 9 h before again plating to assess the relative fraction of each strain. Under these conditions, the majority of the co-cultures showed a minimal shift in their relative populations, with only a few experiments resulting in any substantial change (Figure 2.3). For example, we observed a single trial in which RsbRB-only cells outcompeted RsbRA-only cells (Figure 2.3), but in many strain pairs the results were both modest and of mixed direction and/or strength (e.g., Figure 2.3, WT vs RsbRB-only). We interpret these results as indicating that the 2% ethanol stressor was insufficiently stressful to uncover any substantial fitness differences over the 9-h experimental interval.

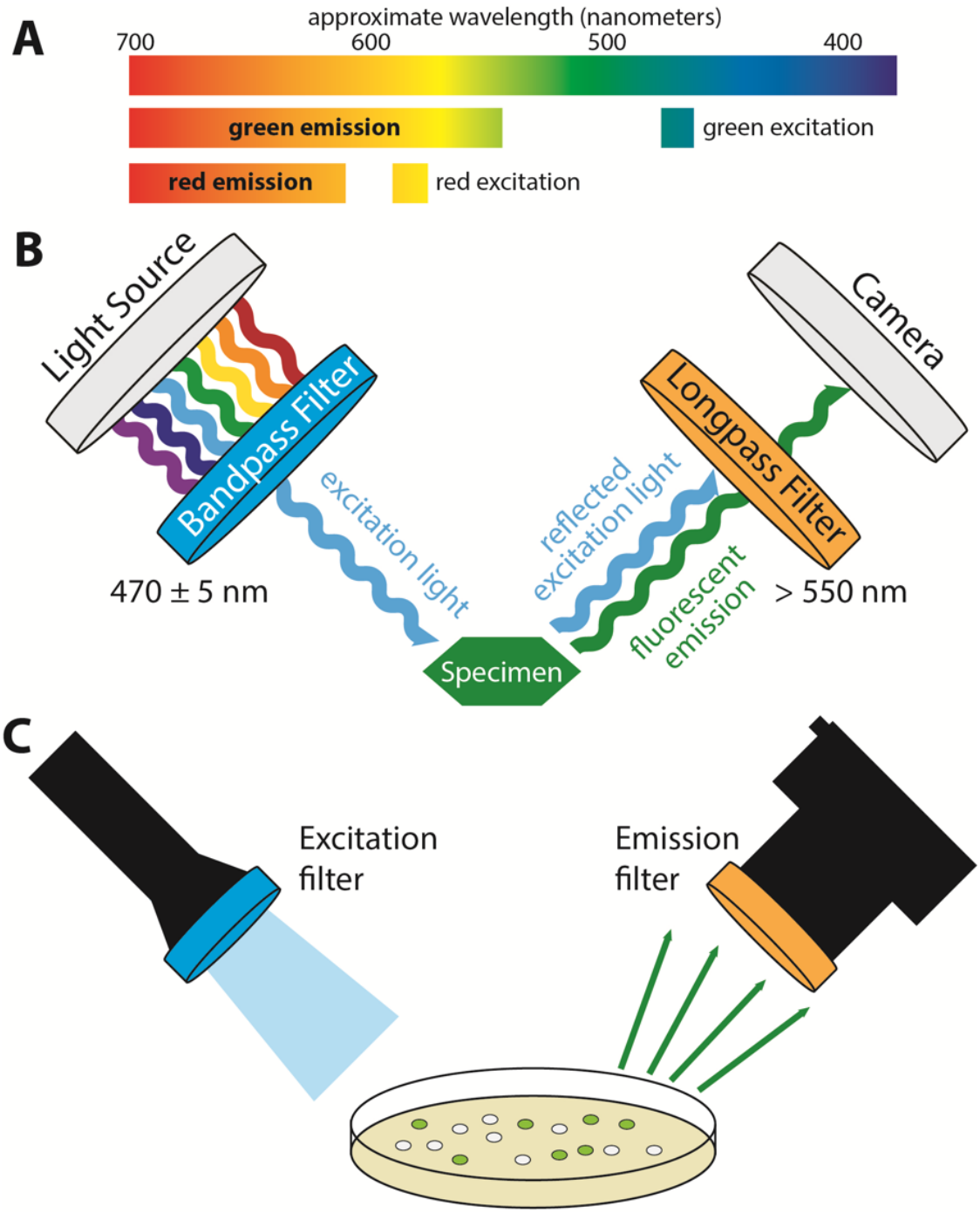

Figure 2.1 Schematic of fluorescence illuminator and principle of operation. **A)** Visible-light spectrum showing excitation and emission regions using the green- and red-fluorescence filter sets described here. **B)** Illustration of fluorescence illumination principles and the use of bandpass and longpass filters to obtain specific wavelengths of light, thereby allowing stimulation of fluorescence emission and subsequent imaging. **C)** Schematic of an LED flashlight equipped with a bandpass filter, allowing excitation of green fluorescent protein-expressing bacterial colonies. The emitted fluorescence is detected by placing a longpass filter (>550 nm) over a digital camera, allowing the specific detection of fluorescent colonies. [56]

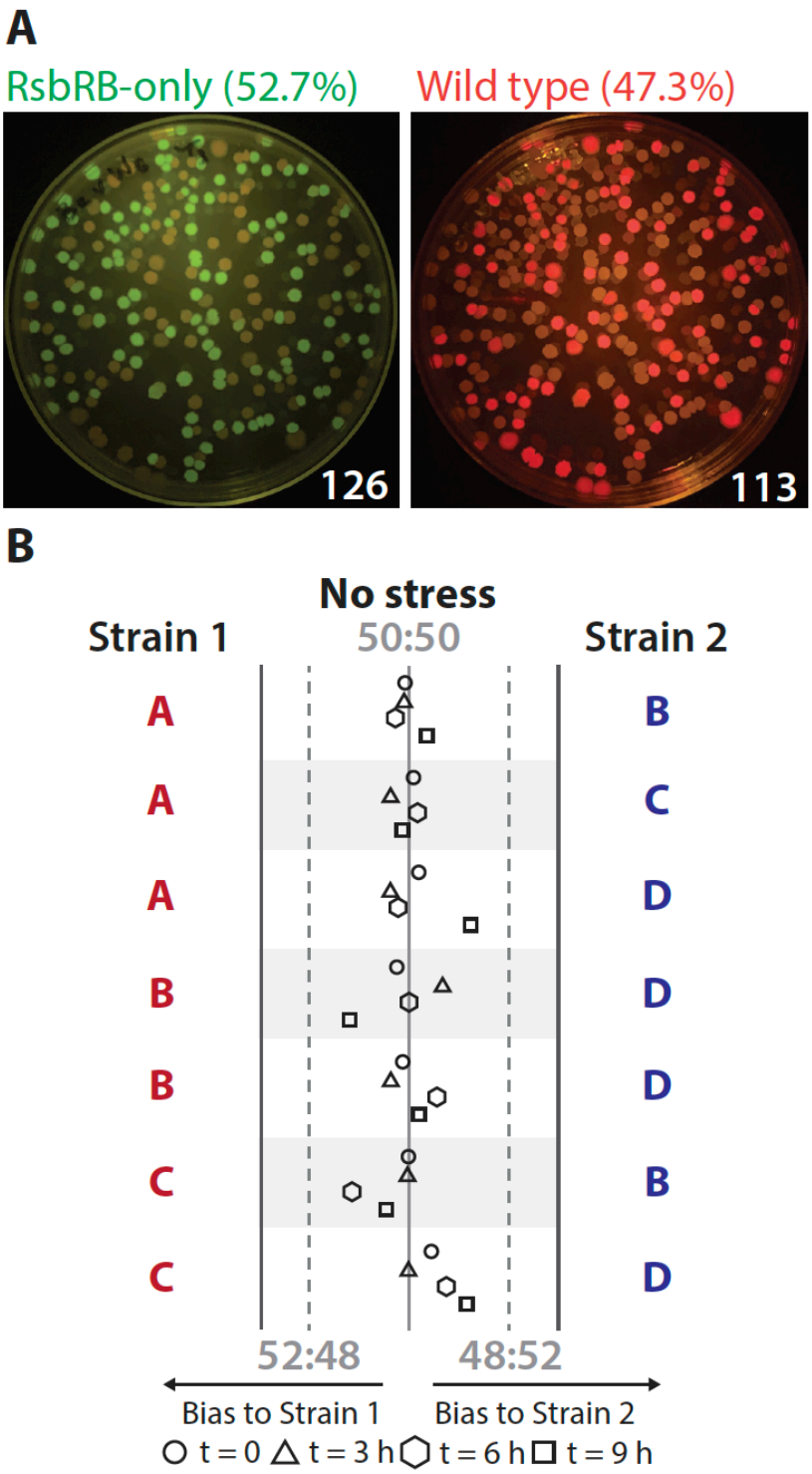

Figure 2.2 A) Representative plate image of RsbRB only cells (GFP) grown together in a flask with wild-type cells (RFP) under no stress. **B)** Comparative colony plate counts between 2 different strains under non-stressed conditions. Strain 1 on the left or strain 2 on the right. The circle represents time point 0, triangle is 3 hours, hexagon is 6 hours, and square denoting 9 hours. We see that when grown together within a flask and no stressor present, single RsbR strains do not manifest a distinct advantage over one another. The dotted line indicates a 2% margin from 50/50. Direction from the median line denotes a movement away from 50/50 growth and indicates a specific strain winning.

2.4.4 Competition in 4% ethanol reveals a fitness hierarchy led by RsbRA-only cells and trailed by RsbRD-only cells

We next asked whether doubling the concentration of ethanol stressor would uncover fitness differences among single-RsbR strains that were not apparent in 2% in ethanol. In 4% ethanol, we began to see a clearer fitness hierarchy among the test strains. The RsbRA-only strain generally outcompeted every co-cultured strain except the wild-type (Figure 2.4). In contrast, the RsbRD-only strain generally lost against every other competitor (Figure 2.4), placing it at the bottom of the fitness hierarchy. Cells containing only RsbRB or RsbRC were in the middle of the hierarchy, generally losing to RsbRA-only cells and winning against RsbRD-only cells (Figure 2.4). Moreover, RsbRB-only, and RsbRC-only cells showed no clear trend when co-cultured together (Figure 2.3), indicating a roughly equal fitness of these two strains. At the top of the fitness hierarchy, RsbRA-only cells and wild-type cells showed similar fitness, with mixed competition results (Figure 2.3). As σ^B activation kinetics are presumably the primary difference between cells containing different RsbR paralogs, it is possible that the σ^B response pattern of a given strain influences its fitness in a given stressful condition. Consistent with this idea, the strain pairs that showed roughly equal fitness (RsbRA-only/wild-type and RsbRB/RsbRC) show similar σ^B activation kinetics in ethanol [16], [56].

2.4.5 Competition in 1 M NaCl shows a different hierarchy led by RsbRD-only cells and trailed by wild-type cells

Our observation of a fitness hierarchy among different single-RsbR strains in 4% ethanol prompted us to ask whether the same hierarchy would manifest in a different environmental stressor. We therefore competed the same strain pairs but used 1 M NaCl, which is also well-known to induce σ^B in *B. subtilis*. In NaCl, the fitness differences were typically more dramatic than in ethanol, with greater population shifts (Figure 2.5). Strikingly, the hierarchy that emerged in NaCl was nearly opposite what we had observed in ethanol. The RsbRD-only strain, which was invariably outcompeted in ethanol, was strongly dominant in NaCl, winning every competition (Figure 2.5). The RsbRA-only strain, in contrast, was

outcompeted by every other single-RsbR strain and won only against wild-type cells, which lost every competition (Figure 2.5). The RsbRB-only and RsbRC-only strains were again in the middle of the hierarchy, with RsbRB dominant over RsbRC (Figure 2.5). These data suggest not only that the RsbR paralog(s) present in a strain influences its fitness under environmental stress, but also that a given genotype may be beneficial or detrimental depending on the stressor encountered.

2.4.6 Strains bearing hybrid RsbR proteins show an advantage for an RsbRA/B hybrid but a disadvantage for an RsbRD/A hybrid

We took advantage of the clear fitness differences of single-RsbR strains in 1 M NaCl to examine how strains bearing single, hybrid RsbR proteins would compare to wild-type or single-RsbR strains. We constructed the hybrid strains by creating gene fusions that would couple the N-terminal half (globin domain) of one RsbR paralog to the C-terminal half (STAS domain) of another. Each hybrid gene was expressed as the only source of RsbR protein in the cell via allelic replacement at the locus of the C-terminal half (e.g., the *rsbRA/B* fusion was expressed from the native promoter at the *rsbRB* locus). We built four different fusions and then competed each with the wild-type and each single-RsbR strain in 1 M NaCl. Interestingly, the RsbRA/B hybrid strain outcompeted all the other strains, even the RsbRD-only strain (Figure 2.6). In contrast, the RsbRD/A hybrid strain was at the bottom of the hierarchy after being outcompeted by every other strain (Figure 2.6), despite having the N-terminal half of RsbRD. An RsbRB/C hybrid, consistent with its constituent parts deriving from strains with intermediate fitness, was in the middle of the hierarchy, losing to RsbRB- and RsbRD-only strains abut outcompeting wild-type, RsbRA-only, and RsbRC-only strains (Figure 2.6). These results further illustrate the influence of RsbR protein identity and sequence on cell fitness under stress conditions. For example, replacing the C-terminal half of RsbRD with the analogous sequence from RsbRA severely affected fitness in 1 M NaCl, causing cells to drop from the top of the fitness hierarchy to its bottom. This particular result suggests that the C-terminal portion of RsbRD is important for its enhanced fitness in 1 M NaCl. Our hybrid results also show that fitness, at least in 1 M NaCl, is not fully optimized with the native protein sequences, as the RsbRA/B hybrid outcompeted all the native single-RsbR strains and the wild-type.

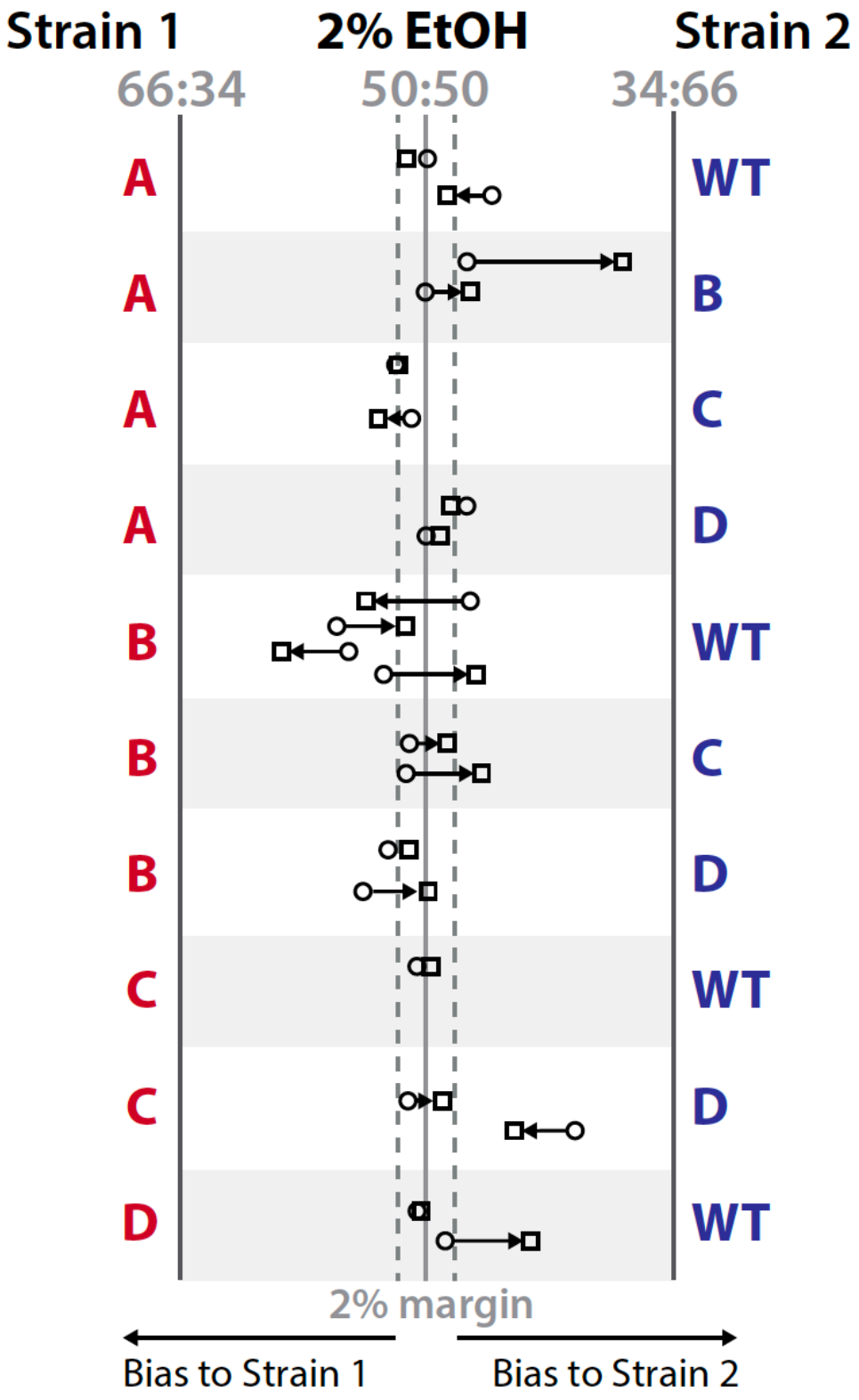

Figure 2.3 Comparative colony plate counts between 2 different strains in a flask containing 2% EtOH, strain 1 on the left or strain 2 on the right. The circle represents time point 0, and square denoting 9 hours. The dotted line indicates a 2% margin from 50/50. Direction from the median line denotes a movement away from 50/50 growth and indicates a specific strain winning.

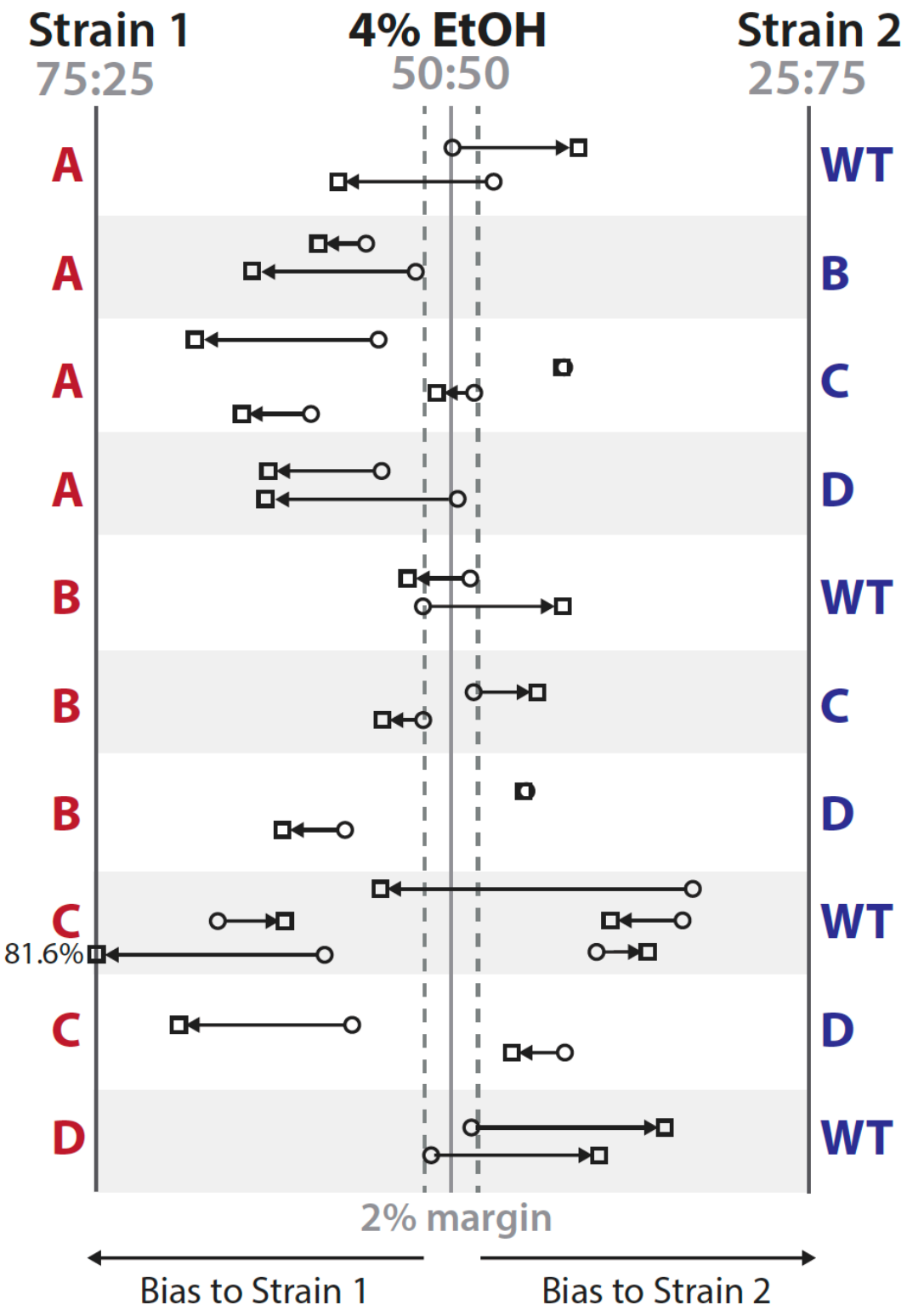

Figure 2.4 Comparative colony plate counts between 2 different strains in a flask containing 4% EtOH, strain 1 on the left or strain 2 on the right. The circle represents time point 0, and square denoting 9 hours. The dotted line indicates a 2% margin from 50/50. Direction from the median line denotes a movement away from 50/50 growth and indicates a specific strain winning.

2.4.7 The presence of RsbRA is detrimental to fitness in 1 M NaCl but is advantageous in 4% ethanol

The competitions between single-RsbR strains in 1 M NaCl showed a clear fitness deficit for strains with RsbRA as the only source of RsbR in the cell, suggesting that an RsbRA-type σ^B response profile is a detriment in NaCl stress conditions [16], [55]. Consistent with this notion, wild-type cells, which have a response profile very similar to RsbRA-only cells [16], [56], were also outcompeted by every single-RsbR strain (Figure 2.5). The similarity between RsbRA-only and wild-type cells with respect to their σ^B response profiles led us to a speculative model in which RsbRA dominates the overall response, even when (as in the wild type) other RsbR paralogs are present [16]. One prediction of this model is that deleting *rsbRA* from a wild-type strain would abrogate its transient σ^B response profile, converting it to a sustained-type response. Because the wild-type (and RsbRA-only) strains were the least fit under 1 M NaCl treatment (Figure 2.5), we hypothesized that deletion of *rsbRA* from a wild-type strain would increase its fitness in NaCl. Conversely, because wild-type cells were at the top of the fitness hierarchy in 4% ethanol, we reasoned that *rsbRA* deletion might compromise fitness under ethanol stress.

We first tested our prediction about how *rsbRA* deletion would impact σ^B profiles. We deleted *rsbRA* from a wild-type strain containing a σ^B-responsive mNeonGreen transcriptional reporter and then monitored the σ^B activity of cells before and after stressor addition in a microfluidic device, as in our previous work [56]. We compared the σ^B profiles of the Δ*rsbRA* strain exposed to 2% ethanol or 500 mM NaCl to data we previously obtained [56] for wild-type cells under the same stressor conditions. We used these concentrations, which are half the concentrations used for the competition experiments, for consistency with our previous data from microfluidics experiments [55]. As we predicted, deletion of *rsbRA* impacted the σ^B response profile, eliminating the sharp response peak of the wild-type strain and replacing it with a much broader peak in ethanol or a sustained response in NaCl. Having established that the σ^B response profile is altered by deletion of *rsbRA*, we then tested our hypotheses that loss of RsbRA would abet fitness in NaCl but hamper fitness in ethanol. We competed the Δ*rsbRA* strain against the wild type in either

4% ethanol or 1 M NaCl, also co-culturing them in the absence of stress to establish that neither strain had an inherent advantage. In the absence of stress, neither strain had an advantage (Figure 2.8), whereas in 4% ethanol the wild type outcompeted the Δ*rsbRA* strain in every trial (Figure 2.8), consistent with RsbRA having a positive effect on fitness in ethanol. In contrast, in 1 M NaCl, the Δ*rsbRA* strain generally outcompeted the wild type in 2 of 3 trials (Figure 2.8), in accord with RsbRA having a negative effect on fitness in NaCl. Collectively, these experiments suggest that a transient, wild type-like response is associated with enhanced fitness in ethanol but poorer fitness in NaCl, whereas a sustained response is associated with enhanced fitness in NaCl but poorer fitness in ethanol.

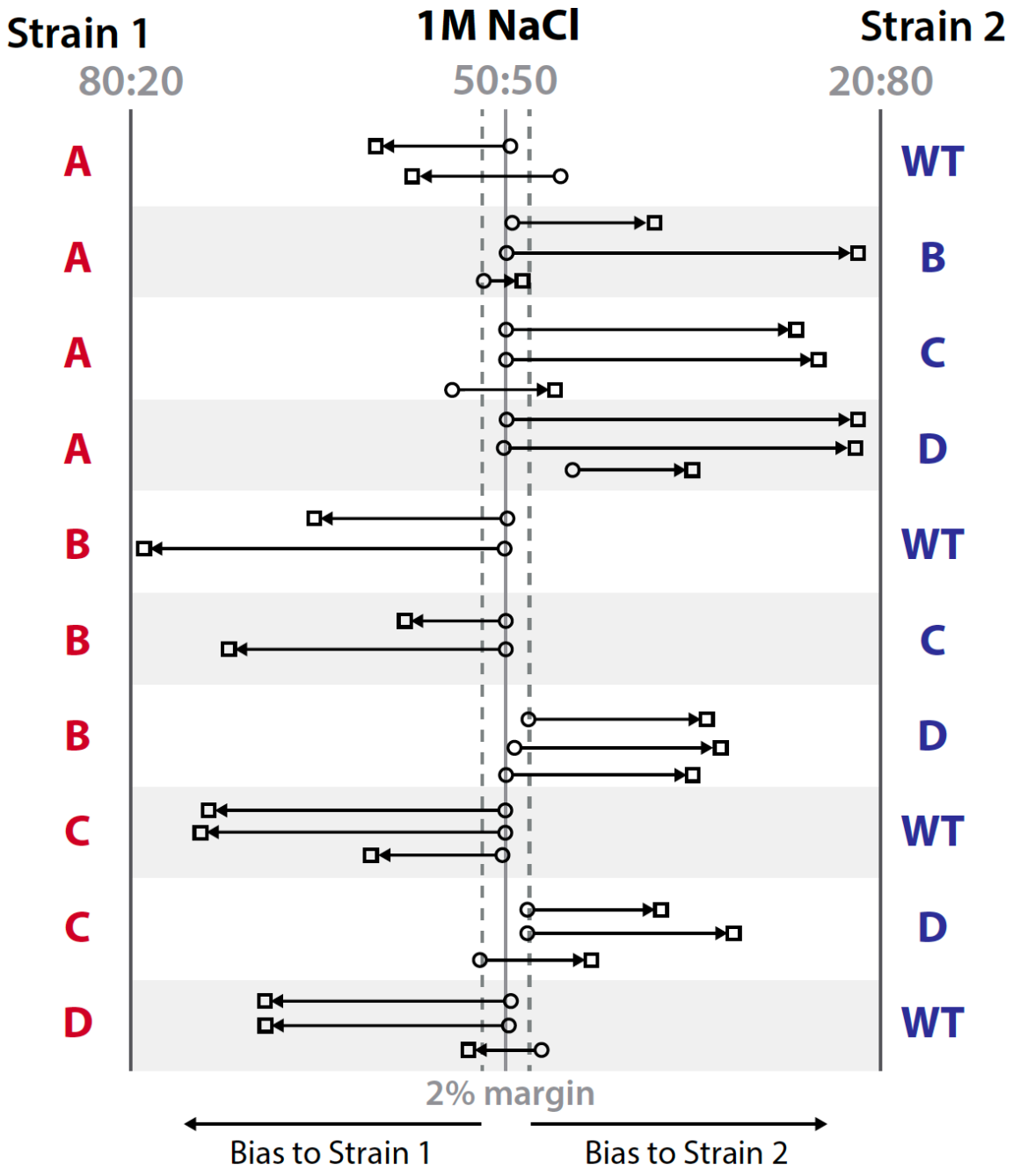

Figure 2.5 Comparative colony plate counts between 2 different strains in a flask containing 1M NaCl, strain 1 on the left or strain 2 on the right. The circle represents time point 0, and square denoting 9 hours. The dotted line indicates a 2% margin from 50/50. Direction from the median line denotes a movement away from 50/50 growth and indicates a specific strain winning.

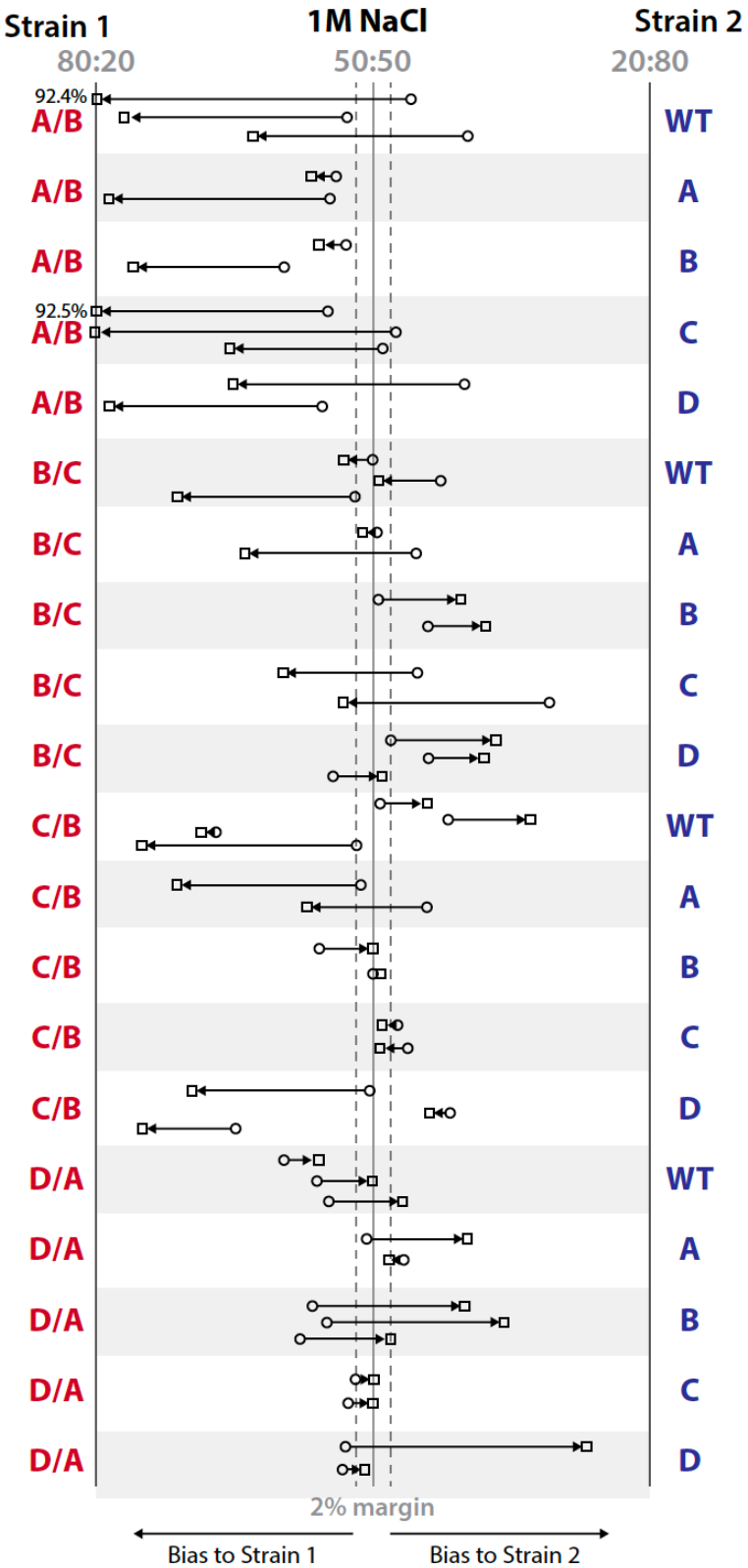

Figure 2.6 Comparative colony plate counts between 2 different strains (hybrid strains and single RsbR strains) in a flask containing 1M NaCl, strain 1 on the left or strain 2 on the right. The circle represents time point 0, and square denoting 9 hours. The dotted line indicates a 2% margin from 50/50. Direction from the median line denotes a movement away from 50/50 growth and indicates a specific strain winning.

2.4.8 Wild-type *B. subtilis* cells show a fitness advantage over cells lacking *rsbRA* within the stressosome when subjected to ethanol stress

We know from previous research that the canonical activation of the general stress response mediated by σ^B involves the quick-on, quick-off, synchronous and transient activation of gene expression (Figure 2.7) [55]. Here, we see that in a strain with RsbRA deleted, but all the other RsbR paralogs present within the stressosome, responds to 2% ethanol with a slower and longer, yet still synchronous initial activation of σ^B compared to the wild type (Figure 2.7A and 2.7C) [55]. *ΔrsbRA* strain did still show a very low level of repeated response as well, although nowhere near the magnitude seen in other repeated responses from single RsbR strains (Figure 2.7A) [55]. Wild-type cells also show a fitness advantage over strains deleted for *rsbRA*, with wild-type cells surviving significantly better when co-cultured with *ΔrsbRA* in the presence of 4% EtOH (Figure 2.8). These findings are consistent with our previous findings showing RsbRA-only strains and wild-type outcompeting all other RsbR paralogs in ethanol, suggesting that RsbRA conveys a fitness advantage in ethanol.

2.4.9 Strains lacking RsbRA outcompete the wild type in the presence of salt stress

In contrast to 4% ethanol, *ΔrsbRA* cells showed a stochastic and sustained response of individual cells, with a repeated response over time and subsequent activation of σ^B to 500 mM NaCl stress (Figure 2.7B). Previous research has shown a repeated activation of σ^B in salt-stress with any individual RsbR paralog other than RsbRA, with the wild-type or RsbRA showing a transient response, suggesting that the presence of *rsbRA* itself is capable of shutting down a repeated response and driving a synchronous and transient response (Figure 2.7B and C) [55]. When *ΔrsbRA* is grown in competition with the wild-type cells, we see that the *ΔrsbRA* strain has a modest advantage over the wild-type in 1M NaCl, supporting our earlier data that the presence of *rsbRA* is disadvantageous in salt stress (Figures 2.5, and 2.8). Taken together, our findings suggest that individual RsbR paralogs can affect the survival of cells through modulation of σ^B activity.

2.4.10 Challenging *B. subtilis* with NaCl results in substantial cell death

During our competition culture experiments, we noticed while enumerating CFUs that there were substantially fewer CFU/ml in cultures challenged with 1 M NaCl than in cultures challenged with ethanol. Further testing indicated that this "death effect" occurred within minutes of NaCl addition. Curious about this observation, we more formally assessed CFU before and after challenge for 5 min with different concentrations of ionic and non-ionic solutes. We observed that short exposures of *B. subtilis* cultures to different osmolytes caused noticeable reductions in cell viability that depended on the concentration of the osmolyte, with higher concentrations causing more severe reductions (Figure 2.10). The death effect appeared to be a general result of hyperosmotic conditions and not due to any specific component, as the effect was similar in sodium and potassium salts with different counterions and in sucrose, a non-ionic osmolyte (Figure 2.9). We attribute at least some of the observed sensitivity of *B. subtilis* to hyperosmotic shock to our culture conditions, as the initial (pre-stress) culture medium is a formulation of LB lacking NaCl and buffered with a relatively low concentration of potassium phosphate.

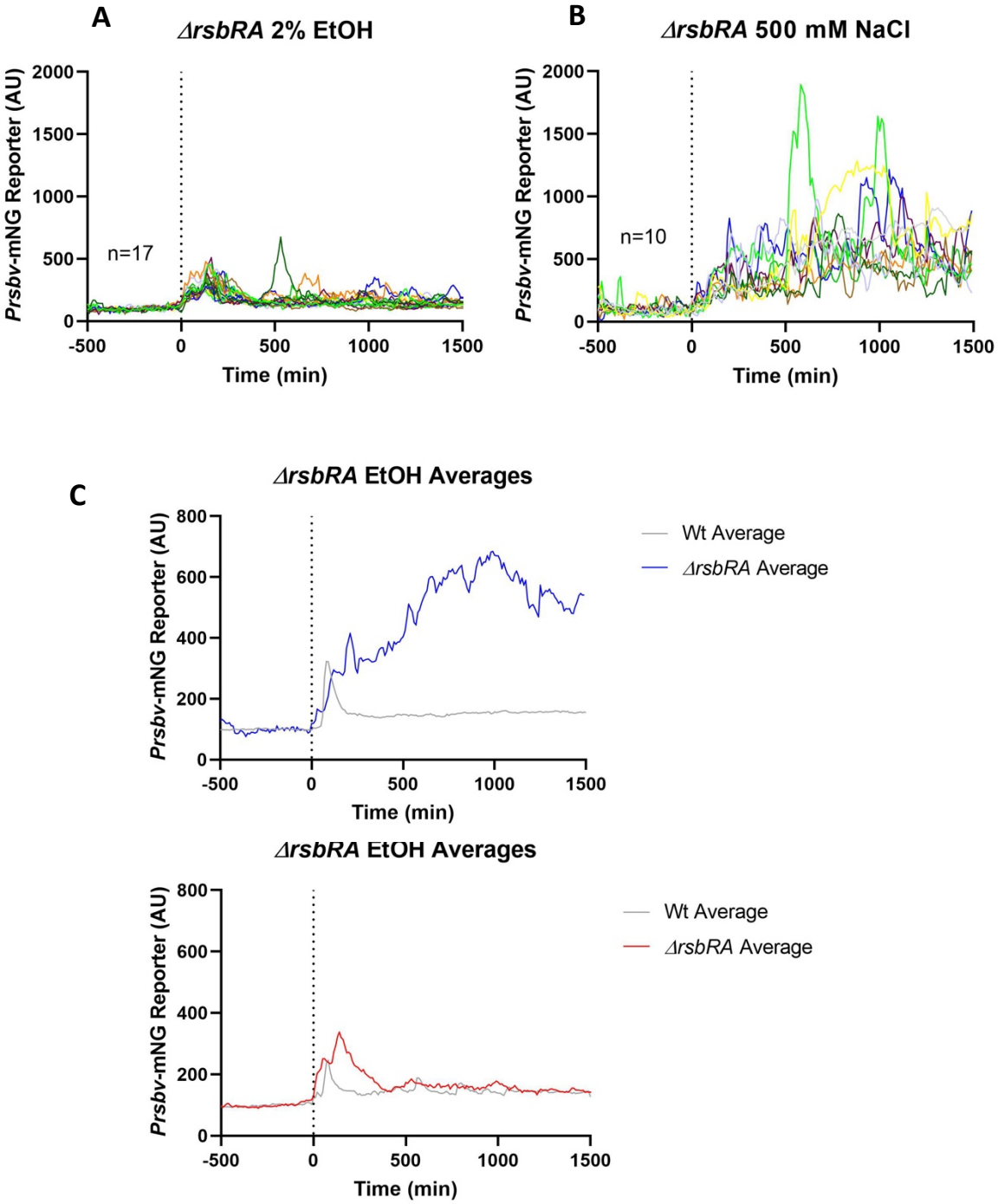

Figure 2.7 Lineage tracking of a *ΔrsbRA* strain exposed to 2% ethanol and 500 mM NaCl imaged via microfluidic fluorescence coupled microscopy. **A)** Individual-lineage intensity traces of a stress-responsive PrsbV-mNeonGreen reporter in an ΔRsbRA strain (MTC1973) before and after the addition (indicated by vertical dotted line) of 2% EtOH. **B)** Individual-lineage intensity traces of a stress-responsive PrsbV-mNeonGreen reporter in an ΔRsbRA strain (MTC1973) before and after the addition (indicated by vertical dotted line) of 500mM NaCl. **C)** Average intensity of the PrsbV-mNeonGreen reporter corresponding to the single-cell traces from panel A and B compared to average traces of the wild-type cells from Hamm et al. 2022 [55]**.**

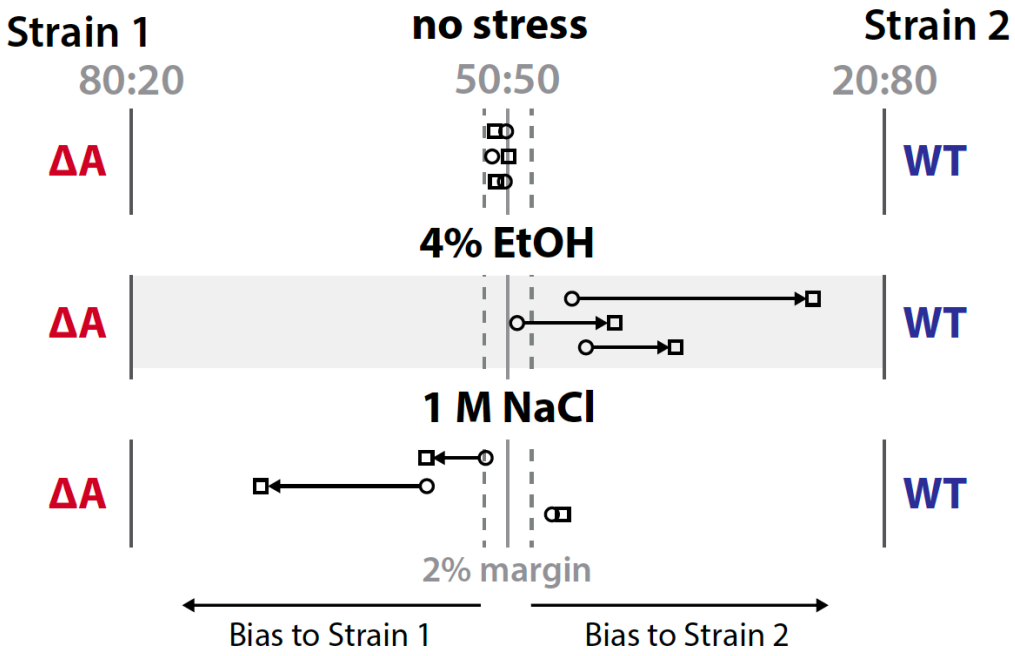

Figure 2.8 Comparative colony plate counts between 2 different strains (wild-type or a △*rsbRA* strain) in a flask containing no stress, 4% EtOH, or 1M NaCl. The circle represents time point 0, and square denoting 9 hours. The dotted line indicates a 2% margin from 50/50. Direction from the median line denotes a movement away from 50/50 growth and indicates a specific strain winning.

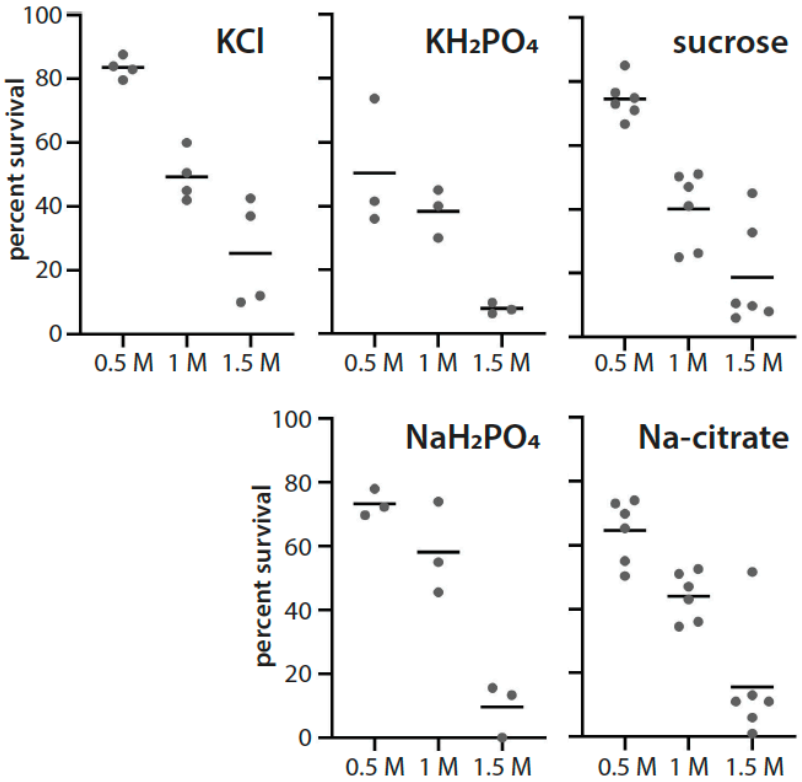

Figure 2.9 Testing survival of *Bacillus subtillis* cells after a 5-minute challenge with different osmolytes. Percent survival was calculated based on plating prior to and after 5-minute exposure to the indicated osmolyte.

Discussion 2.5

Manipulation of the complement of proteins present in the stressosome can clearly impact the dynamics—the magnitude and duration—of the *B. subtilis* σ^B response. Our results here provide evidence that different σ^B response dynamics not only affect cell fitness, but also that the benefit or detriment of a given response pattern varies depending on stressor. We found that the characteristic wild-type σ^B response, characterized by its transience, appears to benefit cells under ethanol stress but represents a disadvantage under NaCl stress. Conversely, a sustained (i.e., repeated in single cells) response confers an advantage in NaCl stress but a disadvantage under ethanol stress. Our experiments competing different hybrid RsbR-bearing strains and competing wild-type and Δ*rsbRA* strains suggest that it is the σ^B response profile, and not necessarily the exact identity of RsbR proteins in the stressosome, that is responsible for the relative fitness of a strain under environmental stress.

One implication of this finding is that the optimally fit σ^B response to one stressor may be different from the optimal response to a different stressor. Under our laboratory conditions, wild-type cells do not appear to change their σ^B profiles in response to different stressors [55]. Hence, one outstanding question is whether *B. subtilis* cells in natural environments do modulate their σ^B responses to optimize fitness under particular conditions. Another important question for the future is how a particular σ^B response profile impacts fitness when cells face simultaneous stresses. How would RsbRA-only and RsbRD-only cells compare if exposed to both ethanol and NaCl stress?

Another interesting and non-exclusive possibility raised by our work is that wild-type cells may not be optimized for all stressors. In fact, wild-type cells were the least fit of all the tested strains in NaCl stress under our experimental conditions. Perhaps cells are forced into a trade-off, such that wild-type cells trade maximal fitness under certain stress conditions in favor of increased fitness across a broad range of stressors. That a trade-off exists is at least supported by our data showing that a strain with the greatest fitness under

one condition (RsbRD-only cells in NaCl, for example) was the least fit under another condition (in ethanol).

We return to the question of why *B. subtilis* encodes four RsbR paralogs. At first glance, our results appear to support the idea that they are, in wild-type cells at least, largely redundant, as wild-type cells respond in a stereotyped way to multiple stressors [55]. However, our genetic manipulations that force cells to use just one paralog highlight the flexibility and breadth of responses that are possible using the stressosome-based GSR pathway of this organism. It is thus tempting to speculate that the different responses, and fitness, that we observe in genetically manipulated, laboratory-grown, exponential-phase cells in rich medium reflect flexibility that exists in nature but that is difficult to detect in the laboratory. For example, in slow-growing or stationary-phase cells exposed to environmental stressors, perhaps differential stability of different RsbR proteins becomes a factor. Alternatively, stressosome composition might be altered on long timescales in cells that become adapted to different stressors.

Acknowledgments 2.6

Sidney Bush, Christopher Hamm, and Matthew Cabeen conceived the study, performed the experimental work, analyzed data, and wrote the paper. Sarah Winburn, Nick Frey, Shelby Sanders, Madeline Toews, Nick Boyne, and Jake Osborne all performed experimental work and analyzed data as well.

Special thanks to Sidney Bush who spearheaded data collection and organization from all the researchers for the competition experiments.

CHAPTER III

PRTN-INDEPENDENT REGULATION OF PYOCIN PRODUCTION BY PRTR

3.1 Abstract

Pseudomonas aeruginosa is a well-known opportunistic pathogen that is responsible for causing infections in immunocompromised individuals and has several antibiotic resistance mechanisms, making it difficult to treat. Recently, we discovered that deletion of the gene *xerC,* encoding a DNA-modifying enzyme called a tyrosine recombinase, causes *P. aeruginosa* cells to overproduce a bacteriocin known as pyocins. Pyocins are bacteriophage tail-like complexes that are released via cell autolysis and kill other strains of *P. aeruginosa*, presenting an attractive alternative or adjunct to antibiotic treatment. Normally, the production of pyocins and the consequent cell lysis is prevented by the transcriptional repressor PrtR, which undergoes RecA-triggered autocleavage when chromosomal DNA damage occurs, thereby allowing pyocin production. Surprisingly, pyocins are produced identically in a Δ*recA* Δ*xerC* double deletion as in Δ*xerC*, despite the trigger (RecA) for cleaving the repressor (PrtR) being absent, suggesting that *xerC* deletion somehow bypasses PrtR-mediated repression. Here, we show that replacement of PrtR with a non-cleavable version ($PrtR_{S162A}$) in a Δ*xerC* background still allows pyocin gene overexpression but somehow blocks production of functional pyocins. The failure of such cells to make functional pyocins is not due to a lysis defect or to incorrect pyocin assembly, but rather lack of assembly, suggesting that $PrtR_{S162A}$ is somehow inhibiting the correct assembly of pyocins. Our data suggests that $PrtR_{S162A}$ does not prevent pyocin assembly by repressing expression, as pyocin gene expression was largely unchanged from Δ*xerC* cells. Moreover, complementation of $PrtR_{S162A}$-downregulated genes failed to restore functional pyocin production in a Δ*xerC prtR*$_{S162A}$ strain. Our ongoing research is

focused on PrtR regulation at the posttranscriptional level by deploying proteomics and probing PrtR interactions with other proteins.

3.2 Introduction

Pseudomonas aeruginosa is a well-known gram-negative opportunistic pathogen with an ability to form biofilms, establishing long term infections that are multidrug-resistant and difficult to treat [57]–[59]. *P. aeruginosa* has an arsenal of virulence factors used to compete with other bacteria in the environment or an infection site. It encodes a host of outer membrane proteins aiding in nutrient uptake and biofilm formation, including proteins such as OprH, which helps binding to surfactant protein A, aiding in adhesion and infection establishment within respiratory tracts [60]. Flagella and type IV pili both aid in motility and establishing infections [61], [62], while type III secretion systems make *Pseudomonas* capable of attacking other cells directly to kill them [63]. Cells produce many other virulence factors like exotoxins, siderophores, and phage-tail like bacteriocins (PTLBs). Known as pyocins in *Pseudomonas*, these PTLBs are capable of directly binding to target cells causing lysis through disruption of cellular membranes.

Pyocins primarily target specific strains within the *P. aeruginosa* species, while also targeting a few other genera, such as *Haemophilus, Neisseria,* and *Campylobacter*, likely helping pyocin-producing cells to effectively compete for resources in the environment [64]–[67]. Within the *P. aeruginosa* genome, there are 3 types of pyocins encoded, namely the S-type, R-type, and F-type pyocins, with both R- and F-types being PTLBs encoded between *trpE* and *trpG* in PAO1 and PA14 [68], [69]. The F-type pyocin is related to phage lambda, while the R-type is more closely related to P2; among the pyocins, R-type function and structure is the best understood [69], [70]. R-type pyocins are composed of a rod-shaped contractile sheath, within which is held an iron-atom tipped “spear-like” core, along with a base plate and tail fibers [71]. The tail fibers are able to recognize highly specific binding sites located in the lipopolysaccharide on the surface of target cells [72], [73]. Once binding occurs, the baseplate undergoes a conformational change and the sheath of the pyocin contracts, forcing the iron-atom tipped spear through the cell envelope and depolarizing the cytoplasmic membrane, causing cell death due to lysis [74]. R-type

pyocins are extremely effective at killing target cells, with only a single pyocin needed to kill a target cell [72].

While the best-known inducer of pyocin production remains DNA damage and subsequent activation of the SOS response, the full range of conditions that license pyocin production remain unknown [75]–[78]. What is known is that the pyocin gene cluster is under the control of PrtN, the activator of the pyocin gene cluster, as well as PrtR, which is a repressor of *prtN* expression (Figure 3.1A) [77]. PrtR keeps the pyocin cluster repressed under normal conditions by binding to the promoter of *prtN*, blocking production of PrtN [77]. Once produced, PrtN can bind to conserved sequences known as "P-boxes" to activate gene expression in the R- and S-type pyocin clusters [77]. Pyocin activation results once PrtR has cleaved itself via autoproteolytic activity triggered by RecA bound to damaged DNA [79]. RecA is a well-known DNA recombination protein found in nearly every species of bacteria, with homologs in both eukaryotes and archaea, and is involved in DNA recombination and repair within cells [80]–[82]. When DNA damage occurs through mutagens such as UV light, reactive oxygen species, chemotherapy, or antibiotics such as ciprofloxacin [83], RecA binds to the damaged DNA to initiate DNA repair mechanisms. RecA binding also triggers autoproteolytic cleavage of LexA which normally represses the SOS response, allowing the cell to respond to damaged DNA [84]–[87]. In a similar manner, PrtR autoproteolytic activity is mediated through RecA, and once PrtR is cleaved subsequent expression of *prtN* can occur, resulting in the production of pyocins (Figure 3.1B) [79], [88].

In order for pyocins to be released from cells, *P. aeruginosa* undergoes explosive cell lysis, releasing pyocins to the environment [88], [89]. It would be quite detrimental to the species to have its entire population lyse all at once, and therefore pyocin production and cell lysis are kept under strict control. In wild-type cells under normal conditions, <1% of the population expresses the pyocin gene cluster, rising after induction of DNA damage [78]. The pyocin gene cluster encodes structural genes as well as lysis genes, presumably to co-regulate lysis of the cell with pyocin production and assembly [68], [72]. The lysis genes include a holin (*hol*) that perforates the cell membrane, allowing the lysin (*lys*) to reach the

peptidoglycan wall and begin degradation [90], [91]. Along with these lysis genes, *P. aeruginosa* also contains a programmed cell death (PCD) system comprising the Alp proteins (AlpB-E), which include a holin (AlpB). The *alpBCDE* operon is regulated similarly to pyocins, with AlpR having an analogous role to PrtR. AlpR is autoproteolyzed under the influence of active RecA, derepressing *alpA*, which like PrtN is the activator of *alpBCDE*; the Alp system may play a role in the release of pyocins [78], [92].

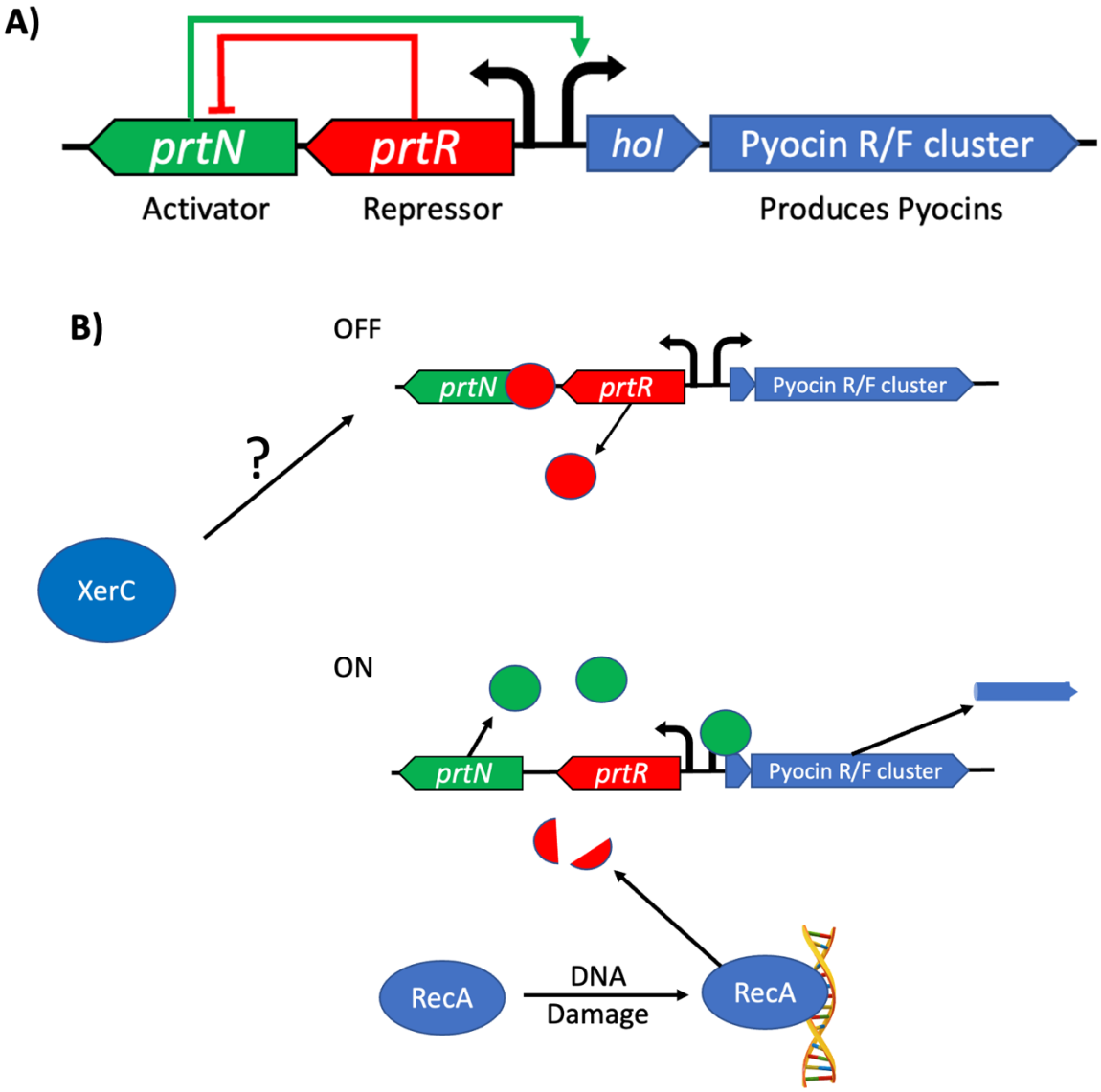

Figure 3.1. A) Schematic of pyocin gene regulation by repressor, PrtR, and the pyocin activator, PrtN and the Holin gene partially responsible for cell lysis and release of pyocins. **B)** Schematic of classic activation of pyocin production via RecA upon DNA damage, triggering the autoproteolysis of PrtR, allowing activation of *prtN*, as well as the newly discovered RecA-independent activation of pyocins that occurs in the absence of *xerC*.

Recent work has discovered an alternative pathway of pyocin activation, outside the canonical RecA-mediated pathway, that is active in the absence of the tyrosine recombinase XerC [78], [93]. XerC is known to be involved in site-specific recombination within the genome of *Escherichia coli* at *dif* sites, as well as functioning in chromosomal decatenation following crossover events during DNA replication [94], [95]. PA14 strains lacking *xerC* showed a large increase in the number of cells producing pyocins, with approximately 16% of cells showing pyocin activity compared to the wild-type of <1%, as well as the total amount of pyocins produced [78]. This increase in pyocin production in Δ*xerC* strains was independent of *recA* and, intriguingly, was further stimulated by DNA damage, even in the absence of RecA [78]. According to the canonical model, a Δ*xerC* Δ*recA* strain would be unable to initiate PrtR autocleavage owing to the absence of RecA. As pyocins are still overproduced in a Δ*xerC* Δ*recA* strain, the implication is that pyocin expression and production totally bypasses PrtR-mediated repression. Despite the dispensability of *recA* in a Δ*xerC* strain, pyocin production remained dependent on PrtN, with deletion of *prtN* shutting down pyocin production entirely in a Δ*xerC* strain [78]. These findings suggest that in a Δ*xerC* strain, *prtN* expression, and hence pyocin expression, is no longer subject to control by PrtR. Here, we further investigate the role of PrtR in pyocin regulation in a Δ*xerC* background, asking whether PrtR cleavage is relevant to RecA-independent pyocin production in *P. aeruginosa*.

3.3 Materials and Methods

3.3.1 Strains and Growth Conditions

Escherichia coli (SM10) and *Pseudomonas aeruginosa* (PA14) were grown in Luria-Bertani (LB) Lennox broth (10 g/L tryptone, 5 g/L yeast extract, 5 g/L NaCl) or on LB agar plates fortified with 1.5% Bacto agar at 37°C. When appropriate, 25 μg/mL Irgasan (to specifically select for P. aeruginosa) plus 75 μg/mL tetracycline, 25 μg/mL Irgasan plus 75 μg/mL gentamicin, 25 μg/mL tetracycline, or 20 μg/mL gentamicin was added to liquid or solid media. *P. aeruginosa* was also selected over *E. coli* for some strains by growth on Vogel-Bonner minimal medium (VBMM) containing citrate as the sole carbon source [96].

The strains used in this work are listed in Table 3.1 and Table S2. Markerless deletions were generated using the pEXG2 vector with counterselection on LB plates containing 6% sucrose or no-salt LB plates containing 15% sucrose [96] and were screened by colony PCR for the presence of deletions. Complementation and reporter strains were constructed by integration of the mini-CTX-1 vector at the neutral chromosomal *attB* locus. Modes of strain and plasmid construction are given in the supplemental material.

Strain	**Genotype or description**	**Source**
MTC1	PA14	Laboratory stock; Stephen Lory, Harvard Medical School
MTC2266	PA14 *ΔxerC*	[78]
MTC2304	PA14 *ΔxerC* prt_{RS162A}	[78]
MTC2297	PA14 *ΔxerC attB::CTX-1*-P_{holin}-*lux*, Tet^r	[78]
MTC2324	PA14 *ΔxerC Δpyocins (Δ07970-08300)*	[78]
MTC2308	PA14 $prtR_{S162A}$ *attB::CTX-1*-P_{holin}-*lux*, Tet^r	[78]
MTC2305	PA14 $prtR_{S162A}$	[78]
MTC2191	13S	Pradeep Singh ab (University of Washington)
MTC2252	PA14 *ΔxerC attB::CTX-1*-P_{holin}-*gfp*, Tet^r	[78]
MTC2280	PA14 *attB::CTX-1*-P_{holin}-*lux*, Tet^r	[78]
MTC2294	PA14 *ΔxerC Δholin Δlysin*	[78]
MTC2307	PA14 *ΔxerC* $prtR_{S162A}$ *attB::CTX-1*-P_{holin}-*lux,* Tet^r	[78]
MTC2424	PA14 *ΔxerC Δholin Δlysin ΔalpB-E*	This study
CSS1180	PA14 *ΔxerC ΔprtR*	This study
MTC2449	PA14 *attB::CTX-1*-P_{holin}-*lux pJN105-prtN*, Tet^r, $Gent^r$	This study

HAM202	PA14 *ΔxerC attB::CTX-1*-P_{holin}-*lux pJN105-prtN*, Tet^r, $Gent^r$	This study
HAM199	*PA14 $prtR_{S162A}$ attB::CTX-1*-P_{holin}-*lux pJN105-prtN*, Tet^r, $Gent^r$	This study
HAM197	PA14 *ΔxerC $prtR_{S162A}$ attB::CTX-1*-P_{holin}-*lux pJN105-prtN*, Tet^r, $Gent^r$	This study
MTC2486	PA14 *ΔxerC $prtR_{S162A}$ attB::CTX-1-gfp,* Tet^r	This study
HAM155	PA14 *attB::CTX-1-gfp pJN105-prtN*, Tet^r, $Gent^r$	This study
HAM157	PA14 *ΔxerC attB::CTX-1-gfp pJN105-prtN*, Tet^r, $Gent^r$	This study
HAM158	PA14 *ΔxerC $prtR_{S162A}$ attB::CTX-1-gfp pJN105-prtN*, Tet^r, $Gent^r$	This study
CSS1206	PA14*ΔxerC ΔprtR attB::CTX-1*-P_{holin}-*lux* Tet^r	This study
CSS1285	PA14*ΔxerC ΔprtR attB::CTX-1*-P_{holin}-*lux pJN105-prtN* Tet^r, $Gent^r$	This study
HAM198	PA14 *ΔxerC $prtR_{S162A}$ pJN105-prtN*, $Gent^r$	This study
HAM185	*PA14 ΔxerC $PrtR_{S162A}$ pJN105-PA14_16250*	This study
HAM186	*PA14 ΔxerC $PrtR_{S162A}$ pJN105-PA14_23680*	This study
HAM187	*PA14 ΔxerC $PrtR_{S162A}$ pJN105-PA14_33510*	This study
HAM188	*PA14 ΔxerC $PrtR_{S162A}$ pJN105-PA14_33560*	This study
HAM189	*PA14 ΔxerC $PrtR_{S162A}$ pJN105-PA14_33580*	This study
HAM190	*PA14 ΔxerC $PrtR_{S162A}$ pJN105-PA14_33590*	This study
HAM191	*PA14 ΔxerC $PrtR_{S162A}$ pJN105-PA14_33600*	This study
HAM192	*PA14 ΔxerC $PrtR_{S162A}$ pJN105-PA14_33830*	This study
HAM193	*PA14 ΔxerC $PrtR_{S162A}$ pJN105-PA14_40290*	This study
HAM194	*PA14 ΔxerC $PrtR_{S162A}$ pJN105-PA14_43850*	This study
HAM195	*PA14 ΔxerC $PrtR_{S162A}$ pJN105-PA14_62970*	This study
HAM196	*PA14 ΔxerC $PrtR_{S162A}$ pJN105-PA14_62990*	This study

Table 3.1. List of strains used in this study.

3.3.2 RNA Isolation and Sequencing

RNA isolation was achieved by growth of strains overnight, back diluted 1,000-fold in the morning and growing until an approximate OD600 of 0.450. Mitomycin C was added to a concentration of 0.1 μg/mL to cultures after 2 hours of growth to further induce pyocin production. Total RNA was isolated from homogenized colonies using the New England Biolabs Monarch total RNA miniprep kit. Subsequent quality control steps, the rRNA depletion, Illumina library preparation, and paired-end high-throughput Illumina sequencing were performed by Novogene (Beijing, China). Sequence mapping and analysis were performed at the Oklahoma University Health Sciences Center Laboratory for Molecular Biology and Cytometry Research using CLC software.

3.3.3 Pyocin Purification for Transmission Electron Microscopy

Cultures of interest were grown overnight and diluted 1,000-fold in 6 mL LB and grown at 37°C. Mitomycin C was added to a concentration of 3 μg/mL to cultures when they reached an OD600 of 0.250 to further induce pyocins in strains, and strains were grown for another 2.5 hours. DNase I was added to a concentration of 2 U/mL and incubated at 37°C for another 30 minutes. Cell debris was removed through centrifugation at 17,000 x g for 1 hour at 4°C. Pyocin particles were collected from the cell debris free supernatant by ultracentrifugation at 58,000 x g for 1 hour at 4°C. Pyocins were resuspended in 1/20th the culture volume of TN50 Buffer (50mM NaCl, 10 mM Tris-HCL pH 7.5), and stored at 4°C until use for imaging. Pyocin extraction protocol adapted from [67].

3.3.4 Growth Curve Analysis

Strains of interest were grown on LB plates overnight, then inoculated into LB liquid broth until late stationary phase was reached (about 18 h). Strains were then diluted 1,000-fold into fresh medium and grown to early exponential phase (about 4 h). The optical density at 600 nm (OD600) was measured, and all cultures were normalized to an OD600 equal to 0.5. Samples were set to appropriate OD and then mixed with ciprofloxacin to a

concentration of 0.03 μg/mL, and then 200 μL of culture with or without ciprofloxacin was aliquoted into a 96-well plate. The plate was incubated in a BioTek Synergy H1 plate reader (BioTek, USA) at 37°C for 20 h with orbital shaking. OD600 measurements were obtained every 10 min.

3.3.5 Kinetic Luciferase Assay

Strains of interest were cultured as described in "Growth curve analysis." Luminescence and OD was measured over a 20-hour period in white, clear-bottom 96-well microtiter plates, and imaged every 10-min at a sensitivity (gain) setting of 135 along with OD600 on a BioTek Synergy H1 plate reader. Final luciferase activity values were calculated by normalizing luciferase luminescence to culture density.

3.3.6 Pyocin Indicator Assays

Strains of interest were grown in 5 mL of LB liquid broth at 37°C until stationary phase was reached (about 16 h). Overnight culture supernatants were harvested and filtered using a 0.22-μm syringe filter to remove any remaining cells. Filtered supernatants were used immediately. Indicator strain 13S (MTC2191) was grown in 3 mL of LB liquid at the same time as the strains of interest. The dense cultures were diluted 1,000-fold into a microcentrifuge tube; then, 100 μL of the diluted cultures was spread plated onto a LB plate using sterile glass beads. After plating the indicator strain on LB, 10 μL of the filtered supernatant of the strains of interest were then spotted on top of the indicator strain plates. The plates were then incubated at 37°C overnight. Lysis defective strain *ΔxerC Δlysin Δholin ΔalpB-E* as well as *ΔxerC prtR*$_{S162A}$ were both disrupted through sonication prior to filtering for spotting.

3.3.7 Fluorescence Time-Lapse Microscopy

Strains of interest were grown in 3 mL of LB liquid broth overnight to obtain a saturated culture. They were then diluted 1,000-fold in fresh LB and grown to early exponential phase (about 4 h). Cells were immobilized by spotting 0.5 μL of the culture onto the pad and covering with cover glass. Imaging was performed on a Nikon Eclipse Ti inverted fluorescence microscope equipped with a Photometrics Prime 95B sCMOS digital camera, a Lumencor SOLA SE II 365 LED Light Engine, and an OKO temperature-controlled enclosure. Snapshot images and time-lapse microscopy of the slides were taken at ×100 magnification in both phase and GFP channels. Automated time-lapse imaging was performed at 37°C.

3.4 Results

3.4.1 Pyocin expression is separable from functional pyocin production

In previous work, we showed that cells lacking the tyrosine recombinase XerC displayed increased pyocin production in PA14 and bypassed the canonical RecA-mediated activation of the pyocin gene cluster [78], [93]. However, the overexpression and production of pyocins in Δ*xerC* cells was abolished by deletion of *prtN* irrespective of the presence of RecA, suggesting that pyocin production in Δ*xerC* cells is dependent on PrtN despite being independent of RecA [78], [93]. The expression of *prtN* is normally repressed by PrtR, which undergoes autoproteolysis upon interaction with activated RecA in the presence of DNA damage, in a similar process to LexA autoproteolysis-mediated triggering of the SOS response [79], [85], [86], [97]. The finding that pyocin expression and production in Δ*xerC* cells is dependent on PrtN but does not require RecA implies that PrtR-mediated repression is bypassed, further suggesting that PrtR autoproteolysis is irrelevant to pyocin production in a Δ*xerC* background.

To test the hypothesis that PrtR autocleavage is irrelevant, we used an S162A point mutant of PrtR ($PrtR_{S162A}$), which inactivates the autoprotease domain of PrtR and thus makes it a

non-cleavable, constitutive repressor in the canonical pathway for pyocin expression. Indeed, PrtR$_{S162A}$ was previously shown to fail to produce pyocins under DNA damage-inducing conditions [88]. When we replaced *prtR* with *prtR*$_{S162A}$ in a Δ*xerC* background, we observed that the pyocin cluster was still expressed, as indicated by our P$_{hol}$-*lux* transcriptional reporter, albeit at a lower level than in Δ*xerC* (Figure 3.2A), suggesting that PrtR$_{S162A}$ exerts a moderate repressive effect. We also saw that P$_{hol}$ expression was further stimulated by ciprofloxacin (Figure 3.2A), consistent with at least partial bypass of PrtR$_{S162A}$-mediated repression. Surprisingly, however, while Δ*xerC prtR*$_{S162A}$ cells strongly expressed P$_{hol}$-*lux*, they failed to produce any detectable functional pyocins (Figure 3.2B). Intrigued by this result, we then tested the effect of a full deletion of the coding sequence of *prtR*. Our prediction was that, without the presence of this repressor, we would observe increased P$_{hol}$-*lux* activity and greater pyocin production. Surprisingly, the Δ*xerC* Δ*prtR* strain failed to activate the P$_{hol}$-*lux* reporter irrespective of whether cells were treated with ciprofloxacin (Figure 3.2A). However, this strain still produced functional R-type pyocins capable of killing the 13S pyocin indicator strain (Figure 3.2B). Moreover, deletion of *prtR* in a wild-type (*xerC*$^{+}$) strain showed the same phenotype, with very low P$_{hol}$-*lux* expression but elevated pyocin production (Figure 3.2B). The failure of these strains to activate the *hol* gene at the start of the pyocin cluster while still producing functional pyocins suggests that the absence of PrtR somehow prevents *hol* expression but permits the expression and production of other genes in the R-type pyocin cluster, resulting in functional pyocin production. Conversely, non-cleavable PrtR$_{S162A}$ has the opposite effect, preventing the expression or production of functional pyocins but not fully blocking *hol* expression. These results suggest that PrtR may have other, previously unappreciated targets for repression within the pyocin cluster. Furthermore, the data imply that there are multiple regulatory sites within the R-pyocin cluster, such that *hol* expression and functional pyocin production can be decoupled.

3.4.2 The failure of Δ*xerC prtR*$_{S162A}$ to produce pyocins is not due to a lysis defect

We first turned our attention to characterizing the curious phenotype of Δ*xerC prtR*$_{S162A}$ cells, with their strong P$_{hol}$ expression but lack of functional pyocin production. One

straightforward explanation for the absence of functional pyocins in culture supernatants might be simply a lysis defect preventing the release of functional pyocins. To test for a lysis defect, we sonicated stationary-phase cell cultures to manually lyse cells prior to filtering and testing for pyocin activity. As a positive control, we used the lysis-defective strain Δ*xerC* Δ*holin* Δ*lysin* Δ*alpB-E*, which produces functional pyocins but lacks the lysis proteins that lyse pyocin-producing cells. As expected, supernatants from this strain showed no pyocin activity, whereas pyocin killing activity was observed when cells of this strain were lysed by sonication (Figure 3.3A). In contrast, no pyocin activity was observed with Δ*xerC prtR*$_{S162A}$ cells irrespective of whether they were sonicated (Figure 3.3A), indicating that the lack of pyocin production was not due merely to a lysis defect.

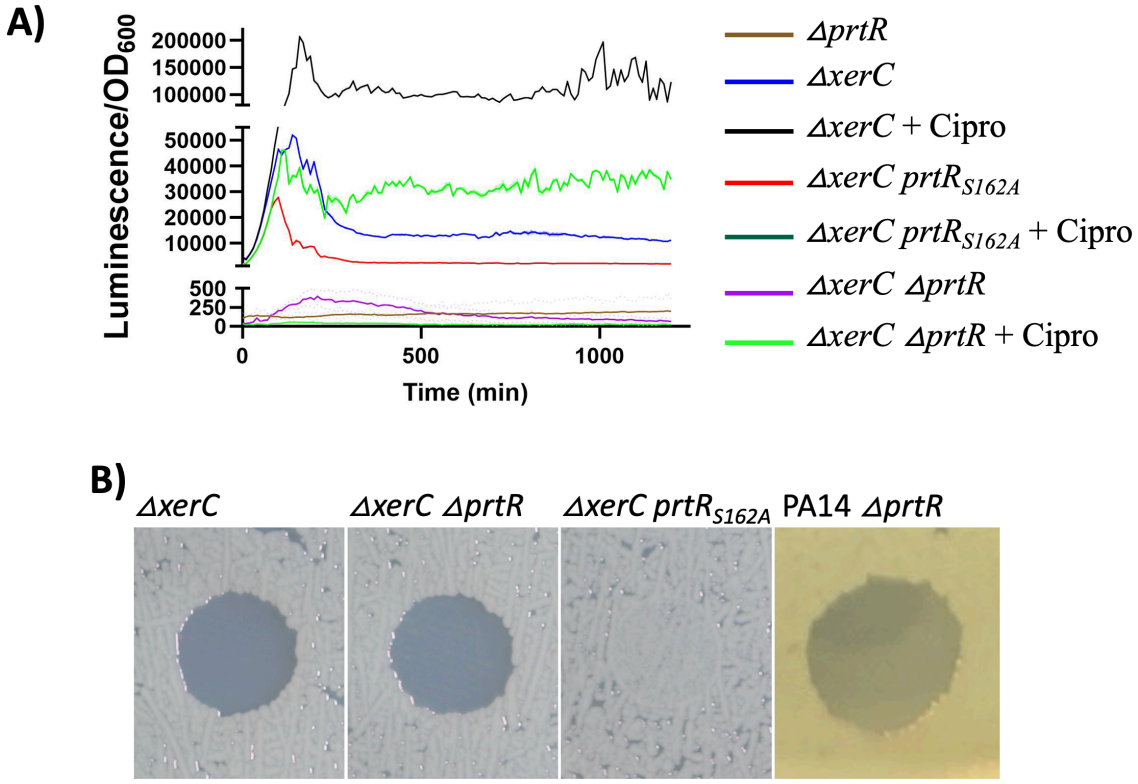

Figure 3.2. **A)** Representative transcriptional profiles (P_{hol}-*lux* reporter) of *ΔxerC* (MTC2297), and *ΔxerC ΔprtR* (CSS1206), and *ΔxerC prtR*$_{S162A}$ (MTC2307) strains with and without 0.03 µg/mL of Ciprofloxacin. *ΔprtR* data was captured during a different experiment but showed no pyocin reporter activity and was adjusted in accordance with the blank LB sample. **B)** Pyocin indicator assays using cell-free stationary-phase culture supernatants from *ΔxerC* (MTC2266), *ΔxerC ΔprtR* (CSS1180), *ΔxerC prtR*$_{S162A}$ (MTC2304) strains.

We also used fluorescence microscopy to monitor the relationship between pyocin production and cell lysis in Δ*xerC prtR*$_{S162A}$. Our previous work showed that pyocin-producing Δ*xerC* cells undergo explosive lysis [78]. In the Δ*xerC prtR*$_{S162A}$ strain, however,

cells expressing pyocins (P_{hol}-*gfp*) were generally dimmer with respect to GFP fluorescence, took much longer to lyse, and often formed long-lasting spheroplasts (Figure 3.3B and 3.3C). Our data also showed the average time to cell lysis in Δ*xerC* is approximately 63 minutes from the onset of pyocin expression, while Δ*xerC* $prtR_{S162A}$ showed an average time to lysis of approximately 109 minutes (Figure 3.3C). The presence of spheroplasts formed by pyocin producers, as well as the length of time prior to lysis seen in Δ*xerC* $prtR_{S162A}$, suggests that $PrtR_{S162A}$ plays a role in suppressing cell lysis but is unable to prevent lysis. Our evidence of pyocin expression in Δ*xerC* $prtR_{S162A}$ cells (Figure 3.2A), as well as their ability to lyse while still failing to produce pyocins capable of killing the indicator strain (Figure 3.2B and 3.3A) point to $PrtR_{S162A}$ affecting the expression or production of a critical pyocin component or somehow impacting the assembly of pyocins. It is possible that while Δ*xerC* $prtR_{S162A}$ shows reporter activity for P_{hol}, $PrtR_{S162A}$ is still capable of binding and inhibiting either another gene in the pyocin cluster, a protein component(s) of the functional pyocin, or something needed for the assembly of pyocins, such as a chaperone protein.

3.4.3 Assembled R-type pyocins can be isolated from Δ*xerC* cells but not Δ*xerC* $prtR_{S162A}$ cells

Based on our previous results showing that Δ*xerC* $prtR_{S162A}$ expresses at least the beginning of the pyocin cluster (P_{hol}) while failing to produce functional pyocins, we next attempted to isolate and visually inspect pyocins to observe if there were any morphological defects in pyocin assembly in Δ*xerC* $prtR_{S162A}$. We thus prepared enriched pyocin extracts from Δ*xerC* and Δ*xerC* $prtR_{S162A}$ cells and used transmission electron microscopy (TEM) to observe individual pyocins. We isolated from the Δ*xerC* mutant numerous fully assembled and functional pyocins, while Δ*xerC* $prtR_{S162A}$ isolates lacked any sign whatsoever of pyocin complexes (Figure 3.4). In the Δ*xerC* extracts we were able to see assembled and primed pyocins, as well as some already contracted pyocins (Figure 3.4A and 3.4C). In Δ*xerC* $prtR_{S162A}$, we failed to see pyocins at any stage of assembly (Figure 3.4B and 3.4D). As a gross test of whether any structural component was missing, we ran the same extracts used for EM by SDS-PAGE and used silver stain to check for obvious differences in the resulting protein bands. We failed to detect any gross changes between the Δ*xerC* extract

and the Δ*xerC prtR*$_{S162A}$ extract (Figure S9). This finding, along with the expression of pyocin genes despite the presence of a non-cleavable PrtR repressor, at least suggests that all the components of pyocins are present but that assembly of functional pyocins is prevented.

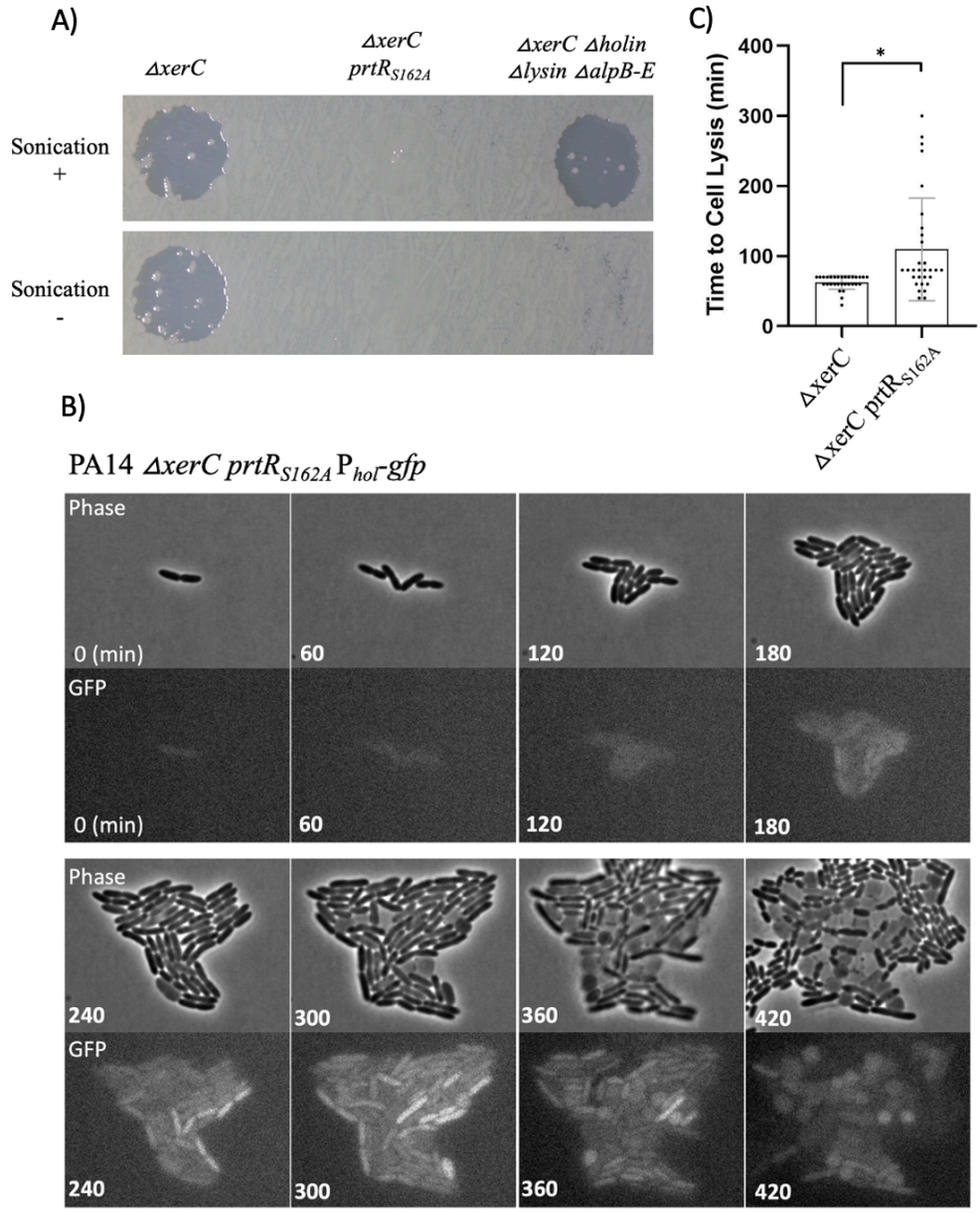

Figure 3.3 A) Pyocin indicator assays using cell-free stationary-phase culture supernatants sonicated or non-sonicated from PA14 *ΔxerC* (MTC2266), PA14 *ΔxerC prtR*$_{S162A}$ (MTC2304), and lysis defective PA14 *ΔxerC Δholin Δlysin ΔalpB-E* (MTC2242). **B)** Representative phase-contrast and fluorescent micrographs of PA14 *ΔxerC prtR*$_{S162A}$ bearing a P$_{hol}$-*gfp* reporter at *attB* (MTC2486). **C)** Counting of cells (n=30) of PA14 *ΔxerC* P$_{hol}$-*gfp* reporter (MTC2252) PA14 *ΔxerC prtR*$_{S162A}$ P$_{hol}$-*gfp* reporter (MTC2486) from start of pyocin expression until cell lysis occurs. Mean of *ΔxerC* time to lysis from onset of pyocin production is 62.67 minutes, while *ΔxerC prtR*$_{S162A}$ is 109.7 minutes. * = p-value of <0.0015.

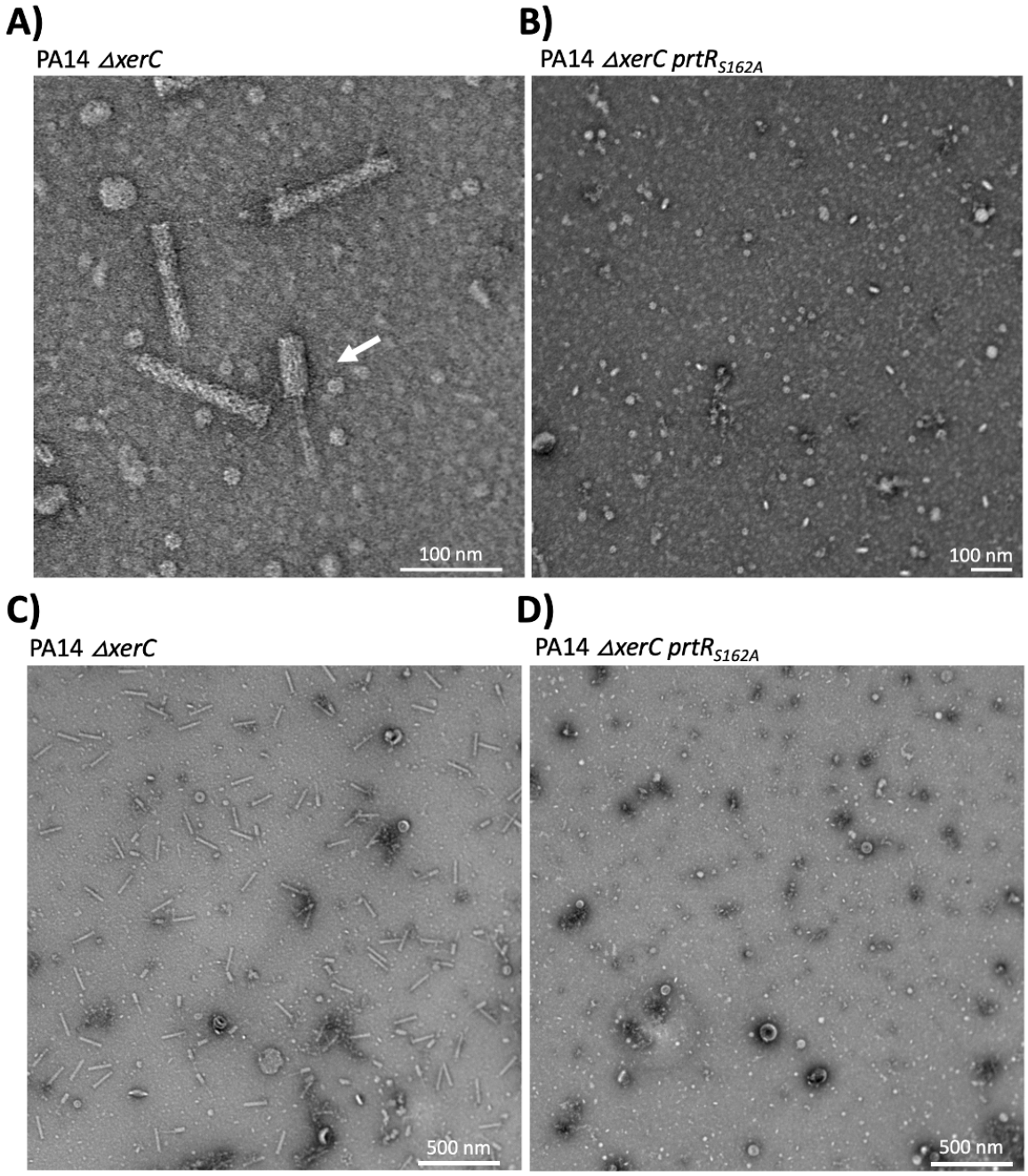

Figure 3.4. Transmission electron micrograph of lysates of cells producing R-type pyocins. **A)** R-type pyocins extracted from PA14 *ΔxerC* (MTC2266). The white arrow indicates a contracted pyocin. **B)** PA14 *ΔxerC prtR*$_{S162A}$ (MTC2304) extracted lysates lacking pyocin. **C)** PA14 *ΔxerC* (MTC2266) purified pyocin extract showing numerous R-type pyocins. **D)** Purified PA14 *ΔxerC prtR*$_{S162A}$ (MTC2304) extracted lysates lacking purified pyocins. Grids were negatively stained with uranyl acetate. Scale bars are shown for each image.

3.4.4 Functional pyocin production in Δ*xerC prtR*$_{S162A}$ is not rescued by inducible *prtN*

The absence of functional pyocins produced by Δ*xerC prtR*$_{S162A}$ cells despite *hol* expression prompted us to investigate whether the effects of PrtR$_{S162A}$ were mediated through repression of *prtN* or whether PrtR has other targets within the pyocin cluster [77]. To test whether *prtN* repression has any role, we sought to fully decouple *prtN* from PrtR by expressing *prtN* on a plasmid with an ectopic, arabinose-inducible P$_{ara}$ promoter. We then determined if we could recover functional pyocins upon *prtN* expression in strains with wild-type PrtR or PrtR$_{S162A}$. In a wild-type background, we saw a large increase (approximately 100-fold) in the amount of pyocin expression (P$_{hol}$-*lux*) when PrtN production was induced (Figure 3.6A) as well as in the number of cells expressing P$_{hol}$-*gfp* (Supplemental Figure 10). We also saw a modest increase in pyocin-mediated killing activity in supernatants from PA14 when PrtN was overexpressed (Figure 3.6B). In a Δ*xerC* background, the already-strong *hol* expression increased approximately 8-fold upon PrtN expression, and supernatants maintained their killing activity (Figure 3.6A and 3.6B and Supplemental Figure S11). Overexpression of *prtN* in the Δ*xerC prtR*$_{S162A}$ mutant resulted in increased *hol* expression, but still showed no recovery of functional pyocin production (Figure 3.6A and 3.5B, Figure S12). This result suggests that PrtR$_{S162A}$ not only represses production of *prtN* but is also somehow capable of blocking production of pyocins, either by binding to DNA at presently unknown binding sites other than the *prtN* promoter, or even through potential interaction with proteins, either structural pyocin proteins or other presently unknown proteins, such as chaperones or assembly proteins that are needed for proper pyocin folding and assembly. In support of PrtR repression acting directly through proteins, it was recently discovered that PrtR binds to *siaD* for direct repression an inhibition of function [98].

3.4.5 Transcriptomic analysis of PrtR$_{S162A}$-regulated genes in a Δ*xerC* background

As a way to identify genes other than *prtN* that may be regulated by PrtR$_{S162A,}$ to prevent the production of functional pyocins, we performed transcriptomic analyses, comparing the gene expression profiles of Δ*xerC prtR*$_{S162A}$ and Δ*xerC*. While many phage-tail like bacteriocins encode their own assembly proteins or may be capable of self-assembly as

structural proteins are made, we considered the possibility that $PrtR_{S162A}$ represses previously unknown targets within the genome or pyocin cluster itself [68], [99], [100]. There are several possibilities for such targets, including a host chaperone protein needed to aid in proper folding or assembly of pyocins. Alternatively, perhaps specific genes within the pyocin cluster are downregulated to prevent pyocin function. Among the differentially regulated genes between Δ*xerC prtR*$_{S162A}$ and Δ*xerC*, we identified 24 candidates with a negative log fold change greater than 2. This list included many hypothetical proteins, as well as some chaperones, proteases, and transcriptional repressors (Table S2). Considering that downregulation of any of these genes might in principle interdict functional pyocin production, we designed arabinose-inducible plasmids to complement the most-downregulated genes and chaperones from the transcriptomic data (Table 3.2) and learn whether complementation would restore functional pyocin production. None of the complementation strains restored functional pyocins when the candidate genes were induced (Figure S13). Several genes within the pyocin cluster were modestly downregulated in Δ*xerC prtR*$_{S162A}$, but no salient changes were identified to suggest the absence of a critical pyocin component (Figure 3.5). While it remains possible that a host chaperone is needed for proper assembly, there is also the possibility that PrtR is directly interacting with a protein causing direct inhibition or disrupting assembly [98].

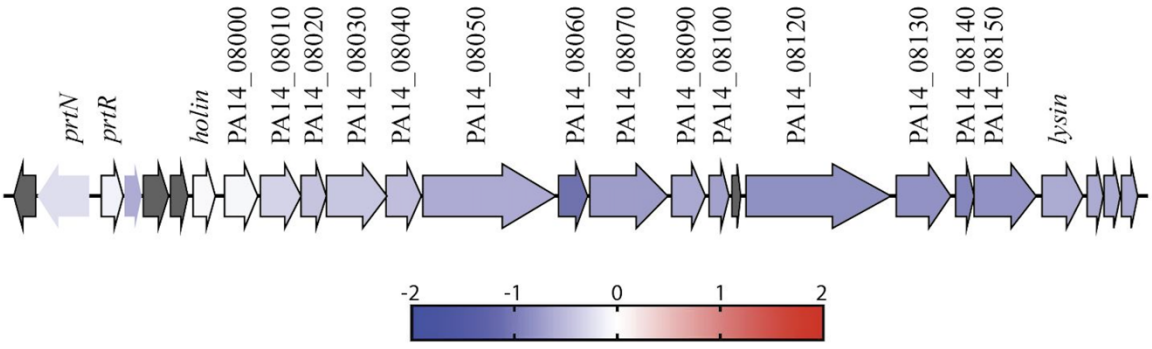

Figure 3.5. Heat map of the log2 fold change of gene expression of the pyocin gene cluster between *ΔxerC* and *ΔxerC prtR*$_{S162A}$ obtained from RNA sequencing data. Genes in dark grey were not found to be differentially regulated in the RNA sequencing data we obtained.

PA14 Gene	Putative Function
PA14_16250	LasB elastase
PA14_23680	Hypothetical heat shock protein IbpA
PA14_33510	Hypothetical MtbH-like protein
PA14_33560	Hypothetical protein for metal ion transport/binding
PA14_33580	Hypothetical protein, function unknown
PA14_33590	Thiamine Pyrophosphate-binding protein
PA14_33600	Hypothetical protein with PepSY domain, a potential regulator of protease activity
PA14_33830	Hypothetical transcriptional repressor
PA14_40290	LasA protease
PA14_43850	Chaperone protein HtpG
PA14_62990	GrpE chaperone binding protein, aids in protein folding

Table 3.2. A list of target genes for complementation in Δ*xerC prtR*$_{S162A}$ to restore functional pyocin production based on RNA sequencing data.

3.4.6 Pyocin activity is neither rescued nor inhibited by secreted compounds from non-pyocin-producing strains

Pyocin production is expressed heterogeneously within a population of cells, with very few cells in the wild-type PA14 expressing pyocins under normal conditions (approximately 0.3% of the population) [78]. This tight regulation of pyocins suggests a coordinated, tightly controlled process, which may be mediated through quorum sensing or through other phenotypic heterogeneity mechanisms similar to those governing persistor cells [101]–[103]. Hence, we at least considered the possibility that cells bearing PrtR$_{S162A}$ might lack a critical component that could be supplied *in trans* by a strain with wild-type PrtR. Alternatively, cells bearing PrtR$_{S162A}$ might produce an inhibitor that could block the activity of pyocins generated by PrtR$^+$ cells, for example by degrading pyocins. To investigate these possibilities, we co-cultured strains together and assessed pyocin killing activity. When Δ*xerC prtR*$_{S162A}$ was co-cultured with Δ*xerC* Δ*pyocins* (the latter strain might provide *in trans* a critical factor but would not itself produce pyocins), we failed to see functional pyocins produced, suggesting that a substance needed for pyocin production was not secreted from PrtR$^+$ cells (Figure 3.6C). We also saw that a Δ*xerC* strain continued

to produce pyocins when co-cultured with Δ*xerC prtR*$_{S162A}$ supporting the hypothesis that no inhibitory molecule was secreted by Δ*xerC prtR*$_{S162A}$ to stop the production of functional pyocins (Figure 6C). Collectively, these results, along with the failure of inducible *prtN* to restore production of pyocins, suggests that PrtR$_{S162A}$ not only targets *prtN* expression and that of known "P-box" binding sites, but also has additional gene or protein targets that prevent the proper production or assembly of pyocins.

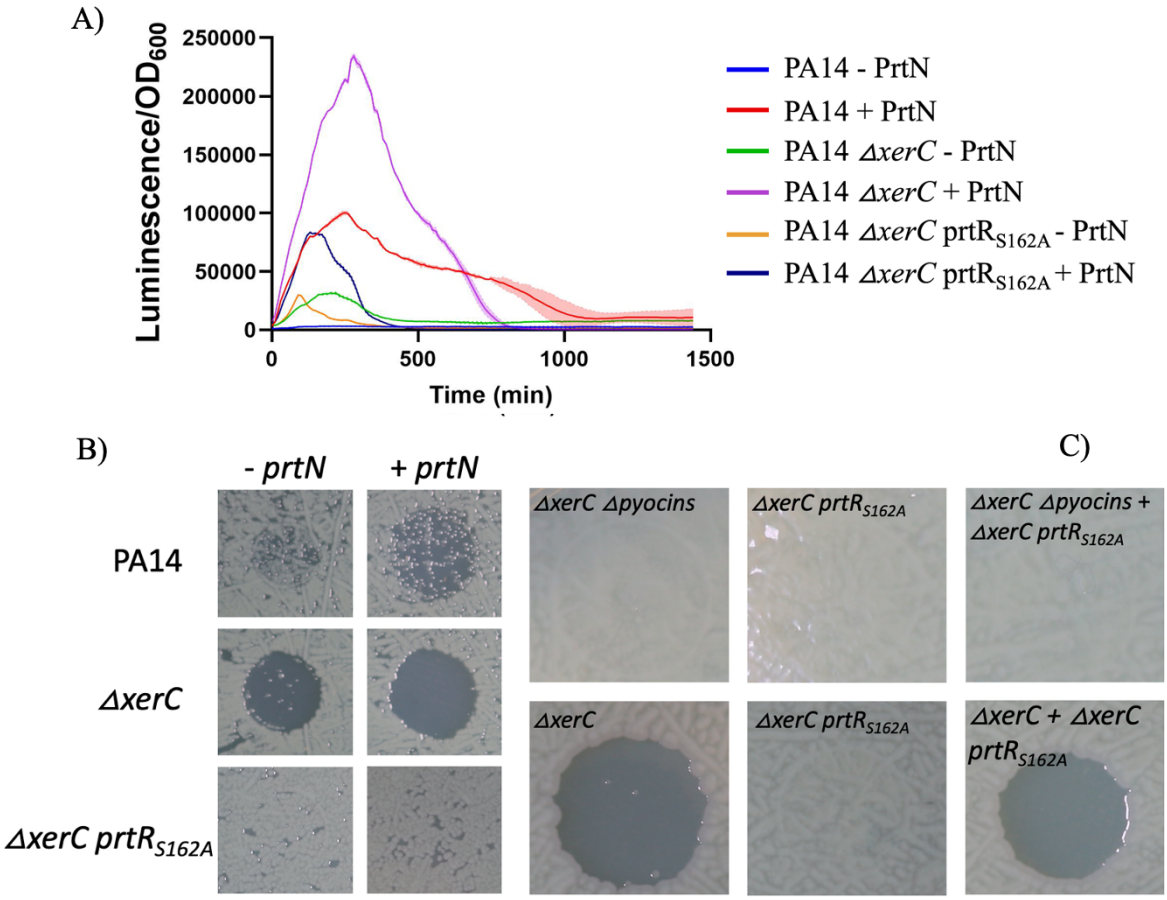

Figure 3.6. (A) Representative transcriptional profiles (P$_{hol}$-*lux* reporter) of wild-type (MTC2449), *ΔxerC* (HAM157), and *ΔxerC prtR*$_{S162A}$ (HAM197) strains with and without 1% arabinose to induce pJN105-*prtN*. **(B)** Pyocin indicator assays using cell-free stationary-phase culture supernatants from PA14 *ΔxerC* (HAM157), *ΔxerC prtR*$_{S162A}$ (HAM197) strains with or without 1% arabinose to induce pJN105-*prtN*. **(C)** Co-culture experiment between *ΔxerC Δpyocins* (MTC2324) and *ΔxerC* prtR$_{S162A}$ (MTC2304), as well as *ΔxerC* (MTC2266) and *ΔxerC prtR*$_{S162A}$ (2304).

3.5 Discussion

PrtR-mediated repression of *prtN* has been known for years, with the model that PrtR keeps *prtN* and hence pyocin expression turned off until RecA bound to damaged DNA stimulates the autocleavage of PrtR together with LexA cleavage-mediated triggering of the SOS response [72], [77], [86], [88], [104]. Recent work has uncovered that deletion of the gene encoding the tyrosine recombinase XerC is able to stimulate overproduction of pyocins via an alternative pathway that is independent of RecA yet still dependent on PrtN while being only partially repressed by $PrtR_{S162A}$ [78], [93]. Here, we show that pyocin expression is separable from pyocin production, with PrtR being necessary for pyocin (P_{hol}) expression but not for pyocin production. We show that strains with uncleavable $PrtR_{S162A}$ express the pyocin gene cluster (*hol*, at least) while failing to produce functional pyocins and exhibiting a morphological defect in which cells activating *hol* expression develop into long-lasting spheroplasts before lysing. Functional pyocin production was not rescued by overexpressing arabinose-inducible *prtN* in the $PrtR_{S162A}$ mutant, suggesting that $PrtR_{S162A}$ is disrupting pyocin production not by regulating *prtN* expression but rather through presently unknown genetic or protein targets.

The failure to activate *holin* expression in the pyocin cluster while still making fully functional pyocins in *prtR*-deleted strains suggests that PrtR may differentially regulate genes within the pyocin cluster. Surprisingly, the non-cleavable, presumably constitutively repressive $PrtR_{S162A}$ mutant still activated expression of the *holin* gene but shut down production of functional pyocins. These findings suggest that while PrtR may be needed for *holin* expression, cleavage of PrtR is essential for expression of the full pyocin cluster and/or for proper assembly of R-type pyocins. PrtR is known to have targets of repression other than *prtN*, such as *ptrB*, which is involved in regulation of type III secretion [77], [105], [106]. PrtR regulation within *Pseudomonas* remains poorly understood, but our findings suggest its regulatory role in the pyocin cluster is not solely due to its repression of *prtN*. It is possible that PrtR is binding to previously unappreciated binding sites within the pyocin cluster or even outside of the pyocin cluster.

Initially, we hypothesized that there was a lysis defect in Δ*xerC prtR*$_{S162A}$ cells, as we saw long-lasting spheroplasts formed by pyocin-expressing cells, that had a delay in cell lysis (Figure 3.3B). As the pyocin cluster encodes both a lysin and a holin, with the promoter of the holin at the start of the pyocin cluster (and being our pyocin expression reporter), we hypothesized that perhaps the lysin-encoding *lys* gene was being somewhat repressed by PrtR$_{S162A}$ mutant. Holin is thought to be responsible for making a hole in the cell membrane, allowing the lysin access to the peptidoglycan layer for degradation [90], [91]. As we saw decreased *hol* expression in Δ*xerC prtR*$_{S162A}$ (Figure 3.2A), we reasoned that perhaps holin and lysin production was enough to disrupt cell shape but not enough to fully lyse the cells, thereby preventing the release of pyocins [91], [107], [108]. However, even when cells were manually lysed by sonication, we failed to see pyocin killing activity, implying that the failure to produce pyocins was not caused by a failure to lyse, but that the PrtR$_{S162A}$ mutant was inhibiting something needed for functional pyocin production.

While the structure of R-type pyocins is well known, how assembly occurs is still poorly understood [68], [109]. Based on the structural similarity to the tail fiber of T4 bacteriophages, the pyocin sheath is thought to assemble around the iron atom-tipped core, using the core as a scaffold until it is assembled in its high-energy, pre-contractile state and the baseplate is added [109], [110]. To investigate the possibility that non-cleavable PrtR$_{S162A}$ was disrupting proper assembly of pyocins, such that pyocins were being assembled in their contracted state, assembling with morphological defects, or not being assembled at all, we extracted pyocins and viewed them directly with transmission electron microscopy (Figure 3.4). While we saw many pyocins in the Δ*xerC* cell lysate, no pyocins at all were seen in the Δ*xerC prtR*$_{S162A}$ lysates, with functional pyocin production failing even when *prtN* was overexpressed (Figure 3.6A), suggesting the PrtR$_{S162A}$ mutant may be capable of inhibiting assembly of pyocins through a presently unknown mechanism. In an attempt to find genes that the PrtR$_{S162A}$ mutant was repressing, we performed RNA sequencing of cell lysates, looking for downregulation of specific genes within the pyocin cluster, as well as potential chaperone proteins or assembly proteins. We saw no salient downregulation of pyocin-cluster genes, and moreover, complementation of the most

strongly downregulated genes failed to restore pyocin production (Table S3, Figure S13). Recent work in PrtR regulation has identified PrtR as a potential global regulator of gene expression [111] that is involved in the regulation of type III secretion systems through repression of *ptrB*; type VI secretion systems; and regulation of the Gac/Rsm systems modulating the switch from transient to chronic infections [79], [98], [105], [112]. PrtR is also involved in regulation of c-di-GMP levels affecting biofilm formation through direct interaction with SiaD, showing that PrtR is capable of regulation via direct protein interactions and not just by binding to DNA [98]. Given the ability of PrtR to regulate so many different systems through both DNA binding to promoters for repression and direct protein-protein interactions, the ability of $PrtR_{S162A}$ to shut down production of functional pyocins may be due to direct protein interactions blocking assembly of pyocin components, which would be permitted under normal circumstances by autocleavage of PrtR. Ongoing experiments include proteomic analysis to identify any pyocin proteins that are missing from $PrtR_{S162A}$-bearing strains and interaction analyses (e.g., pull-down assays) to investigate protein-protein interactions of PrtR. The results of these ongoing experiments may help us formulate a better understanding of PrtR regulation during the production of pyocins. Our findings in this work indicate that PrtR-mediated regulation of pyocins in *P. aeruginosa* is more complex than the standard model in which PrtR represses of *prtN* and that PrtR likely plays other roles in the regulation of pyocins and other cellular processes in *P. aeruginosa.*

3.6 Acknowledgments

Thank you to members of the Cabeen lab for many fruitful discussions throughout the research project.

C.W.H. and M.T.C. conceived the study, performed the experimental work, analyzed data, and wrote the paper. Trenton Skinner and Creed Killgore also performed experimental work and helped analyzed data.

CHAPTER IV

FUTURE PROJECTS IN THE LAB

Note: The following chapter is a list of projects I spearheaded in the lab that have generated their own projects to be carried out by future graduate students in the Cabeen lab.

4.1 Pyocins from *Pseudomonas aeruginosa* can extend antibiotic effectiveness

Pseudomonas aeruginosa is a notorious gram-negative human pathogen causing diseases that can be difficult to treat due to the antibiotic resistance nature of *Pseudomonas*, and often this can lead to the establishment of chronic infections in patients with Cystic Fibrosis [113], [114]. *Pseudomonas'* ability to resist antibiotics, both through intrinsic and acquired mechanisms, continues to be a major concern and has prompted the search for alternatives to antibiotics [115]. Pyocins, which are phage tail-like complexes that *P. aeruginosa* uses to kill and compete for resources with other *P. aeruginosa* strains, represent a possible alternative or adjunct to antibiotics in the treatment of *Pseudomonas* infections [67], [116]. These pyocins are typically released in response to DNA damage via RecA binding to the damaged DNA, and like phages they are released by producer cell lysis. Recent work found that strains lacking the tyrosine recombinase XerC strongly express pyocins via a novel RecA-independent but DNA damage-inducible pathway [78]. We sought to test whether Δ*xerC* cells, which are hypersensitive to ciprofloxacin, would extend the effect of this antibiotic to other pyocin-sensitive strains which are ciprofloxacin resistant.

A *⊿xerC* strain is still capable of responding to DNA damage independently of RecA, with approximately 16% of cells already producing pyocins, the number of cells expressing pyocins increases several fold in the presence of a sublethal concentration of a DNA damage inducing antibiotic such as ciprofloxacin [78]. As producer cells must lyse to release pyocins, we investigated whether a sublethal concentration of antibiotics causing DNA damage would stimulate a large portion of the population into killing themselves to release pyocins capable of killing other pyocin sensitive strains which may be antibiotic resistant. While further studies need to be done to map out which strains of *Pseudomonas* are sensitive to the specific pyocins produced by strains, initial studies showing heterogeneous susceptibility of clinical isolates to pyocins presents a promising potential for investigation [64], [65]. Pyocins have been showing promising results in treating *Pseudomonas* infections, as well as burn wounds as an alternative to antibiotics [117], [118].

We found that a sublethal concentration of ciprofloxacin did not substantially block or impact the growth of the clinical isolate 13S, which is sensitive to R-type pyocins released by PA14 (Figure 4.1) [119]. However, when 13S was co-cultured with Δ*xerC* cells, sublethal ciprofloxacin (0.03μg/mL) treatment effectively inhibited the growth of both *⊿xerC* and 13S, with preferential killing of the 13S cells (Figure 4.1 and S14). Moreover, the inhibition depended on pyocin production, with the growth of 13S not being inhibited nor impacted when the pyocin cluster was deleted in a *⊿xerC* background (Figure 4.1 and S15). Our data represent a proof of principle that XerC-deficient strains can increase the effectiveness of antibiotics against *P. aeruginosa*, opening the door to future therapeutic strategies. Our future goal is to perform a small molecule drug screen to identify compounds capable of mimicking a XerC deletion phenotype, causing an increased production of pyocins within local infections by *Pseudomonas* cells. An increase in strains producing pyocins, with or without the addition of antibiotics will hopefully provoke strains to attack one another with pyocins, killing one another and killing themselves in the process, like an old west shootout.

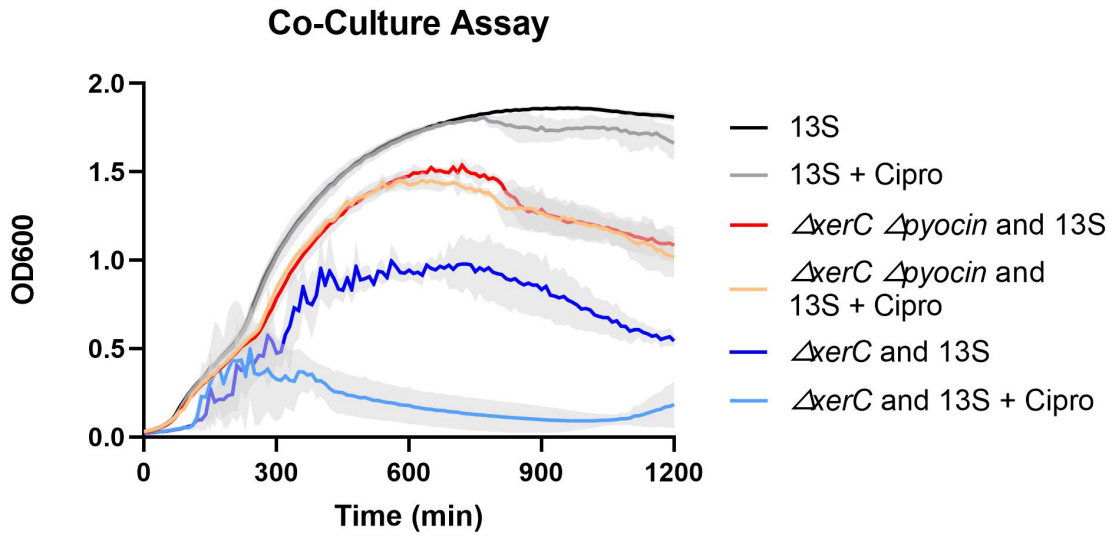

Figure 4.1. Clinical isolate 13S which is resistant to Ciprofloxacin was grown in the presence and absence of 0.03 µg/mL of ciprofloxacin, and co-cultured with a *ΔxerC* strain, or *ΔxerC Δpyocins* to assess pyocin activity against 13S.

4.2 Investigation into other tyrosine recombinases and their potential activity on pyocin production

Recent work has found that a deletion of the tyrosine recombinase XerC increased the number of cells producing pyocins, suggesting XerC is capable of regulating pyocins through a previously unknown RecA-independent pathway [78], [93]. In *E. coli* XerC is known to bind to *dif* sites to aide in chromosomal decatenation, normally binding cooperatively with XerD, and upon deletion of XerC cells exhibit a cell division error with a filamentous cell phenotype [120]–[122]. *Pseudomonas aeruginosa* also encodes XerD, and we investigated if a deletion of XerD would have a similar effect as the XerC deletion on pyocin regulation. Upon deletion of XerD, we see a similar phenotype to a XerC deletion with about 10% of cells expressing pyocins (Figure 4.2A). A double deletion of XerCD also showed an increased number of cells producing pyociins, equivalent with a single deletion of XerC or XerD, with no filamentous cells nor other strucutre anomallies noted during time-lapse microscopy (Figure 4.2B). These findings suggest a there may be an alternative to XerCD within *Pseudomonas* for chromosomal decatenation, as cells seem to be able to divide normally without a cell division defect in the absence of XerCD.

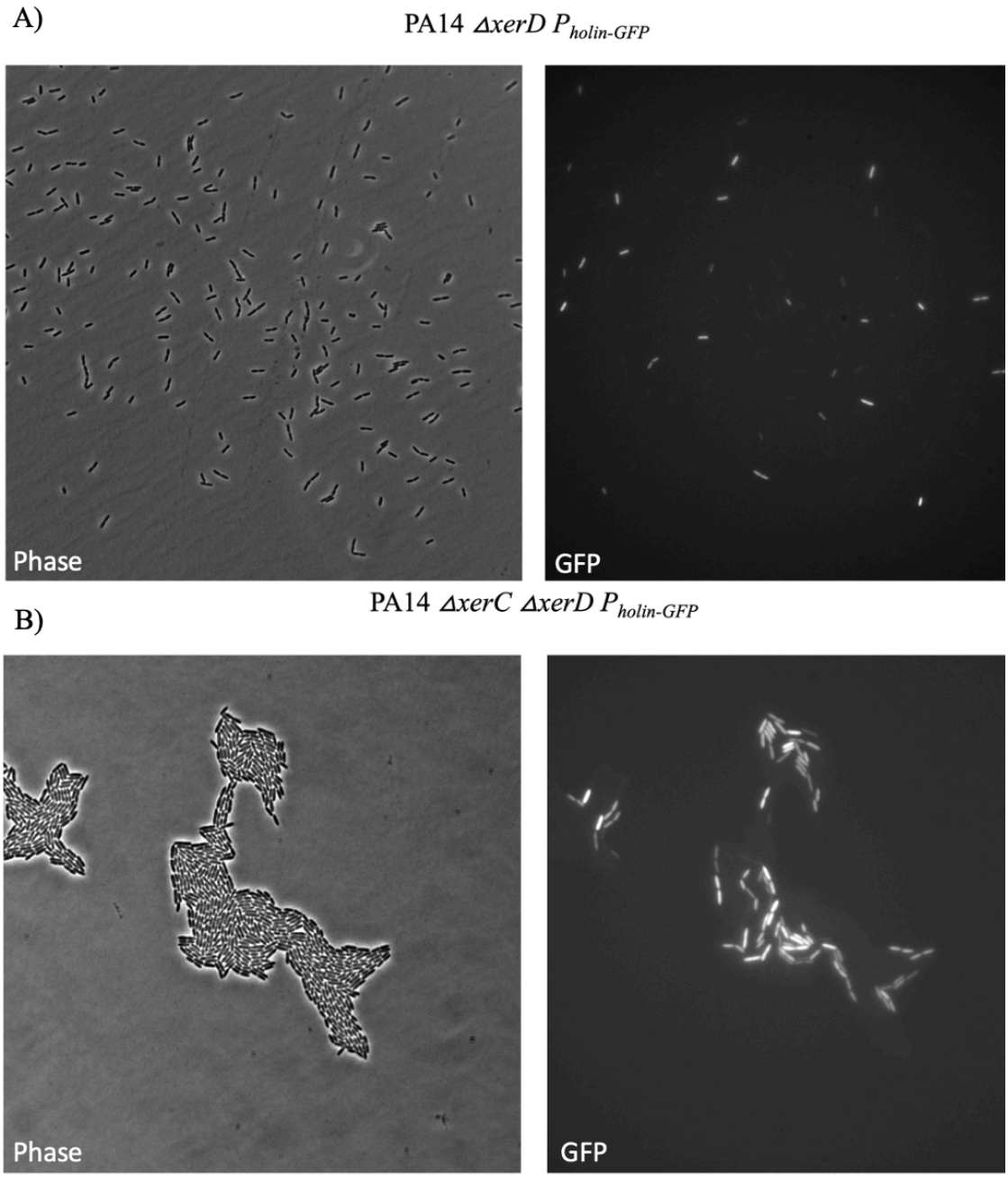

Figure 4.2. **A)** Representative images of phase and GFP fluorescent microscopy on an agarose pad of PA14 *ΔxerD* P_{holin}-gfp (MTC2520). Approximately 10% of cells are expressing pyocins. **B)** Representative images of phase and GFP fluorescent microscopy on an agarose pad of PA14 *ΔxerC ΔxerD* P_{holin}-gfp (HAM125). Approximately 10% of cells are expressing pyocins.

Within the genome of PA14 there is a XerC-like integrase PA_51650 (Figure 4.3), as well as a XerD-like integrase PA_60140 (Figure 4.4) that were identified on Pseudomonas Genome DB. We theorized that these XerC and XerD like genes may function as a backup for XerCD and that they may be able to perform a similar function in the absence of XerCD.

To test this, we made single deletions as well as double, triple, and quadruple deletions these proteins to see if they affected the expression of pyocins as well as their effects on cell division. Upon deletion of PA_60140 alone we saw similar expression of the pyocin cluster as in the wild-type (Figure 4.5C). We still failed to see a growth defect or detect the filamentous growth phenotype seen in *E. coli* upon a deletion of XerCD [120], in a triple or quad deletion while still maintaining similar expression rates of pyocins as seen before, approximately 10.5% (Figure 4.5A and 4.5B), suggesting XerC and XerD like proteins may not be essential for chromosomal decatenation in *Pseudomonas aeruginosa.* It is possible that there are other proteins involved in the process and that *xerC*, as well as *xerD* and XerCD like proteins may aide another unknown protein in PA14, but not be wholly responsible. Further studies need to be performed to investigate other possible proteins involved in cell division during cell growth within *Pseudomonas*, as well as potential protein-protein interactions with *xerC* and *xerD*.

```
XerC        ----------------------MRADLDAFLEHLRSERQVSAHTLDGYRRDLLKILALA    37
PA14_51650  MTPQQLTEEYIFAHDLREASAKIYRAATKALLKHFGPTA---------------------    39
                                  **  .*:*:*:

XerC        EKAGLSDWNALDTRSLRTFVARLHQQGQSSRSLARLLSATRGLYQYLLREGRCRHDPANG    97
PA14_51650  ------TVQEVDHRSVLGWRRKVLEQGLSKRSWNTYSNHLRTIWGYAIEHELVTHSQVNP    93
                   : :* **:  :  :: :** *.**     .  * :: * :..    *. .*

XerC        LSAP--KSPRKLPRTLDADRAL------QLLDGAV------EDDFIARRDQALLELFYSS    143
PA14_51650  FRKTTVIPPRRASKTVAAEAILRARNWLNMQVGAERCTGDRARITPAWFWLCTFEVFYFT    153
            :       **:  :*: *:  *      ::  **            *    . :*:** :

XerC        GLRLSELVGLDLEWLDLKEGLVRVRGKGNKVREL---PVGKAARQALEAWLPLRAQAA-P    199
PA14_51650  GIRLNALLCIRKRDIDWENQLILIRGETEKTHKEFVVPITEGLVPHLSRLLQEADRAGFA    213
            *:**. *: :  . :* :: *: :**: :*.::    *: :.    *.  *    :*.

XerC        EDGAVF-IGRGGKRLTPRAIQL----RVRQAGVRELGQHLHPHMLRHSFASHLLESS-GD    253
PA14_51650  DDDQLFNVNRFSPHYKSKVMNSDQVEAMYRKLTEKVGVRMTPHRFRHTLATDLMKAPERN    273
            :*. :* :.* . : . :.::      : :  ..::* :: ** :**::*:.*:::   :

XerC        LRAVQELLGHADIATTQIYTHLDFQHLASVYDRAHPRAK-----R----KGNADGGNDP-    303
PA14_51650  IHLTKCLLNHSNIQTTMSYIEADYDHMRAVLHARSLAQGALENVRKVDYSGSPQASAKPK    333
            :: .: **.*::* **  * . *::*: :* .            *    .*. :.. .*

XerC        ------------------------------------------------------------    303
PA14_51650  PCGQPLARMGEAPPQEARTEPAEPREHTPGTGIQGDATAWEEALPQPPDTFEQSVLFTLM    393


XerC        ---------------------------------       303
PA14_51650  AQHLSNRAATASAASTATSGSGGWGSTARSSLA       426
```

Figure 4.3. Sequence alignment of PA14_XerC and XerC-like protein PA14_51650. Protein sequence alignment was generated using sequences from Pseudomonas Genome DB aligned with EMBL-EBI Clustal Omega. Sequence similarity scored at 43.3%. A . (period) indicates weakly similar proteins, a : (colon) indicates strongly similar proteins with similar features, and an * (asterix) indicates a conserved residue.

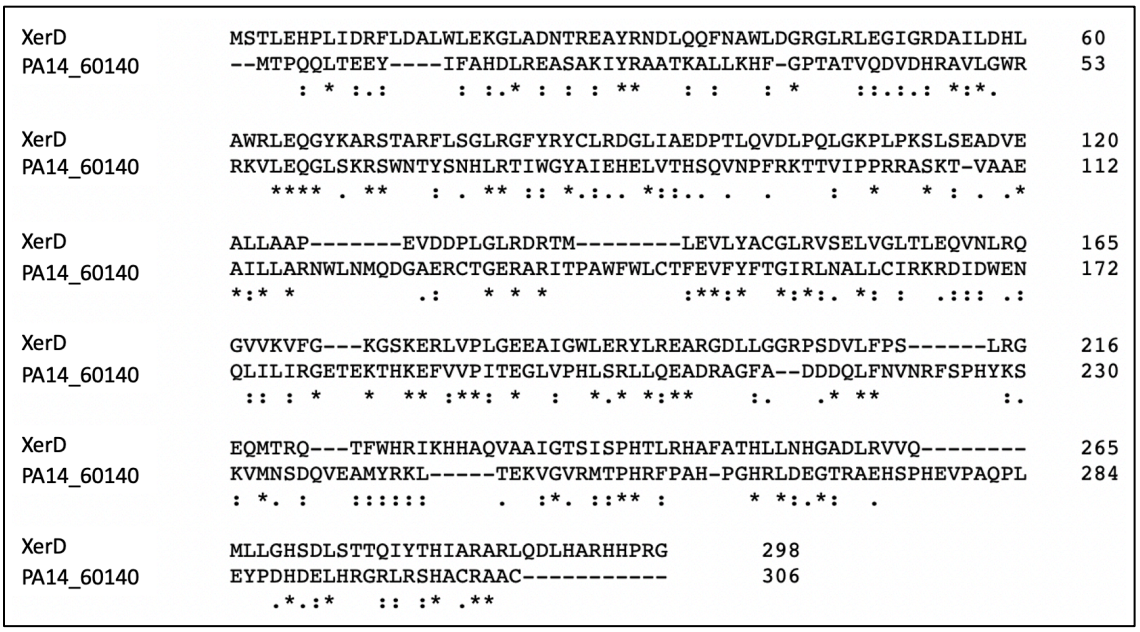

Figure 4.4 Sequence alignment of PA14_XerD and XerD like PA14_60140. Protein sequence alignment was generated using sequences from Pseudomonas Genome DB aligned with EMBL-EBI Clustal Omega. Sequence similarity scored at 38.2%. A . (period) indicates weakly similar proteins, a : (colon) indicates strongly similar proteins with similar features, and an * (asterix) indicates a conserved residue.

4.3 Materials and Methods

4.3.1 Kinetic luciferase assay

Strains of interest were cultured as described in "Growth curve analysis." Luminescence and OD was measured over a 20-hour period in white, clear-bottom 96-well microtiter plates, and imaged every 10-min at a sensitivity (gain) setting of 135 along with OD600 on a BioTek Synergy H1 plate reader. Final luciferase activity values were calculated by normalizing luciferase luminescence to culture density.

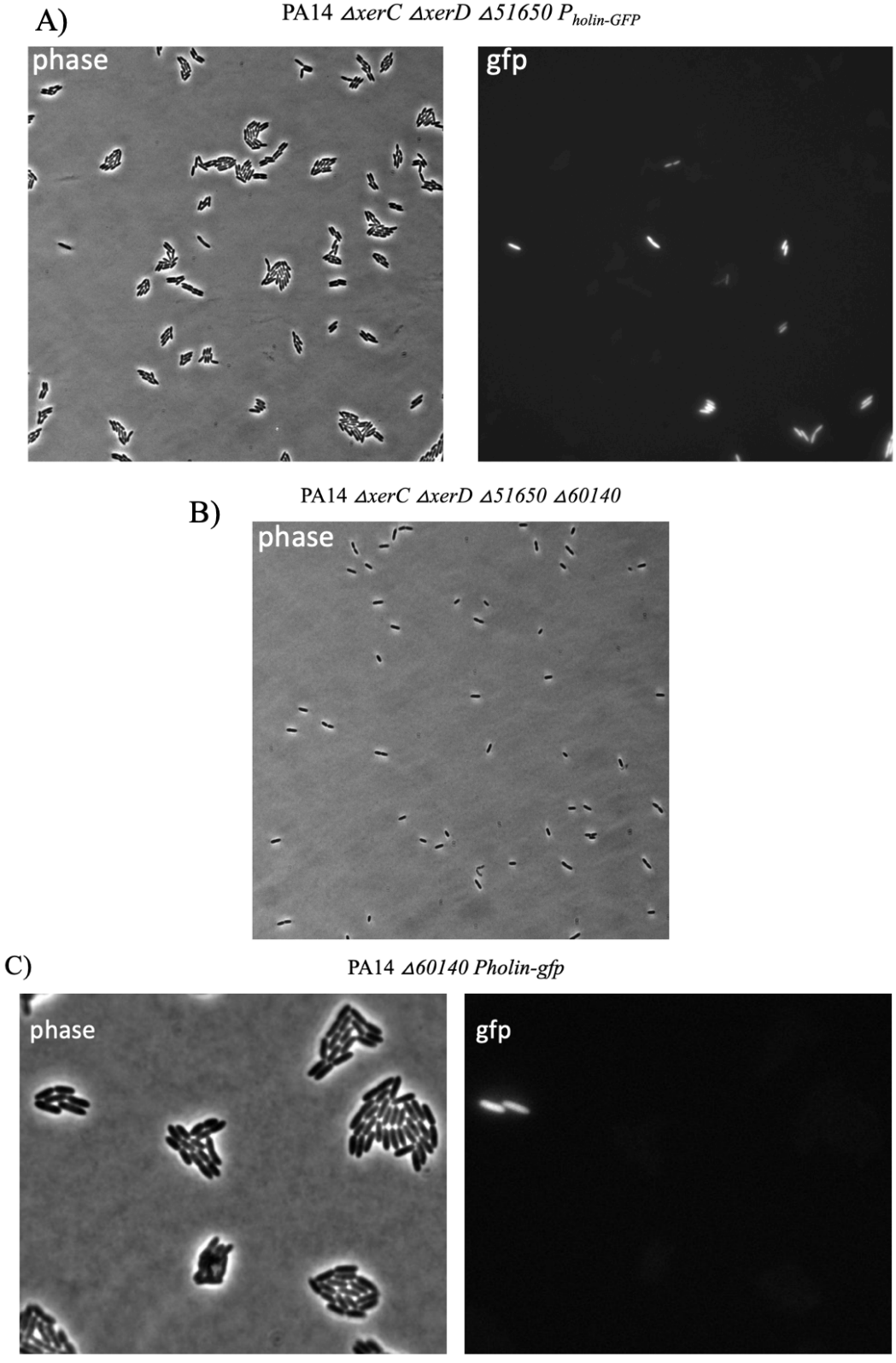

Figure 4.5. **A)** Representative images of phase and GFP microscopy on an agarose pad of PA14 *ΔxerC ΔxerD Δ51650* P_{holin}-gfp (HAM138). Approximately 10.6% of cells are expressing pyocins. **B)** Representative images of phase microscopy on an agarose pad of PA14 *ΔxerC ΔxerD Δ51650 Δ60140* (HAM154). **C)** Representative images of phase microscopy on an agarose pad of PA14 *Δ60140* (HAM205).

4.3.2 Fluorescence time-lapse microscopy

Strains of interest were grown in 3 mL of LB liquid broth overnight to obtain a saturated culture. They were then diluted 1,000-fold in fresh LB and grown to early exponential phase (about 3-4 h). Cells were immobilized by spotting 0.5 μL of the culture onto the agarose pad and covering with cover glass. Imaging was performed on a Nikon Eclipse Ti inverted fluorescence microscope equipped with a Photometrics Prime 95B sCMOS digital camera, a Lumencor SOLA SE II 365 LED Light Engine, and an OKO temperature-controlled enclosure. Snapshot images and time-lapse microscopy of the slides were taken at ×100 magnification in both phase and GFP channels. Automated time-lapse imaging was performed at 37°C.

4.3.3 Strain construction

Strains were constructed by amplifying genes of interest or for deletion by polymerase chain reaction, run on a DNA electrophoresis gel and extracted using OMEGA E.N.Z.A Gel Extraction Kit. Extracted bands were assembled into cut pEXG2 using isothermal assembly and selected on Gent 20 μg/mL LB plates. Donor *E. coli* and recipient PA14 strains were then grown overnight and then mated on LB plate for approximately 6 hours, before being scraped up, resuspended in LB, and plated on VBMM Gent20 plates for selection of *Pseudomonas* strain with plasmid. Colonies from these plates were streaked onto no salt LB plates (NSLB) with 15% sucrose, which are later picked and patched on LB and LB Gent20 plates for screening for the loss of pEXG2 plasmid. These colonies are then screened by PCR to confirm if the deletion or the wild-type gene is present. VBMM stock: 2g $MgSO_4$*7(H_2O), 100g K_2HPO_4, 20g of citric acid, and 35g $Na(NH)_4(HPO)_4$ in 1 L of ultrapure water, pH set to 7.0 and filter sterilized.

References

[1] H. E. Schellhorn, "Function, Evolution, and Composition of the RpoS Regulon in Escherichia coli," *Front. Microbiol.*, vol. 11, p. 560099, Sep. 2020, doi: 10.3389/fmicb.2020.560099.

[2] S. Lacour and P. Landini, "σ^S -Dependent Gene Expression at the Onset of Stationary Phase in *Escherichia coli* : Function of σ^S -Dependent Genes and Identification of Their Promoter Sequences," *J Bacteriol*, vol. 186, no. 21, pp. 7186–7195, Nov. 2004, doi: 10.1128/JB.186.21.7186-7195.2004.

[3] M. Jishage and A. Ishihama, "Regulation of RNA polymerase sigma subunit synthesis in Escherichia coli: intracellular levels of sigma 70 and sigma 38," *J Bacteriol*, vol. 177, no. 23, pp. 6832–6835, Dec. 1995, doi: 10.1128/jb.177.23.6832-6835.1995.

[4] D. B. Straus, W. A. Walter, and C. A. Gross, "The heat shock response of E. coli is regulated by changes in the concentration of σ32," *Nature*, vol. 329, no. 6137, pp. 348–351, Sep. 1987, doi: 10.1038/329348a0.

[5] M. Hecker, J. Pané-Farré, and V. Uwe, "SigB-Dependent General Stress Response in *Bacillus subtilis* and Related Gram-Positive Bacteria," *Annu. Rev. Microbiol.*, vol. 61, no. 1, pp. 215–236, Oct. 2007, doi: 10.1146/annurev.micro.61.080706.093445.

[6] M. Hecker and U. Völker, "General stress response of Bacillus subtilis and other bacteria," in *Advances in Microbial Physiology*, Elsevier, 2001, pp. 35–91. doi: 10.1016/S0065-2911(01)44011-2.

[7] U. Völker, B. Maul, and M. Hecker, "Expression of the sigmaB-dependent general stress regulon confers multiple stress resistance in Bacillus subtilis," *J Bacteriol*, vol. 181, no. 13, pp. 3942–3948, Jul. 1999, doi: 10.1128/JB.181.13.3942-3948.1999.

[8] M. Brigulla, T. Hoffmann, A. Krisp, A. Völker, E. Bremer, and U. Völker, "Chill Induction of the SigB-Dependent General Stress Response in *Bacillus subtilis* and Its Contribution to Low-Temperature Adaptation," *J Bacteriol*, vol. 185, no. 15, pp. 4305–4314, Aug. 2003, doi: 10.1128/JB.185.15.4305-4314.2003.

[9] C.-C. Chen, R. J. Lewis, R. Harris, M. D. Yudkin, and O. Delumeau, "A supramolecular complex in the environmental stress signalling pathway of Bacillus subtilis," *Mol Microbiol*, vol. 49, no. 6, pp. 1657–1669, Sep. 2003, doi: 10.1046/j.1365-2958.2003.03663.x.

[10] C. W. Price, "General Stress Response," in *Bacillus subtilis and Its Closest Relatives*, A. L. Sonenshein, J. A. Hoch, and R. Losick, Eds., Washington, DC, USA: ASM Press, 2014, pp. 369–384. doi: 10.1128/9781555817992.ch26.

[11] S. A. Boylan, A. R. Redfield, M. S. Brody, and C. W. Price, "Stress-induced activation of the sigma B transcription factor of Bacillus subtilis," *J Bacteriol*, vol. 175, no. 24, pp. 7931–7937, Dec. 1993, doi: 10.1128/jb.175.24.7931-7937.1993.

[12] A. K. Benson and W. G. Haldenwang, “The sigma B-dependent promoter of the Bacillus subtilis sigB operon is induced by heat shock,” *J Bacteriol*, vol. 175, no. 7, pp. 1929–1935, Apr. 1993, doi: 10.1128/jb.175.7.1929-1935.1993.
[13] C. M. Kang, K. Vijay, and C. W. Price, “Serine kinase activity of a Bacillus subtilis switch protein is required to transduce environmental stress signals but not to activate its target PP2C phosphatase,” *Mol Microbiol*, vol. 30, no. 1, pp. 189–196, Oct. 1998, doi: 10.1046/j.1365-2958.1998.01052.x.
[14] M. S. Brody, K. Vijay, and C. W. Price, “Catalytic function of an alpha/beta hydrolase is required for energy stress activation of the sigma(B) transcription factor in Bacillus subtilis,” *J Bacteriol*, vol. 183, no. 21, Art. no. 21, Nov. 2001, doi: 10.1128/JB.183.21.6422-6428.2001.
[15] V. Tran, K. Geraci, G. Midili, W. Satterwhite, R. Wright, and C. Y. Bonilla, “Resilience to oxidative and nitrosative stress is mediated by the stressosome, RsbP and SigB in *Bacillus subtilis*,” *J Basic Microbiol*, vol. 59, no. 8, pp. 834–845, Aug. 2019, doi: 10.1002/jobm.201900076.
[16] M. T. Cabeen, J. R. Russell, J. Paulsson, and R. Losick, “Use of a microfluidic platform to uncover basic features of energy and environmental stress responses in individual cells of Bacillus subtilis,” *PLoS Genet*, vol. 13, no. 7, p. e1006901, Jul. 2017, doi: 10.1371/journal.pgen.1006901.
[17] S. Akbar, C. M. Kang, T. A. Gaidenko, and C. W. Price, “Modulator protein RsbR regulates environmental signalling in the general stress pathway of Bacillus subtilis,” *Mol Microbiol*, vol. 24, no. 3, pp. 567–578, May 1997, doi: 10.1046/j.1365-2958.1997.3631732.x.
[18] T.-J. Kim, T. A. Gaidenko, and C. W. Price, “A multicomponent protein complex mediates environmental stress signaling in Bacillus subtilis,” *J Mol Biol*, vol. 341, no. 1, pp. 135–150, Jul. 2004, doi: 10.1016/j.jmb.2004.05.043.
[19] S. Akbar, T. A. Gaidenko, C. M. Kang, M. O’Reilly, K. M. Devine, and C. W. Price, “New family of regulators in the environmental signaling pathway which activates the general stress transcription factor sigma(B) of Bacillus subtilis,” *J Bacteriol*, vol. 183, no. 4, pp. 1329–1338, Feb. 2001, doi: 10.1128/JB.183.4.1329-1338.2001.
[20] S. Alper, A. Dufour, D. A. Garsin, L. Duncan, and R. Losick, “Role of adenosine nucleotides in the regulation of a stress-response transcription factor in Bacillus subtilis,” *J Mol Biol*, vol. 260, no. 2, pp. 165–177, Jul. 1996, doi: 10.1006/jmbi.1996.0390.
[21] O. Delumeau, R. J. Lewis, and M. D. Yudkin, “Protein-protein interactions that regulate the energy stress activation of sigma(B) in Bacillus subtilis,” *J Bacteriol*, vol. 184, no. 20, pp. 5583–5589, Oct. 2002, doi: 10.1128/JB.184.20.5583-5589.2002.
[22] U. Voelker, A. Voelker, B. Maul, M. Hecker, A. Dufour, and W. G. Haldenwang, “Separate mechanisms activate sigma B of Bacillus subtilis in response to environmental and metabolic stresses,” *J Bacteriol*, vol. 177, no. 13, pp. 3771–3780, Jul. 1995, doi: 10.1128/jb.177.13.3771-3780.1995.
[23] O. Delumeau, C.-C. Chen, J. W. Murray, M. D. Yudkin, and R. J. Lewis, “High-molecular-weight complexes of RsbR and paralogues in the environmental signaling pathway of Bacillus subtilis,” *J Bacteriol*, vol. 188, no. 22, Art. no. 22, Nov. 2006, doi: 10.1128/JB.00892-06.

[24] T. A. Gaidenko, X. Yang, Y. M. Lee, and C. W. Price, “Threonine phosphorylation of modulator protein RsbR governs its ability to regulate a serine kinase in the environmental stress signaling pathway of Bacillus subtilis,” *Journal of Molecular Biology*, vol. 288, no. 1, pp. 29–39, Apr. 1999, doi: 10.1006/jmbi.1999.2665.
[25] D. N. Guerreiro *et al.*, “Acid stress signals are integrated into the σB-dependent general stress response pathway via the stressosome in the food-borne pathogen Listeria monocytogenes,” *PLoS Pathog*, vol. 18, no. 3, p. e1010213, Mar. 2022, doi: 10.1371/journal.ppat.1010213.
[26] X. Yang, C. M. Kang, M. S. Brody, and C. W. Price, “Opposing pairs of serine protein kinases and phosphatases transmit signals of environmental stress to activate a bacterial transcription factor,” *Genes Dev*, vol. 10, no. 18, pp. 2265–2275, Sep. 1996, doi: 10.1101/gad.10.18.2265.
[27] A. K. Benson and W. G. Haldenwang, “Bacillus subtilis sigma B is regulated by a binding protein (RsbW) that blocks its association with core RNA polymerase,” *Proc Natl Acad Sci U S A*, vol. 90, no. 6, pp. 2330–2334, Mar. 1993, doi: 10.1073/pnas.90.6.2330.
[28] A. Dufour and W. G. Haldenwang, “Interactions between a Bacillus subtilis anti-sigma factor (RsbW) and its antagonist (RsbV),” *J Bacteriol*, vol. 176, no. 7, pp. 1813–1820, Apr. 1994, doi: 10.1128/jb.176.7.1813-1820.1994.
[29] A.-H. Teh *et al.*, “Structure of the RsbX phosphatase involved in the general stress response of *Bacillus subtilis*,” *Acta Crystallogr D Biol Crystallogr*, vol. 71, no. 6, pp. 1392–1399, Jun. 2015, doi: 10.1107/S1399004715007166.
[30] M. B. Quin, J. M. Berrisford, J. A. Newman, A. Baslé, R. J. Lewis, and J. Marles-Wright, “The Bacterial Stressosome: A Modular System that Has Been Adapted to Control Secondary Messenger Signaling,” *Structure*, vol. 20, no. 2, pp. 350–363, Feb. 2012, doi: 10.1016/j.str.2012.01.003.
[31] C. Dessaux, D. N. Guerreiro, M. G. Pucciarelli, C. P. O’Byrne, and F. García-del Portillo, “Impact of osmotic stress on the phosphorylation and subcellular location of Listeria monocytogenes stressosome proteins,” *Sci Rep*, vol. 10, no. 1, p. 20837, Dec. 2020, doi: 10.1038/s41598-020-77738-z.
[32] J. Marles-Wright *et al.*, “Molecular architecture of the ‘stressosome,’ a signal integration and transduction hub,” *Science*, vol. 322, no. 5898, pp. 92–96, Oct. 2008, doi: 10.1126/science.1159572.
[33] J. W. Murray, O. Delumeau, and R. J. Lewis, “Structure of a nonheme globin in environmental stress signaling,” *Proc. Natl. Acad. Sci. U.S.A.*, vol. 102, no. 48, pp. 17320–17325, Nov. 2005, doi: 10.1073/pnas.0506599102.
[34] S. Choi, Y. Nakasone, K. J. Hellingwerf, and M. Terazima, “Photoreaction Dynamics of a Full-Length Protein YtvA and Intermolecular Interaction with RsbRA,” *Biochemistry*, vol. 59, no. 50, pp. 4703–4710, Dec. 2020, doi: 10.1021/acs.biochem.0c00888.
[35] M. Avila-Pérez, K. J. Hellingwerf, and R. Kort, “Blue light activates the sigmaB-dependent stress response of Bacillus subtilis via YtvA,” *J Bacteriol*, vol. 188, no. 17, pp. 6411–6414, Sep. 2006, doi: 10.1128/JB.00716-06.
[36] T. A. Gaidenko, T.-J. Kim, A. L. Weigel, M. S. Brody, and C. W. Price, “The blue-light receptor YtvA acts in the environmental stress signaling pathway of Bacillus

subtilis," *J Bacteriol*, vol. 188, no. 17, pp. 6387–6395, Sep. 2006, doi: 10.1128/JB.00691-06.
[37] J. B. van der Steen and K. J. Hellingwerf, "Activation of the General Stress Response of *Bacillus subtilis* by Visible Light," *Photochem Photobiol*, vol. 91, no. 5, pp. 1032–1045, Sep. 2015, doi: 10.1111/php.12499.
[38] A. Reeves, L. Martinez, and W. Haldenwang, "Expression of, and in vivo stressosome formation by, single members of the RsbR protein family in Bacillus subtilis," *Microbiology (Reading)*, vol. 156, no. Pt 4, pp. 990–998, Apr. 2010, doi: 10.1099/mic.0.036095-0.
[39] L. Martinez, A. Reeves, and W. Haldenwang, "Stressosomes Formed in *Bacillus subtilis* from the RsbR Protein of *Listeria monocytogenes* Allow σ ^{B} Activation following Exposure to either Physical or Nutritional Stress," *J Bacteriol*, vol. 192, no. 23, pp. 6279–6286, Dec. 2010, doi: 10.1128/JB.00467-10.
[40] T. M. Norman, N. D. Lord, J. Paulsson, and R. Losick, "Memory and modularity in cell-fate decision making," *Nature*, vol. 503, no. 7477, pp. 481–486, Nov. 2013, doi: 10.1038/nature12804.
[41] D. K. Bol and R. E. Yasbin, "Characterization of an inducible oxidative stress system in Bacillus subtilis," *J Bacteriol*, vol. 172, no. 6, pp. 3503–3506, Jun. 1990, doi: 10.1128/jb.172.6.3503-3506.1990.
[42] R. E. Marquis, "Salt-induced contraction of bacterial cell walls," *J Bacteriol*, vol. 95, no. 3, pp. 775–781, Mar. 1968, doi: 10.1128/jb.95.3.775-781.1968.
[43] T. KovÃ¡cs, A. Hargitai, K. L. KovÃ¡cs, and I. MÃ©cs, "pH-dependent activation of the alternative transcriptional factor σ ^{B} in *Bacillus subtilis*," *FEMS Microbiology Letters*, vol. 165, no. 2, pp. 323–328, Aug. 1998, doi: 10.1111/j.1574-6968.1998.tb13164.x.
[44] B. C. A. Dowds, "The oxidative stress response in *Bacillus subtilis*," *FEMS Microbiology Letters*, vol. 124, no. 3, pp. 255–263, Dec. 1994, doi: 10.1111/j.1574-6968.1994.tb07294.x.
[45] M. Mols and T. Abee, "Primary and secondary oxidative stress in *Bacillus*: Oxidative stress in Bacilli," *Environmental Microbiology*, vol. 13, no. 6, pp. 1387–1394, Jun. 2011, doi: 10.1111/j.1462-2920.2011.02433.x.
[46] H. Antelmann, S. Engelmann, R. Schmid, and M. Hecker, "General and oxidative stress responses in Bacillus subtilis: cloning, expression, and mutation of the alkyl hydroperoxide reductase operon," *J Bacteriol*, vol. 178, no. 22, pp. 6571–6578, Nov. 1996, doi: 10.1128/jb.178.22.6571-6578.1996.
[47] J. B. van der Steen, M. Avila-Pérez, D. Knippert, A. Vreugdenhil, P. van Alphen, and K. J. Hellingwerf, "Differentiation of function among the RsbR paralogs in the general stress response of Bacillus subtilis with regard to light perception," *J Bacteriol*, vol. 194, no. 7, pp. 1708–1716, Apr. 2012, doi: 10.1128/JB.06705-11.
[48] J. W. Young, J. C. W. Locke, and M. B. Elowitz, "Rate of environmental change determines stress response specificity," *Proc. Natl. Acad. Sci. U.S.A.*, vol. 110, no. 10, pp. 4140–4145, Mar. 2013, doi: 10.1073/pnas.1213060110.
[49] T. A. Gaidenko, X. Bie, E. P. Baldwin, and C. W. Price, "Two Surfaces of a Conserved Interdomain Linker Differentially Affect Output from the RST Sensing Module of the Bacillus subtilis Stressosome," *J Bacteriol*, vol. 194, no. 15, pp. 3913–3921, Aug. 2012, doi: 10.1128/JB.00583-12.

[50] J. C. W. Locke, J. W. Young, M. Fontes, M. J. Hernández Jiménez, and M. B. Elowitz, "Stochastic pulse regulation in bacterial stress response," *Science*, vol. 334, no. 6054, pp. 366–369, Oct. 2011, doi: 10.1126/science.1208144.
[51] T. A. Gaidenko and C. W. Price, "General Stress Transcription Factor ς ^{B} and Sporulation Transcription Factor ς ^{H} Each Contribute to Survival of *Bacillus subtilis* under Extreme Growth Conditions," *J Bacteriol*, vol. 180, no. 14, pp. 3730–3733, Jul. 1998, doi: 10.1128/JB.180.14.3730-3733.1998.
[52] S. Gottesman, "Trouble is coming: Signaling pathways that regulate general stress responses in bacteria," *Journal of Biological Chemistry*, vol. 294, no. 31, pp. 11685–11700, Aug. 2019, doi: 10.1074/jbc.REV119.005593.
[53] J. B. van der Steen, *The general stress response of Bacillus subtilis*. S.l: s.n., 2013.
[54] F. Rodriguez Ayala, M. Bartolini, and R. Grau, "The Stress-Responsive Alternative Sigma Factor SigB of Bacillus subtilis and Its Relatives: An Old Friend With New Functions," *Front. Microbiol.*, vol. 11, p. 1761, Sep. 2020, doi: 10.3389/fmicb.2020.01761.
[55] C. W. Hamm, D. R. Butler, and M. T. Cabeen, "Bacillus subtilis Stressosome Sensor Protein Sequences Govern the Ability To Distinguish among Environmental Stressors and Elicit Different σ ^{B} Response Profiles," *mBio*, vol. 13, no. 6, pp. e02001-22, Dec. 2022, doi: 10.1128/mbio.02001-22.
[56] C. W. Hamm, S. F. Winburn, and M. T. Cabeen, "Using Fluorescence in Biotechnology Instruction to Visualize Antibiotic Resistance & DNA," *The American Biology Teacher*, vol. 83, no. 6, pp. 395–401, Aug. 2021, doi: 10.1525/abt.2021.83.6.395.
[57] J. Jeljaszewicz and J. Hawiger, "The resistance to antibiotics of strains of Streptococcus viridans, Streptococcus faecalis, Escherichia coli, Pseudomonas aeruginosa, Proteus and Klebsiella isolated in Poland," *Bull World Health Organ*, vol. 35, no. 2, pp. 243–246, 1966.
[58] I. Jurado-Martín, M. Sainz-Mejías, and S. McClean, "Pseudomonas aeruginosa: An Audacious Pathogen with an Adaptable Arsenal of Virulence Factors," *IJMS*, vol. 22, no. 6, p. 3128, Mar. 2021, doi: 10.3390/ijms22063128.
[59] N. Høiby, O. Ciofu, and T. Bjarnsholt, "*Pseudomonas aeruginosa* biofilms in cystic fibrosis," *Future Microbiology*, vol. 5, no. 11, pp. 1663–1674, Nov. 2010, doi: 10.2217/fmb.10.125.
[60] M. Qadi *et al.*, "Surfactant Protein A Recognizes Outer Membrane Protein OprH on *Pseudomonas aeruginosa* Isolates From Individuals With Chronic Infection," *J Infect Dis.*, vol. 214, no. 9, pp. 1449–1455, Nov. 2016, doi: 10.1093/infdis/jiw387.
[61] C. Schwarzer, H. Fischer, and T. E. Machen, "Chemotaxis and Binding of Pseudomonas aeruginosa to Scratch-Wounded Human Cystic Fibrosis Airway Epithelial Cells," *PLoS ONE*, vol. 11, no. 3, p. e0150109, Mar. 2016, doi: 10.1371/journal.pone.0150109.
[62] L. L. Burrows, "*Pseudomonas aeruginosa* Twitching Motility: Type IV Pili in Action," *Annu. Rev. Microbiol.*, vol. 66, no. 1, pp. 493–520, Oct. 2012, doi: 10.1146/annurev-micro-092611-150055.
[63] A. Anantharajah, M.-P. Mingeot-Leclercq, and F. Van Bambeke, "Targeting the Type Three Secretion System in Pseudomonas aeruginosa," *Trends in Pharmacological Sciences*, vol. 37, no. 9, pp. 734–749, Sep. 2016, doi: 10.1016/j.tips.2016.05.011.

[64] M. Mei, J. Thomas, and S. P. Diggle, "Heterogenous Susceptibility to R-Pyocins in Populations of Pseudomonas aeruginosa Sourced from Cystic Fibrosis Lungs," *mBio*, vol. 12, no. 3, pp. e00458-21, Jun. 2021, doi: 10.1128/mBio.00458-21.
[65] O. Oluyombo, C. N. Penfold, and S. P. Diggle, "Competition in Biofilms between Cystic Fibrosis Isolates of *Pseudomonas aeruginosa* Is Shaped by R-Pyocins," *mBio*, vol. 10, no. 1, pp. e01828-18, Feb. 2019, doi: 10.1128/mBio.01828-18.
[66] R. D. Waite and M. A. Curtis, "*Pseudomonas aeruginosa* PAO1 Pyocin Production Affects Population Dynamics within Mixed-Culture Biofilms," *J Bacteriol*, vol. 191, no. 4, pp. 1349–1354, Feb. 2009, doi: 10.1128/JB.01458-08.
[67] S. R. Williams, D. Gebhart, D. W. Martin, and D. Scholl, "Retargeting R-Type Pyocins To Generate Novel Bactericidal Protein Complexes," *Appl Environ Microbiol*, vol. 74, no. 12, pp. 3868–3876, Jun. 2008, doi: 10.1128/AEM.00141-08.
[68] D. Scholl, "Phage Tail–Like Bacteriocins," *Annu. Rev. Virol.*, vol. 4, no. 1, pp. 453–467, Sep. 2017, doi: 10.1146/annurev-virology-101416-041632.
[69] K. Nakayama *et al.*, "The R-type pyocin of Pseudomonas aeruginosa is related to P2 phage, and the F-type is related to lambda phage," *Mol Microbiol*, vol. 38, no. 2, pp. 213–231, Oct. 2000, doi: 10.1046/j.1365-2958.2000.02135.x.
[70] S. Saha *et al.*, "F-type Pyocins are Diverse Non-Contractile Phage Tail-Like Weapons for Killing *Pseudomonas aeruginosa*," Microbiology, preprint, Feb. 2021. doi: 10.1101/2021.02.16.431561.
[71] P. Ge *et al.*, "Action of a minimal contractile bactericidal nanomachine," *Nature*, vol. 580, no. 7805, pp. 658–662, Apr. 2020, doi: 10.1038/s41586-020-2186-z.
[72] Y. Michel-Briand and C. Baysse, "The pyocins of Pseudomonas aeruginosa," *Biochimie*, vol. 84, no. 5–6, pp. 499–510, May 2002, doi: 10.1016/S0300-9084(02)01422-0.
[73] T. Köhler, V. Donner, and C. van Delden, "Lipopolysaccharide as Shield and Receptor for R-Pyocin-Mediated Killing in *Pseudomonas aeruginosa*," *J Bacteriol*, vol. 192, no. 7, pp. 1921–1928, Apr. 2010, doi: 10.1128/JB.01459-09.
[74] Y. Uratani and T. Hoshino, "Pyocin R1 inhibits active transport in Pseudomonas aeruginosa and depolarizes membrane potential," *J Bacteriol*, vol. 157, no. 2, pp. 632–636, Feb. 1984, doi: 10.1128/jb.157.2.632-636.1984.
[75] R. T. Cirz, B. M. O'Neill, J. A. Hammond, S. R. Head, and F. E. Romesberg, "Defining the *Pseudomonas aeruginosa* SOS Response and Its Role in the Global Response to the Antibiotic Ciprofloxacin," *J Bacteriol*, vol. 188, no. 20, pp. 7101–7110, Oct. 2006, doi: 10.1128/JB.00807-06.
[76] W. Chang, D. A. Small, F. Toghrol, and W. E. Bentley, "Microarray analysis of Pseudomonas aeruginosa reveals induction of pyocin genes in response to hydrogen peroxide," *BMC Genomics*, vol. 6, no. 1, p. 115, Dec. 2005, doi: 10.1186/1471-2164-6-115.
[77] H. Matsui, Y. Sano, H. Ishihara, and T. Shinomiya, "Regulation of pyocin genes in Pseudomonas aeruginosa by positive (prtN) and negative (prtR) regulatory genes," *J Bacteriol*, vol. 175, no. 5, pp. 1257–1263, Mar. 1993, doi: 10.1128/jb.175.5.1257-1263.1993.
[78] N. S. Baggett, A. S. Bronson, and M. T. Cabeen, "SOS-Independent Pyocin Production in P. aeruginosa Is Induced by XerC Recombinase Deficiency," *mBio*, vol. 12, no. 6, p. e0289321, Dec. 2021, doi: 10.1128/mBio.02893-21.

[79] Z. Sun *et al.*, "PrtR Homeostasis Contributes to Pseudomonas aeruginosa Pathogenesis and Resistance against Ciprofloxacin," *Infect Immun*, vol. 82, no. 4, pp. 1638–1647, Apr. 2014, doi: 10.1128/IAI.01388-13.
[80] M. M. Cox, "Recombinational DNA Repair in Bacteria and the RecA Protein," in *Progress in Nucleic Acid Research and Molecular Biology*, Elsevier, 1999, pp. 311–366. doi: 10.1016/S0079-6603(08)60726-6.
[81] E. M. Seitz, J. P. Brockman, S. J. Sandler, A. J. Clark, and S. C. Kowalczykowski, "RadA protein is an archaeal RecA protein homolog that catalyzes DNA strand exchange," *Genes Dev*, vol. 12, no. 9, pp. 1248–1253, May 1998, doi: 10.1101/gad.12.9.1248.
[82] A. Shinohara, H. Ogawa, and T. Ogawa, "Rad51 protein involved in repair and recombination in S. cerevisiae is a RecA-like protein," *Cell*, vol. 69, no. 3, pp. 457–470, May 1992, doi: 10.1016/0092-8674(92)90447-k.
[83] R. N. Klitgaard, B. Jana, L. Guardabassi, K. L. Nielsen, and A. Løbner-Olesen, "DNA Damage Repair and Drug Efflux as Potential Targets for Reversing Low or Intermediate Ciprofloxacin Resistance in E. coli K-12," *Front. Microbiol.*, vol. 9, p. 1438, Jul. 2018, doi: 10.3389/fmicb.2018.01438.
[84] T. Horii, T. Ogawa, T. Nakatani, T. Hase, H. Matsubara, and H. Ogawa, "Regulation of SOS functions: purification of E. coli LexA protein and determination of its specific site cleaved by the RecA protein," *Cell*, vol. 27, no. 3 Pt 2, pp. 515–522, Dec. 1981, doi: 10.1016/0092-8674(81)90393-7.
[85] B. Gao, L. Liang, L. Su, A. Wen, C. Zhou, and Y. Feng, "Structural basis for regulation of SOS response in bacteria," *Proc. Natl. Acad. Sci. U.S.A.*, vol. 120, no. 2, p. e2217493120, Jan. 2023, doi: 10.1073/pnas.2217493120.
[86] E. M. Witkin, "RecA protein in the SOS response: milestones and mysteries," *Biochimie*, vol. 73, no. 2–3, pp. 133–141, Feb. 1991, doi: 10.1016/0300-9084(91)90196-8.
[87] K. C. Giese, C. B. Michalowski, and J. W. Little, "RecA-Dependent Cleavage of LexA Dimers," *Journal of Molecular Biology*, vol. 377, no. 1, pp. 148–161, Mar. 2008, doi: 10.1016/j.jmb.2007.12.025.
[88] J. Penterman, P. K. Singh, and G. C. Walker, "Biological Cost of Pyocin Production during the SOS Response in Pseudomonas aeruginosa," *J Bacteriol*, vol. 196, no. 18, pp. 3351–3359, Sep. 2014, doi: 10.1128/JB.01889-14.
[89] L. Turnbull *et al.*, "Explosive cell lysis as a mechanism for the biogenesis of bacterial membrane vesicles and biofilms," *Nat Commun*, vol. 7, no. 1, p. 11220, Apr. 2016, doi: 10.1038/ncomms11220.
[90] R. Young, "Bacteriophage lysis: mechanism and regulation," *Microbiol Rev*, vol. 56, no. 3, pp. 430–481, Sep. 1992, doi: 10.1128/mr.56.3.430-481.1992.
[91] R. Young, "Bacteriophage holins: deadly diversity," *J Mol Microbiol Biotechnol*, vol. 4, no. 1, pp. 21–36, Jan. 2002.
[92] K. A. McFarland *et al.*, "A self-lysis pathway that enhances the virulence of a pathogenic bacterium," *Proc. Natl. Acad. Sci. U.S.A.*, vol. 112, no. 27, pp. 8433–8438, Jul. 2015, doi: 10.1073/pnas.1506299112.
[93] A. S. Bronson, N. S. Baggett, and M. T. Cabeen, "DNA Damage-Inducible Pyocin Expression Is Independent of RecA in *xerC* -Deleted Pseudomonas aeruginosa,"

Microbiol Spectr, vol. 10, no. 4, pp. e01167-22, Aug. 2022, doi: 10.1128/spectrum.01167-22.
[94] G. Blakely, S. Colloms, G. May, M. Burke, and D. Sherratt, "Escherichia coli XerC recombinase is required for chromosomal segregation at cell division," *New Biol*, vol. 3, no. 8, pp. 789–798, Aug. 1991.
[95] S. C. Y. Ip, "Decatenation of DNA circles by FtsK-dependent Xer site-specific recombination," *The EMBO Journal*, vol. 22, no. 23, pp. 6399–6407, Dec. 2003, doi: 10.1093/emboj/cdg589.
[96] L. R. Hmelo *et al.*, "Precision-engineering the Pseudomonas aeruginosa genome with two-step allelic exchange," *Nat Protoc*, vol. 10, no. 11, pp. 1820–1841, Nov. 2015, doi: 10.1038/nprot.2015.115.
[97] Z. Podlesek and D. Žgur Bertok, "The DNA Damage Inducible SOS Response Is a Key Player in the Generation of Bacterial Persister Cells and Population Wide Tolerance," *Front. Microbiol.*, vol. 11, p. 1785, Aug. 2020, doi: 10.3389/fmicb.2020.01785.
[98] H. Jiao, F. Li, T. Wang, J. K. H. Yam, L. Yang, and H. Liang, "The Pyocin Regulator PrtR Regulates Virulence Expression of Pseudomonas aeruginosa by Modulation of Gac/Rsm System and c-di-GMP Signaling Pathway," *Infect Immun*, vol. 89, no. 2, pp. e00602-20, Jan. 2021, doi: 10.1128/IAI.00602-20.
[99] C. Weigel and H. Seitz, "Bacteriophage replication modules," *FEMS Microbiol Rev*, vol. 30, no. 3, pp. 321–381, May 2006, doi: 10.1111/j.1574-6976.2006.00015.x.
[100] A. A. Aksyuk and M. G. Rossmann, "Bacteriophage Assembly," *Viruses*, vol. 3, no. 3, pp. 172–203, Feb. 2011, doi: 10.3390/v3030172.
[101] J. Grote, D. Krysciak, and W. R. Streit, "Phenotypic Heterogeneity, a Phenomenon That May Explain Why Quorum Sensing Does Not Always Result in Truly Homogenous Cell Behavior," *Appl Environ Microbiol*, vol. 81, no. 16, pp. 5280–5289, Aug. 2015, doi: 10.1128/AEM.00900-15.
[102] S. E. Darch, S. A. West, K. Winzer, and S. P. Diggle, "Density-dependent fitness benefits in quorum-sensing bacterial populations," *Proc. Natl. Acad. Sci. U.S.A.*, vol. 109, no. 21, pp. 8259–8263, May 2012, doi: 10.1073/pnas.1118131109.
[103] A. Podbielski and B. Kreikemeyer, "Cell density – dependent regulation: basic principles and effects on the virulence of Gram-positive cocci," *International Journal of Infectious Diseases*, vol. 8, no. 2, pp. 81–95, Mar. 2004, doi: 10.1016/j.ijid.2003.04.003.
[104] Y. Sano and M. Kageyama, "The sequence and function of the recA gene and its protein in Pseudomonas aeruginosa PAO," *Mol Gen Genet*, vol. 208, no. 3, pp. 412–419, Jul. 1987, doi: 10.1007/BF00328132.
[105] W. Wu and S. Jin, "PtrB of *Pseudomonas aeruginosa* Suppresses the Type III Secretion System under the Stress of DNA Damage," *J Bacteriol*, vol. 187, no. 17, pp. 6058–6068, Sep. 2005, doi: 10.1128/JB.187.17.6058-6068.2005.
[106] M. Fernandez *et al.*, "Characterization of the bacteriocins and the PrtR regulator in a plant-associated Pseudomonas strain," *Journal of Biotechnology*, vol. 307, pp. 182–192, Jan. 2020, doi: 10.1016/j.jbiotec.2019.11.003.
[107] S. Garde, P. K. Chodisetti, and M. Reddy, "Peptidoglycan: Structure, Synthesis, and Regulation," *EcoSal Plus*, vol. 9, no. 2, p. ecosalplus.ESP-0010-2020, Dec. 2021, doi: 10.1128/ecosalplus.ESP-0010-2020.

[108] Ž. Pandur, M. Dular, R. Kostanjšek, and D. Stopar, "Bacterial cell wall material properties determine E. coli resistance to sonolysis," *Ultrasonics Sonochemistry*, vol. 83, p. 105919, Feb. 2022, doi: 10.1016/j.ultsonch.2022.105919.

[109] P. Ge, D. Scholl, P. G. Leiman, X. Yu, J. F. Miller, and Z. H. Zhou, "Atomic structures of a bactericidal contractile nanotube in its pre- and postcontraction states," *Nat Struct Mol Biol*, vol. 22, no. 5, pp. 377–382, May 2015, doi: 10.1038/nsmb.2995.

[110] F. Arisaka, J. Tschopp, R. van Driel, and J. Engel, "Reassembly of the bacteriophage T4 tail from the core-baseplate and the monomeric sheath protein P18: A co-operative association process," *Journal of Molecular Biology*, vol. 132, no. 3, pp. 369–386, Aug. 1979, doi: 10.1016/0022-2836(79)90266-3.

[111] L. Xiang *et al.*, "CRISPR-dCas9-mediated knockdown of *prtR* , an essential gene in *Pseudomonas aeruginosa*," *Lett Appl Microbiol*, p. lam.13337, Jun. 2020, doi: 10.1111/lam.13337.

[112] H. Mikkelsen, M. Sivaneson, and A. Filloux, "Key two-component regulatory systems that control biofilm formation in Pseudomonas aeruginosa: Two-component systems in Pseudomonas aeruginosa biofilms," *Environmental Microbiology*, vol. 13, no. 7, pp. 1666–1681, Jul. 2011, doi: 10.1111/j.1462-2920.2011.02495.x.

[113] J. C. Davies, "Pseudomonas aeruginosa in cystic fibrosis: pathogenesis and persistence," *Paediatric Respiratory Reviews*, vol. 3, no. 2, pp. 128–134, Jun. 2002, doi: 10.1016/S1526-0550(02)00003-3.

[114] J. Davies and D. Davies, "Origins and Evolution of Antibiotic Resistance," *MMBR*, vol. 74, no. 3, pp. 417–433, Sep. 2010, doi: 10.1128/MMBR.00016-10.

[115] Z. Pang, R. Raudonis, B. R. Glick, T.-J. Lin, and Z. Cheng, "Antibiotic resistance in Pseudomonas aeruginosa: mechanisms and alternative therapeutic strategies," *Biotechnology Advances*, vol. 37, no. 1, pp. 177–192, Jan. 2019, doi: 10.1016/j.biotechadv.2018.11.013.

[116] M. Redero, C. López-Causapé, J. Aznar, A. Oliver, J. Blázquez, and A. I. Prieto, "Susceptibility to R-pyocins of Pseudomonas aeruginosa clinical isolates from cystic fibrosis patients," *Journal of Antimicrobial Chemotherapy*, vol. 73, no. 10, pp. 2770–2776, Oct. 2018, doi: 10.1093/jac/dky261.

[117] A. Six, K. Mosbahi, M. Barge, C. Kleanthous, T. Evans, and D. Walker, "Pyocin efficacy in a murine model of *Pseudomonas aeruginosa* sepsis," *Journal of Antimicrobial Chemotherapy*, vol. 76, no. 9, pp. 2317–2324, Aug. 2021, doi: 10.1093/jac/dkab199.

[118] A. Alqahtani *et al.*, "Recombinant R2-pyocin cream is effective in treating *Pseudomonas aeruginosa*- infected wounds," *Can. J. Microbiol.*, vol. 67, no. 12, pp. 919–932, Dec. 2021, doi: 10.1139/cjm-2021-0207.

[119] D. Scholl and D. W. Martin, "Antibacterial Efficacy of R-Type Pyocins towards *Pseudomonas aeruginosa* in a Murine Peritonitis Model," *Antimicrob Agents Chemother*, vol. 52, no. 5, pp. 1647–1652, May 2008, doi: 10.1128/AAC.01479-07.

[120] F. Hayes and D. J. Sherratt, "Recombinase binding specificity at the chromosome dimer resolution site dif of Escherichia coli 1 1Edited by I. B. Holland," *Journal of Molecular Biology*, vol. 266, no. 3, pp. 525–537, Feb. 1997, doi: 10.1006/jmbi.1996.0828.

[121] F. Castillo, A. Benmohamed, and G. Szatmari, “Xer Site Specific Recombination: Double and Single Recombinase Systems,” *Front. Microbiol.*, vol. 8, Mar. 2017, doi: 10.3389/fmicb.2017.00453.

[122] M. Tecklenburg, A. Naumer, O. Nagappan, and P. Kuempel, “The dif resolvase locus of the Escherichia coli chromosome can be replaced by a 33-bp sequence, but function depends on location.,” *Proc. Natl. Acad. Sci. U.S.A.*, vol. 92, no. 5, pp. 1352–1356, Feb. 1995, doi: 10.1073/pnas.92.5.1352.

APPENDICES

Note: The following Text S1 and Figure S1-S8 is published in the ASM journal mBio, with published work located at [55].

Supplemental Text S1. Detailed Modes of Strain and Plasmid Construction, Strains and Primer Sequences

The markerless gene replacement in the strains below were added in succession using the pminiMAD vector (gift of Daniel Kearns). A pminiMAD vector propagated in E. coli and containing the desired gene was directly transformed into PY79 via competence {Wilson, 1968 #1148} and selected on MLS (0.5 μg/ml erythromycin and 2.5 μg/ml lincomycin). A phage SPP1 lysate was prepared from that intermediate strain, and the recipient strain was phage-transduced with the PY79 strain containing the desired chromosomally integrated pminiMAD vector and again selected on MLS. Five to 10 transductants were then inoculated into liquid LB and kept in exponential phase at approximately 25°C for several hours to permit plasmid excision before being repeatedly diluted and grown in liquid LB at 37°C (restrictive for plasmid replication) to promote loss of excised plasmid. The cells were then plated, and single colonies were screened for the successful replacement by colony PCR, restreaked for single colonies, patched on plain LB and LB/MLS plates to verify plasmid loss, restreaked, verified by PCR and stored at -80°C.

MTC2540

MTC 1761 was transduced with lysate from PY79 pminiMAD-rsbRC/A as described above to produce 3610 hagA233V ΔytvA ΔrsbRB ΔrsbRC ΔrsbRD rsbRA::RsbRC/A.

MTC2541

MTC 1765 was transduced with lysate from PY79 pminiMAD-rsbRA/C as described above to produce 3610 hagA233V ΔytvA ΔrsbRA ΔrsbRB ΔrsbRD rsbRC::RsbRA/C.

MTC2542

MTC 1763 was transduced with lysate from PY79 *pminiMAD-rsbRC/B* as described above to produce 3610 *hagA233V ΔytvA ΔrsbRA ΔrsbRC ΔrsbRD rsbRB::RsbRC/B*.

MTC2543

MTC 1765 was transduced with lysate from PY79 *pminiMAD-rsbRB/C* as described above to produce 3610 *hagA233V ΔytvA ΔrsbRA ΔrsbRB ΔrsbRD rsbRC::RsbRB/C*.

MTC2544

MTC 1761 was transduced with lysate from PY79 *pminiMAD-rsbRD/A* as described above to produce 3610 *hagA233V ΔytvA ΔrsbRB ΔrsbRC ΔrsbRD rsbRA::RsbRD/A*.

MTC2545

MTC 1767 was transduced with lysate from PY79 *pminiMAD-rsbRA/D* as described above to produce 3610 *hagA233V ΔytvA ΔrsbRA ΔrsbRC ΔrsbRD rsbRD::RsbRA/D*.

MTC2546

MTC 1761 was transduced with lysate from PY79 *pminiMAD-rsbRB/A* as described above to produce 3610 *hagA233V ΔytvA ΔrsbRA ΔrsbRB ΔrsbRD rsbRC::RsbRB/A*.

MTC2547

MTC 1763 was transduced with lysate from PY79 *pminiMAD-rsbRA/B* as described above to produce 3610 *hagA233V ΔytvA ΔrsbRB ΔrsbRC ΔrsbRD rsbRA::RsbRA/B*.

Plasmid construction

pminiMAD-rsbRC/A

Plasmid pminiMAD was linearized with EcoRI and HindIII. An upstream fragment containing the 5' flanking region upstream of *rsbRA* was amplified with primers 689/776. The middle fragment, containing the gene sequence encoding the variable region of RsbRC, was amplified with primers 777/778. The downstream fragment, containing the

gene sequence encoding the conserved region of RsbRA and the flanking 3' region was amplified with primers 779/692. Each fragment contained an overlapping region with the adjacent fragment to allow stitching of all pieces together. All fragments were gel purified, and then isothermally assembled {Gibson, 2009 #989} with the linearized pminiMAD. The resulting plasmid was propagated in E. coli and confirmed by sequencing.

pminiMAD-rsbRA/C

Plasmid pminiMAD was linearized with EcoRI and HindIII. An upstream fragment containing the 5' flanking region upstream of *rsbRC* was amplified with primers 694/948. The middle fragment, containing the gene sequence encoding the variable region of RsbRA, was amplified with primers 949/950. The downstream fragment, containing the gene sequence encoding the conserved region of RsbRC and the flanking 3' region was amplified with primers 951/700. Each fragment contained an overlapping region with the adjacent fragment to allow stitching of all pieces together. All fragments were gel purified, and then isothermally assembled {Gibson, 2009 #989} with the linearized pminiMAD. The resulting plasmid was propagated in E. coli and confirmed by sequencing.

pminiMAD-rsbRA/D

Plasmid pminiMAD was linearized with EcoRI and HindIII. An upstream fragment containing the 5' flanking region upstream of *rsbRD* was amplified with primers 701/1058. The middle fragment, containing the gene sequence encoding the variable region of RsbRA, was amplified with primers 1059/1060. The downstream fragment, containing the gene sequence encoding the conserved region of RsbRD and the flanking 3' region was amplified with primers 1061/704. Each fragment contained an overlapping region with the adjacent fragment to allow stitching of all pieces together. All fragments were gel purified, and then isothermally assembled {Gibson, 2009 #989} with the linearized pminiMAD. The resulting plasmid was propagated in E. coli and confirmed by sequencing.

pminiMAD-rsbRD/A

Plasmid pminiMAD was linearized with EcoRI and HindIII. An upstream fragment containing the 5' flanking region upstream of *rsbRA* was amplified with primers 689/1070.

The middle fragment, containing the gene sequence encoding the variable region of RsbRD, was amplified with primers 1071/1072. The downstream fragment, containing the gene sequence encoding the conserved region of RsbRA and the flanking 3' region was amplified with primers 1073/692. Each fragment contained an overlapping region with the adjacent fragment to allow stitching of all pieces together. All fragments were gel purified, and then isothermally assembled {Gibson, 2009 #989} with the linearized pminiMAD. The resulting plasmid was propagated in E. coli and confirmed by sequencing.

pminiMAD-rsbRB/A

Plasmid pminiMAD was linearized with EcoRI and HindIII. An upstream fragment containing the 5' flanking region upstream of *rsbRA* was amplified with primers 689/1062. The middle fragment, containing the gene sequence encoding the variable region of RsbRB, was amplified with primers 1063/1064. The downstream fragment, containing the gene sequence encoding the conserved region of RsbRA and the flanking 3' region was amplified with primers 1065/692. Each fragment contained an overlapping region with the adjacent fragment to allow stitching of all pieces together. All fragments were gel purified, and then isothermally assembled {Gibson, 2009 #989} with the linearized pminiMAD. The resulting plasmid was propagated in E. coli and confirmed by sequencing.

pminiMAD-rsbRA/B

Plasmid pminiMAD was linearized with EcoRI and HindIII. An upstream fragment containing the 5' flanking region upstream of *rsbRB* was amplified with primers 693/1066. The middle fragment, containing the gene sequence encoding the variable region of RsbRA, was amplified with primers 1067/1068. The downstream fragment, containing the gene sequence encoding the conserved region of RsbRB and the flanking 3' region was amplified with primers 1069/696. Each fragment contained an overlapping region with the adjacent fragment to allow stitching of all pieces together. All fragments were gel purified, and then isothermally assembled {Gibson, 2009 #989} with the linearized pminiMAD. The resulting plasmid was propagated in E. coli and confirmed by sequencing.

pminiMAD-rsbRB/C

Plasmid pminiMAD was linearized with EcoRI and HindIII. An upstream fragment containing the 5' flanking region upstream of *rsbRC* was amplified with primers 697/952. The middle fragment, containing the gene sequence encoding the variable region of RsbRB, was amplified with primers 953/954. The downstream fragment, containing the gene sequence encoding the conserved region of RsbRC and the flanking 3' region was amplified with primers 955/700. Each fragment contained an overlapping region with the adjacent fragment to allow stitching of all pieces together. All fragments were gel purified, and then isothermally assembled {Gibson, 2009 #989} with the linearized pminiMAD. The resulting plasmid was propagated in E. coli and confirmed by sequencing.

pminiMAD-rsbRC/B

Plasmid pminiMAD was linearized with EcoRI and HindIII. An upstream fragment containing the 5' flanking region upstream of *rsbRB* was amplified with primers 693/956. The middle fragment, containing the gene sequence encoding the variable region of RsbRC, was amplified with primers 957/958. The downstream fragment, containing the gene sequence encoding the conserved region of RsbRB and the flanking 3' region was amplified with primers 959/696. Each fragment contained an overlapping region with the adjacent fragment to allow stitching of all pieces together. All fragments were gel purified, and then isothermally assembled {Gibson, 2009 #989} with the linearized pminiMAD. The resulting plasmid was propagated in E. coli and confirmed by sequencing.

Strains or plasmid	**Relevant genotype or description**	**Source or reference**
B. subtilis Strains		
MTC52	PY79	Cabeen et al. 2017
MTC53	3610	Cabeen et al. 2017
Plasmids		
pminiMAD	Suicide plasmid for *B. subtilis* markerless allelic replacement	Lab Strain from Daniel Kearns
pminiMAD -RsbRC/A	pminiMAD-based markerless deletion plasmid for *rsbRC/A*	This Study

pminiMAD-RsbRA/C	pminiMAD-based markerless deletion plasmid for *rsbRA/C*	This Study
pminiMAD-RsbRC/B	pminiMAD-based markerless deletion plasmid for *rsbRC/B*	This Study
pminiMAD-RsbRB/A	pminiMAD-based markerless deletion plasmid for *rsbRB/C*	This Study
pminiMAD-RsbRD/A	pminiMAD-based markerless deletion plasmid for *rsbRD/A*	This Study
pminiMAD-RsbRA/D	pminiMAD-based markerless deletion plasmid for *rsbRA/D*	This Study
pminiMAD-RsbRB/A	pminiMAD-based markerless deletion plasmid for *rsbRB/A*	This Study
pminiMAD-RsbRA/B	pminiMAD-based markerless deletion plasmid for *rsbRA/B*	This Study
Primer Name	**Primer Sequence (often contains 5' extensions for assembly that do not anneal to the template)**	
689	AACAGCTATGACCATGATTACGCCAAGCTTCGGCTATATGGAAATGGCG	Cabeen et al. 2017
692	CGTTGTAAAACGACGGCCAGTGAATTCTTCCTCTGTCTGCGACCTG	Cabeen et al. 2017
693	AACAGCTATGACCATGATTACGCCAAGCTTTCGCCGCCAAGAACCTTC	Cabeen et al. 2017
696	CGTTGTAAAACGACGGCCAGTGAATTCTGTCGGCATCTCTCTCGGG	Cabeen et al. 2017
697	AACAGCTATGACCATGATTACGCCAAGCTTGGCAGCCATGAATTTTGCG	Cabeen et al. 2017
700	CGTTGTAAAACGACGGCCAGTGAATTCCAAGAGCTCATCAACGCTTGC	Cabeen et al. 2017
701	AACAGCTATGACCATGATTACGCCAAGCTTATATCCAAGCTGCACGTC	Cabeen et al. 2017
704	CGTTGTAAAACGACGGCCAGTGAATTCGTGCTGTTTTCCATGCTGAC	Cabeen et al. 2017
776	TTTTTGCCATCAAATTCGCTTACCTCCCAATAAAAAAC	This Study
777	AGCGAATTTGATGGCAAAAAACAAAAAATTATTCGAG	This Study
778	GCGCAGACAGTTCAGTAATCATATCTTTTTGGGCC	This Study
779	GATTACTGAACTGTCTGCGCCGCTTATCC	This Study
948	AGTCTGGTTCGACATGATTGATCACCTCTTTTAAA	This Study
949	AAGAGGTGATCAATCATGTCGAACCAGACTGTATA	This Study
950	GGAGCGCTCAACTCTTGCAGCG	This Study
951	GCTGCAAGAGTTGAGCGCTCCGGTC	This Study
952	TTCATTCAGTTTCATGATTGATCACCTCTT	This Study
953	CATTTAAAAGAGGTGATCAATCATGAAACTGAATGA	This Study

954	GCACGATGACCGGAGCGCTCAATTCCAATATCAT	This Study
955	TGATATTGGAATTGAGCGCTCCGG	This Study
956	TTTTTTGTTTTTTGCCATGACACTGCTCCT	This Study
957	GAGCAGTGTCATGGCAAAAAACAA	This Study
958	GGGTAATGACAGGTGAGCTCAATTCAGTAA	This Study
959	ATATGATTACTGAATTGAGCTCACCTGTCATTA=	This Study
1058	ACAGTCTGGTTCGACATCTTAATGAGTTACC	This Study
1059	AACTCATTAAGATGTCGAACCAGACTGTAT	This Study
1060	GCATAATCGGCGCACTCAACTCTTGCAG	This Study
1061	AGAGTTGAGTGCGCCGATTATGC	This Study
1062	TCAGTTTCATCAAATTCGCTTACCTCCCAAT	This Study
1063	GGAGGTAAGCGAATTTGATGAAACTGAATGA	This Study
1064	CGGCGCAGACAGTAATTCCAATATCATTT	This Study
1065	TGATATTGGAATTACTGTCTGCGCCGCTTA	This Study
1066	GTTCGACATGACACTGCTCCTTTCCCCAAC	This Study
1067	GGAAAGGAGCAGTGTCATGTCGAAC	This Study
1068	CAGGTGAGCTTAACTCTTGCAGCGCGATTT	This Study
1069	GCGCTGCAAGAGTTAAGCTCACCTGTCATT	This Study
1070	ATCAAGAGCTATCATCAAATTCGCTTACC	This Study
1071	AAGCGAATTTGATGATAGCTCTTGATCAG	This Study
1072	AGCGGCGCAGACAGTTCATTAATCATTTC	This Study
1073	AATGATTAATGAACTGTCTGCGCCGCTTA	This Study

Supplemental Table 1. A list of primers used in the study of chapter 1.

Supplemental Text S2. Detailed Modes of Strain and Plasmid Construction, Strains and Primer Sequences

The markerless gene replacement in the strains below were added in succession using the pminiMAD vector (gift of Daniel Kearns). A pminiMAD vector propagated in E. coli and containing the desired gene was directly transformed into PY79 via competence {Wilson, 1968 #1148} and selected on MLS (0.5 μg/ml erythromycin and 2.5 μg/ml lincomycin). A phage SPP1 lysate was prepared from that intermediate strain, and the recipient strain was phage-transduced with the PY79 strain containing the desired chromosomally integrated pMiniMAD vector and again selected on MLS. Five to 10 transductants were then inoculated into liquid LB and kept in exponential phase at approximately 25°C for several hours to permit plasmid excision before being repeatedly diluted and grown in liquid LB at 37°C (restrictive for plasmid replication) to promote loss of excised plasmid. The cells were then plated, and single colonies were screened for the successful replacement by colony PCR, restreaked for single colonies, patched on plain LB and LB/MLS plates to verify plasmid loss, restreaked, verified by PCR and stored at -80°C. Hybrid strain construction was performed as specified below using PY79 lysates from Hamm et al, 2022 [55].

CSS 408

MTC 1672 was transduced with lysate from PY79 containing constitutive mKate2 as described above to produce 3610 *ΔytvA*.

CSS 409

MTC 1697 was transduced with lysate from PY79 containing constitutive mKate2 as described above to produce 3610 *ΔytvA ΔrsbRB ΔrsbRC ΔrsbRD*.

CSS 410

MTC 1695 was transduced with lysate from PY79 containing constitutive mKate2 as described above to produce 3610 *ΔytvA ΔrsbRA ΔrsbRC ΔrsbRD*.

CSS 411

MTC 1693 was transduced with lysate from PY79 containing constitutive mKate2 as described above to produce 3610 *ΔytvA ΔrsbRA ΔrsbRB ΔrsbRD*.

CSS 412

MTC 1691 was transduced with lysate from PY79 containing constitutive mKate2 as described above to produce 3610 *ΔytvA ΔrsbRA ΔrsbRB ΔrsbRC*.

CSS 414

MTC 1672 was transduced with lysate from PY79 containing constitutive GFP as described above to produce 3610 *ΔytvA*.

CSS 415

MTC 1697 was transduced with lysate from PY79 containing constitutive GFP as described above to produce 3610 *ΔytvA ΔrsbRB ΔrsbRC ΔrsbRD*.

CSS 416

MTC 1695 was transduced with lysate from PY79 containing constitutive GFP as described above to produce 3610 *ΔytvA ΔrsbRA ΔrsbRC ΔrsbRD*.

CSS 417

MTC 1693 was transduced with lysate from PY79 containing constitutive GFP as described above to produce 3610 *ΔytvA ΔrsbRA ΔrsbRB ΔrsbRD*.

CSS 418

MTC 1691 was transduced with lysate from PY79 containing constitutive GFP as described above to produce 3610 *ΔytvA ΔrsbRA ΔrsbRB ΔrsbRC*

MTC 1973

MTC 1801 was transduced with lysate from PY79 containing a phage JRR227 producing a *ΔrsbRA* phenotype.

CSS 1256

MTC 1697 was transduced with a lysate from a phage from PY79 *pminiMAD-rsbRD/A* as described above to produce 3610 *ΔytvA ΔrsbRB ΔrsbRC ΔrsbRD rsbRA::RsbRD/A*. This strain was then transduced again with either a constitutive GFP or RFP reporter.

CSS 1259

MTC 1695 was transduced with a lysate from a phage from PY79 *pminiMAD-rsbRA/B* as described above to produce 3610 *ΔytvA ΔrsbRA ΔrsbRC ΔrsbRD rsbRB::RsbRA/B*. This strain was then transduced again with either a constitutive GFP or RFP reporter.

CSS 1262

MTC 1693 was transduced with a lysate from a phage from PY79 *pminiMAD-rsbRB/C* as described above to produce 3610 *ΔytvA ΔrsbRA ΔrsbRB ΔrsbRD rsbRC::RsbRB/C*. This strain was then transduced again with either a constitutive GFP or RFP reporter.

CSS 1265

MTC 1695 was transduced with a lysate from a phage from PY79 *pminiMAD-rsbRC/B* as described above to produce 3610 *ΔytvA ΔrsbRA ΔrsbRC ΔrsbRD rsbRB::RsbRC/B*. This strain was then transduced again with either a constitutive GFP or RFP reporter.

CSS 1265

MTC 1695 was transduced with a lysate from a phage from PY79 *pminiMAD-rsbRC/B* as described above to produce 3610 *ΔytvA ΔrsbRA ΔrsbRC ΔrsbRD rsbRB::RsbRC/B*. This strain was then transduced again with either a constitutive GFP or RFP reporter.

CSS 1268

MTC 1691 was transduced with a lysate from a phage from PY79 *pminiMAD-rsbRA/D* as described above to produce 3610 *ΔytvA ΔrsbRA ΔrsbRB ΔrsbRC rsbRD::RsbRA/D*. This strain was then transduced again with either a constitutive GFP or RFP reporter.

CSS 1271

MTC 1693 was transduced with a lysate from a phage from PY79 *pminiMAD-rsbRA/C* as described above to produce 3610 *ΔytvA ΔrsbRA ΔrsbRB ΔrsbRD rsbRC::RsbRA/C*. This strain was then transduced again with either a constitutive GFP or RFP reporter.

CSS 1274

MTC 1697 was transduced with a lysate from a phage from PY79 *pminiMAD-rsbRB/A* as described above to produce 3610 *ΔytvA ΔrsbRA ΔrsbRC ΔrsbRD rsbRA::RsbRB/A*. This strain was then transduced again with either a constitutive GFP or RFP reporter.

CSS 1277

MTC 1697 was transduced with a lysate from a phage from PY79 *pminiMAD-rsbRC/A* as described above to produce 3610 *ΔytvA ΔrsbRA ΔrsbRC ΔrsbRD rsbRA::RsbRC/A*. This strain was then transduced again with either a constitutive GFP or RFP reporter.

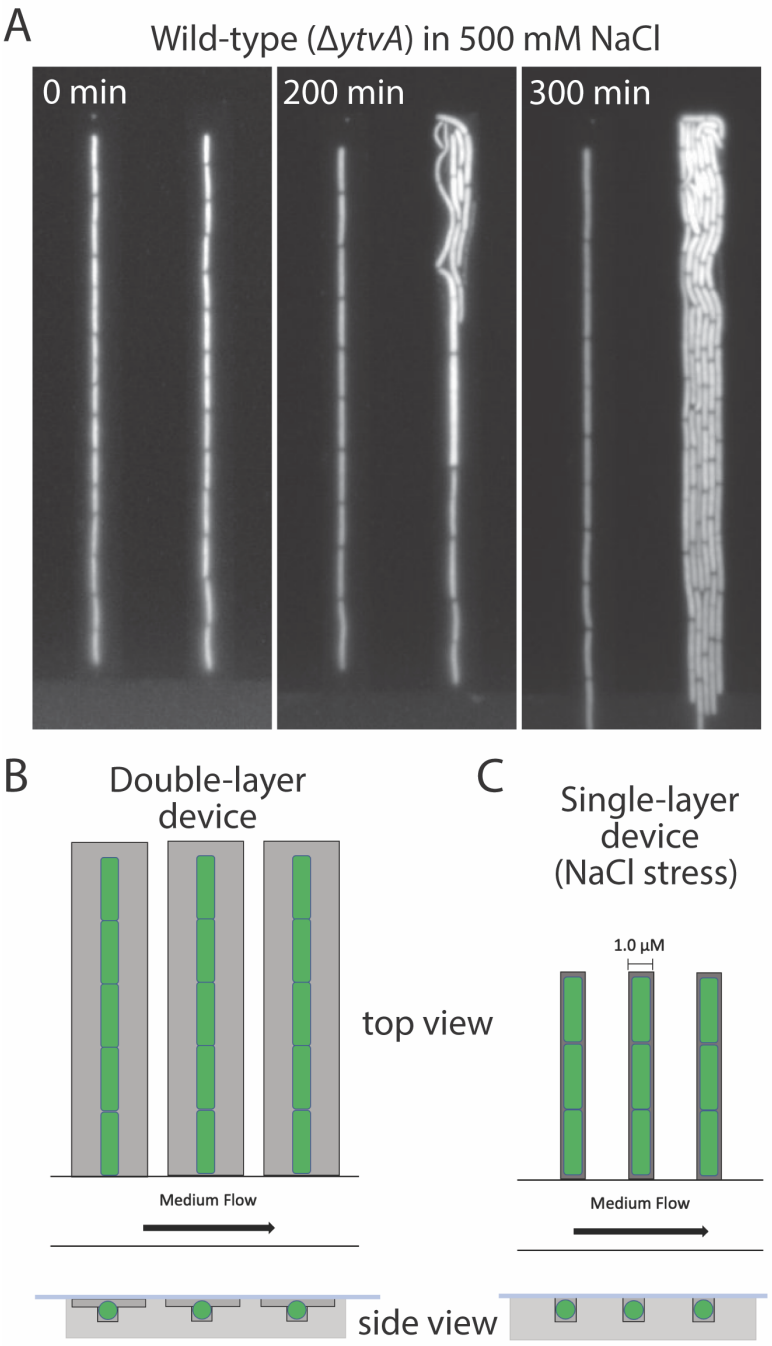

Figure S1. Microfluidic devices with and without a shallow channel surround. **(A)** Micrographs illustrating the filling of the shallow region surrounding the central cell channel with cells undergoing NaCl treatment. At an early time point (0 min), the cells were confined to the central deep channel. However, 200 min later, cells began to fill the shallow surrounding region, and the region was completely filled with cells 300 min later. **(B)** Schematic of cells confined in the central cell channel in a double-layer device (with two feature depths) with shallow surrounding region. The channel length is not to scale. **(C)** Schematic of cells confined in a single-layer device to prevent cell escape from a single-file line. The length is not to scale, but such channels are shorter to ensure diffusion of nutrients and additives to cells.

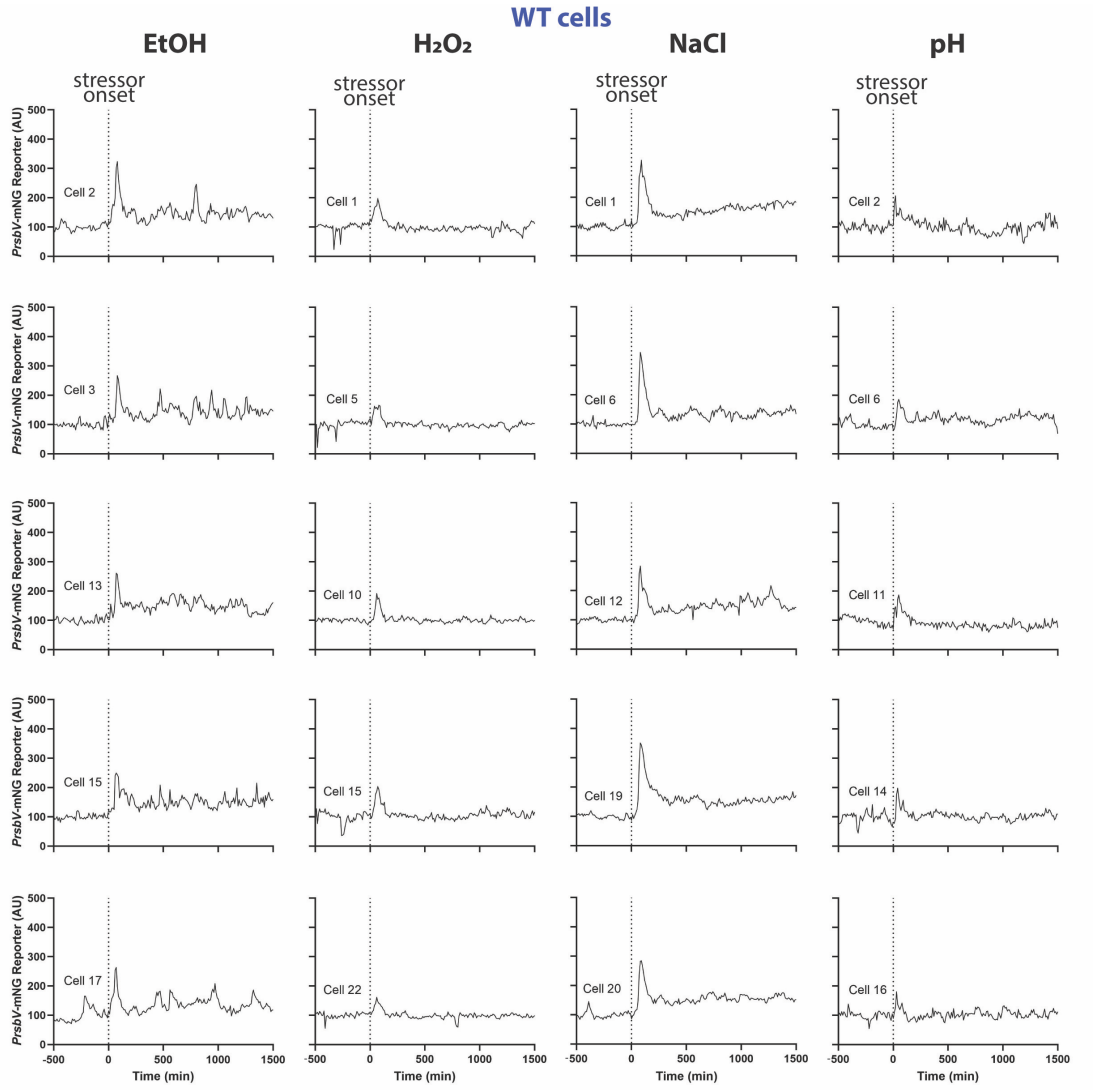

Figure S2. P_{rsbV}-mNeonGreen (σ^B reporter) traces for individual wild-type cell lineages in different stressors. Traces from individual cells, corresponding to the ensemble and average traces shown in Figure 1.3, are shown. Each column shows traces from five individual cells challenged with the stressor shown at the top of the column. EtOH, 2% ethanol; H_2O_2, 0.005% hydrogen peroxide; NaCl, 500 mM NaCl; pH, shift from pH 6.5 to 6.25.

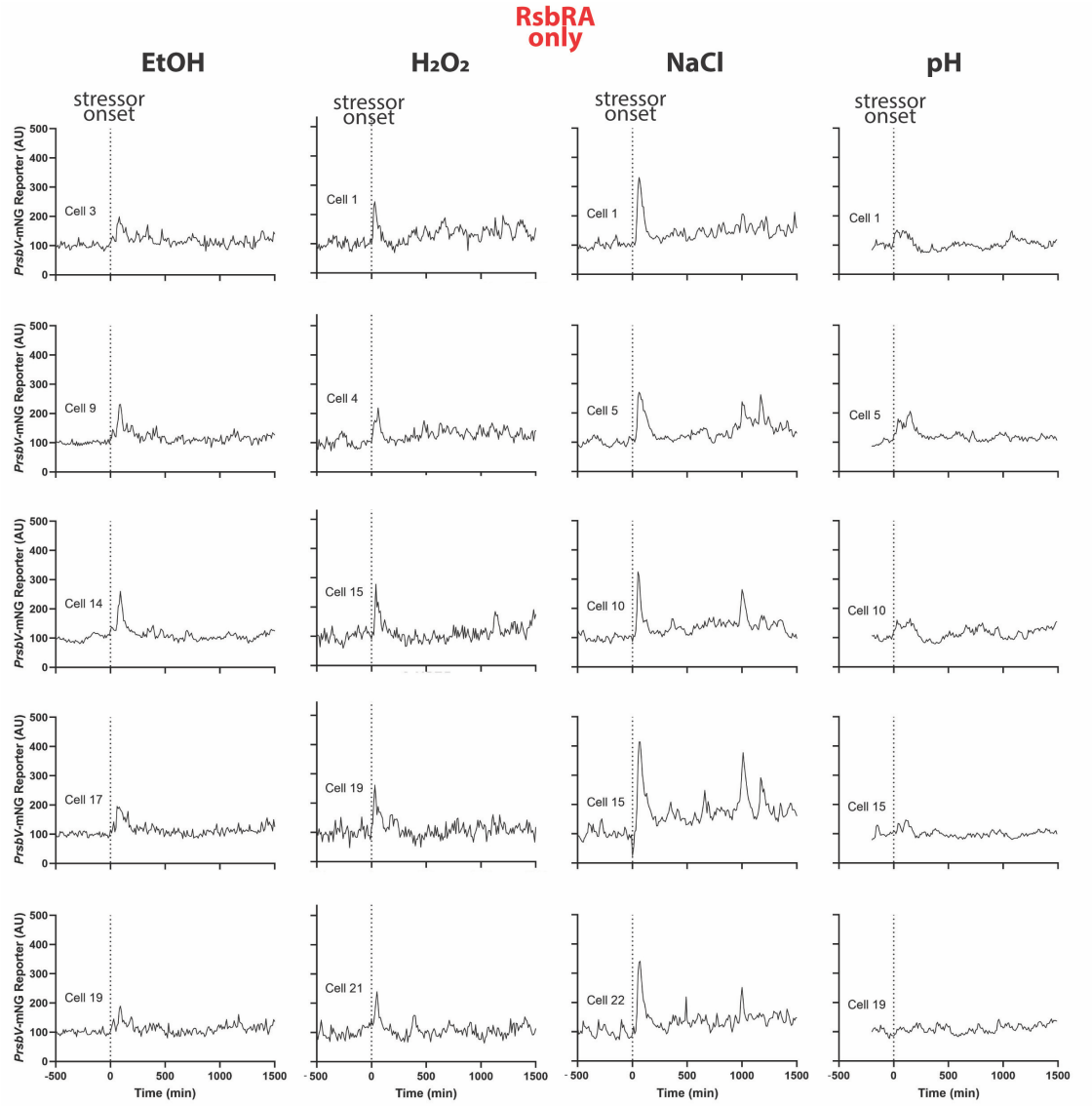

Figure S3. P*rsbV*-mNeonGreen (σ^B reporter) traces for individual RsbRA-only cell lineages in different stressors. Traces from individual cells, corresponding to the ensemble and average traces shown in Figure 1.4, are shown. Each column shows traces from five individual cells challenged with the stressor shown at the top of the column. EtOH, 2% ethanol; H_2O_2, 0.005% hydrogen peroxide; NaCl, 500 mM NaCl; pH, shift from pH 6.5 to 6.25.

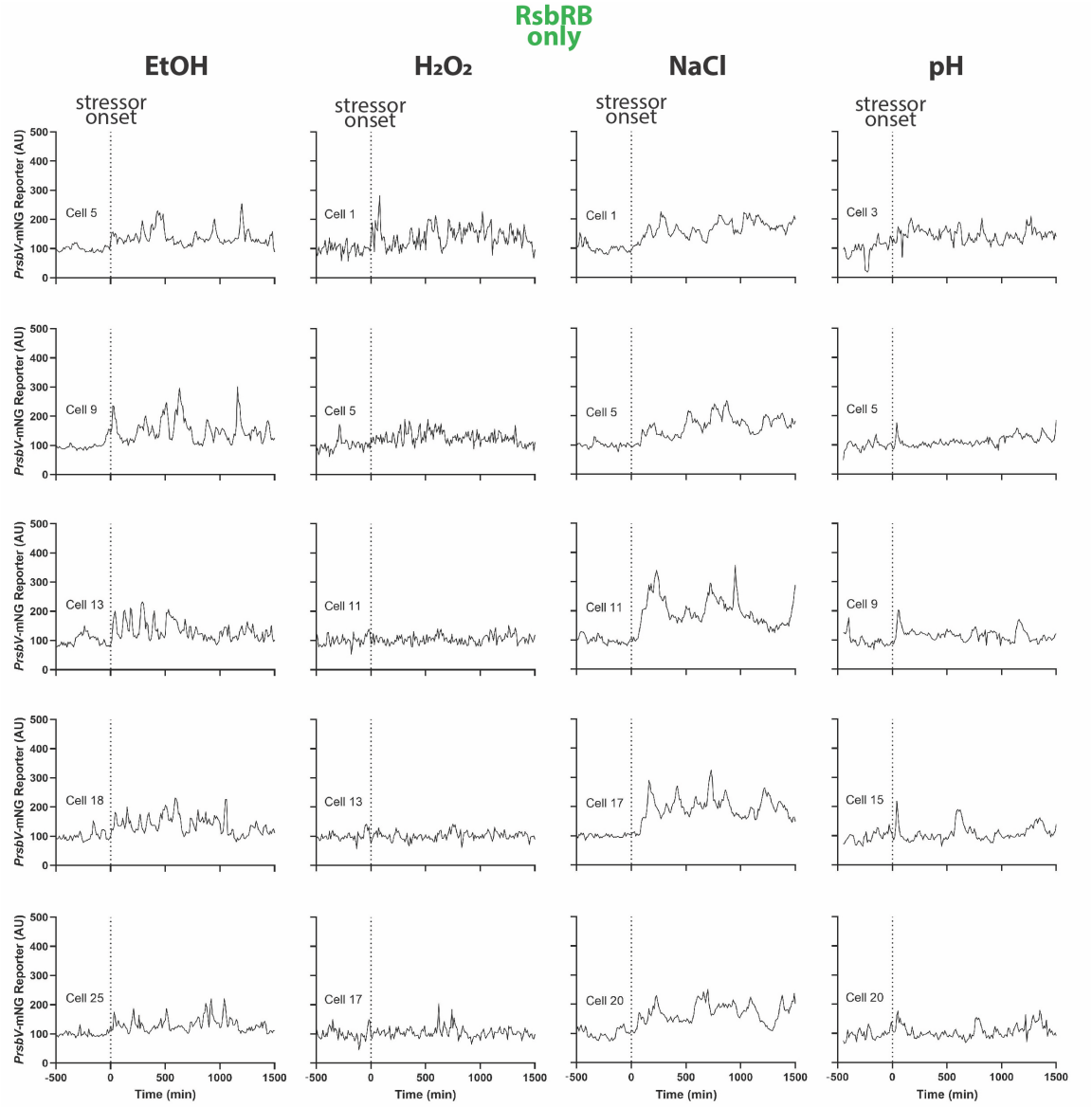

Figure S4. P*rsbV*-mNeonGreen (σ^B reporter) traces for individual RsbRB-only cell lineages in different stressors. Traces from individual cells, corresponding to the ensemble and average traces shown in Figure 1.5, are shown. Each column shows traces from five individual cells challenged with the stressor shown at the top of the column. EtOH, 2% ethanol; H_2O_2, 0.005% hydrogen peroxide; NaCl, 500 mM NaCl; pH, shift from pH 6.5 to 6.25

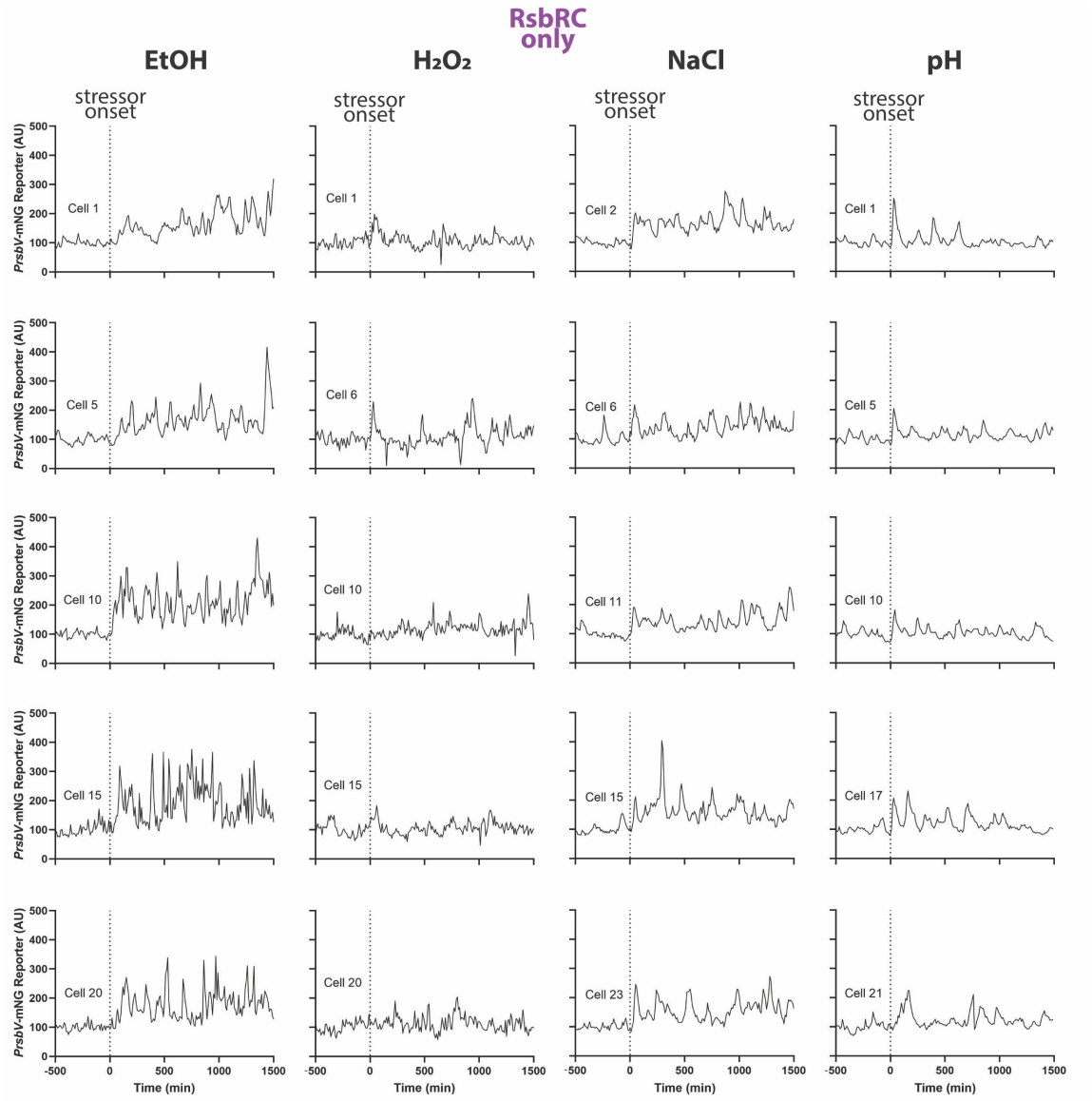

Figure S5. P*rsbV*-mNeonGreen (σ^B reporter) traces for individual RsbRC-only cell lineages in different stressors. Traces from individual cells, corresponding to the ensemble and average traces shown in Figure 1.6, are shown. Each column shows traces from five individual cells challenged with the stressor shown at the top of the column. EtOH, 2% ethanol; H_2O_2, 0.005% hydrogen peroxide; NaCl, 500 mM NaCl; pH, shift from pH 6.5 to 6.25.

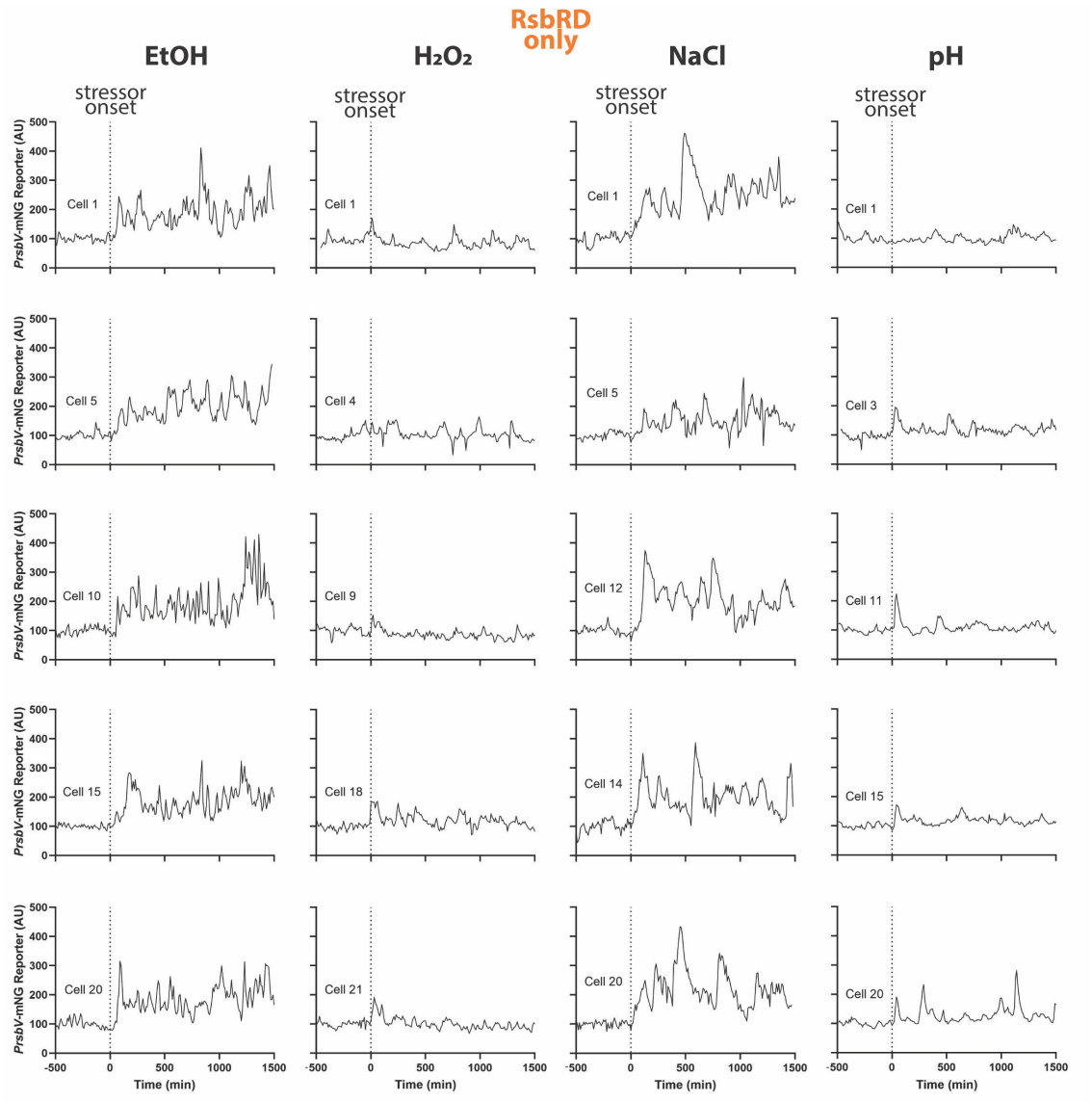

Figure S6. P*rsbV*-mNeonGreen (σ^B reporter) traces for individual RsbRD-only cell lineages in different stressors. Traces from individual cells, corresponding to the ensemble and average traces shown in Figure 1.7, are shown. Each column shows traces from five individual cells challenged with the stressor shown at the top of the column. EtOH, 2% ethanol; H_2O_2, 0.005% hydrogen peroxide; NaCl, 500 mM NaCl; pH, shift from pH 6.5 to 6.25.

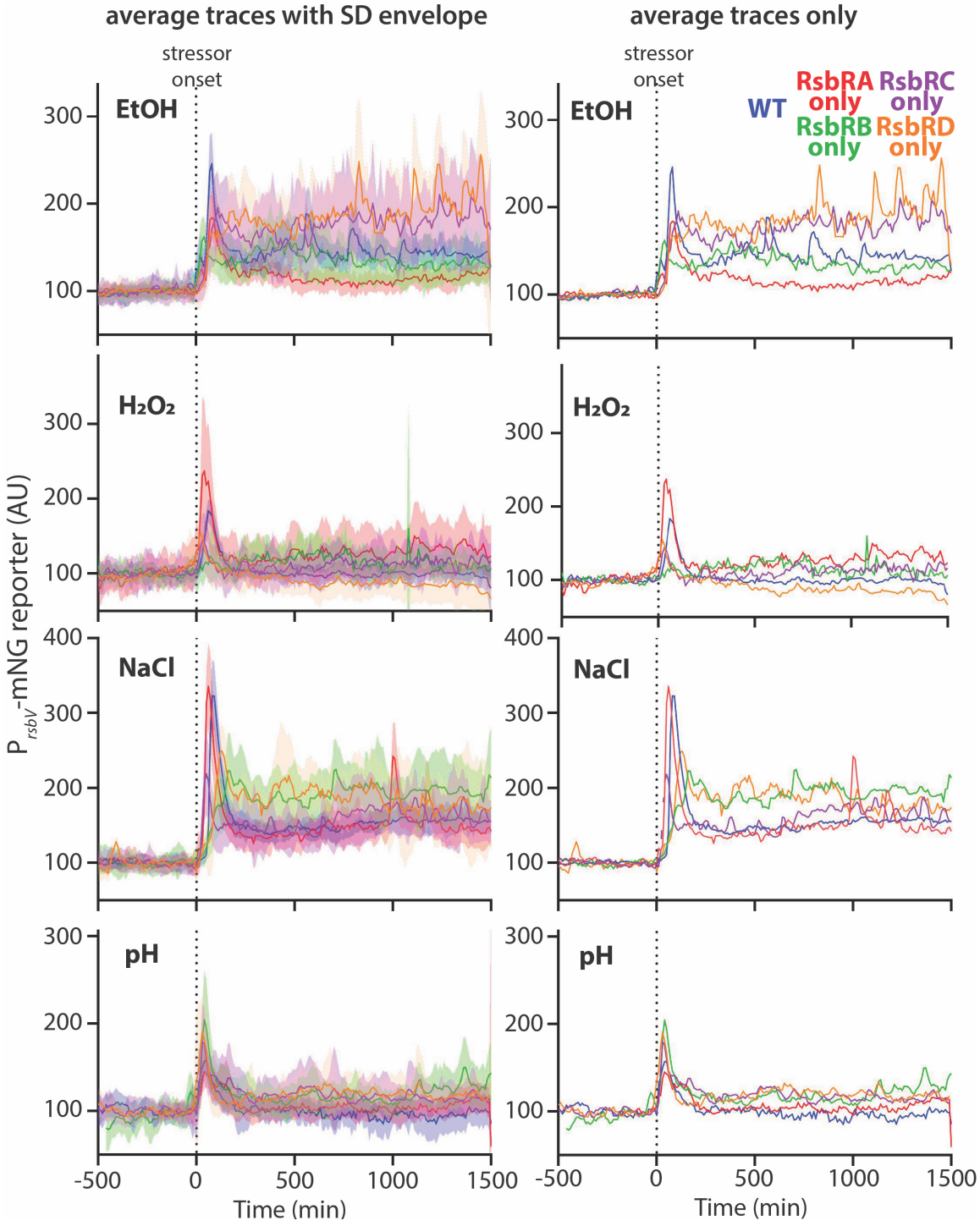

Figure S7. Average σ^B reporter traces grouped by stressor. For convenient comparison, the average traces for each strain (wild-type and each RsbR paralog on its own) in the indicated stressor are shown in different colors on the same plot. The left column shows the average traces with a shaded standard deviation envelope. The right column shows the same average traces without the envelope, for clarity. EtOH, 2% ethanol; H_2O_2, 0.005% hydrogen peroxide; NaCl, 500 mM NaCl; pH, shift from pH 6.5 to 6.25.

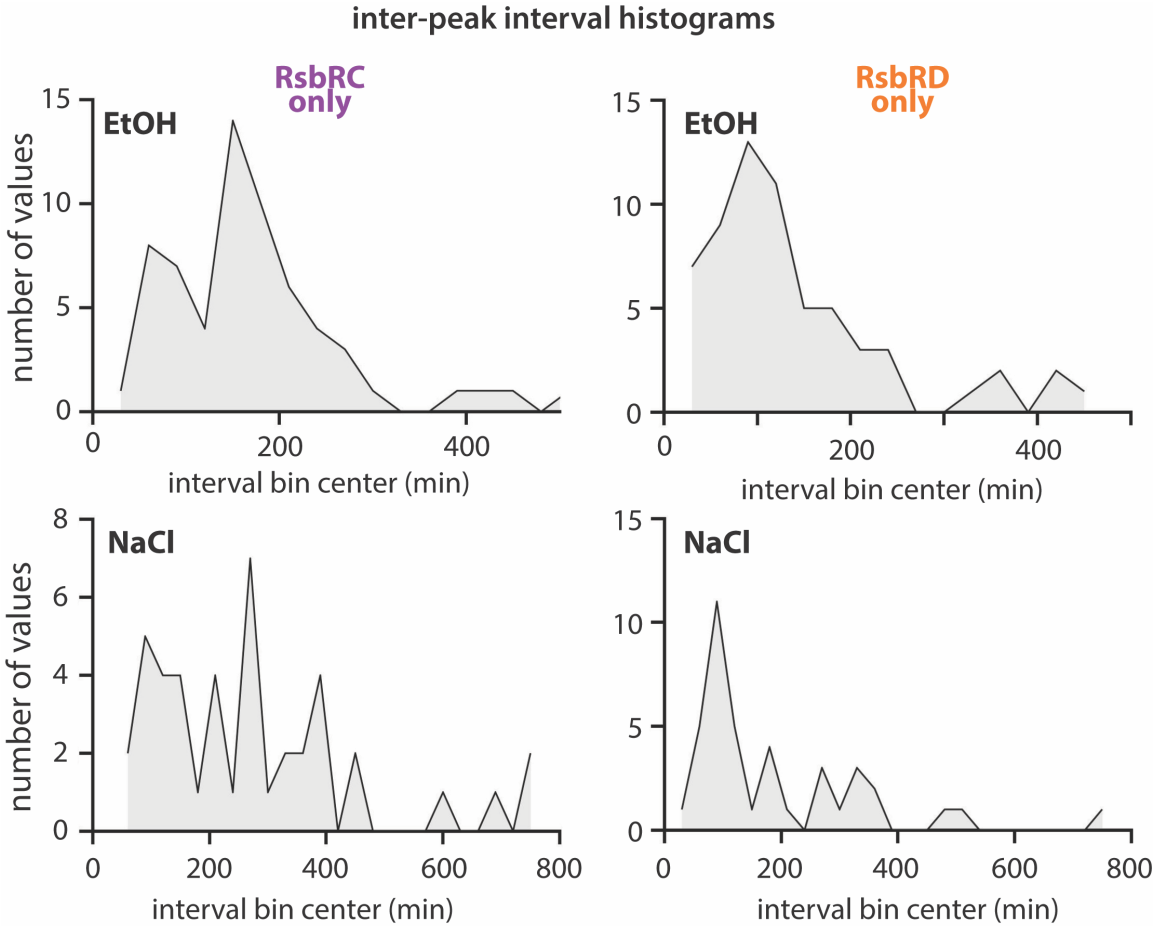

Figure S8. Distributions of intervals between response peaks in selected strain/stressor combinations. To detect whether the repeated σ^B responses observed in certain strains had any characteristic frequency, a set of at least five randomly selected cells from two different strains (RsbRC-only, RsbRD-only) and two different stressors (EtOH and NaCl) were manually analyzed for inter-response peak times (between 40 and 62 intervals were analyzed for each strain/stressor combination). Thresholds of 150 and 200 arbitrary fluorescence units were used to identify peaks in NaCl and EtOH, respectively. The interpeak times were then plotted as histograms (20-min bins) to display the frequency distribution.

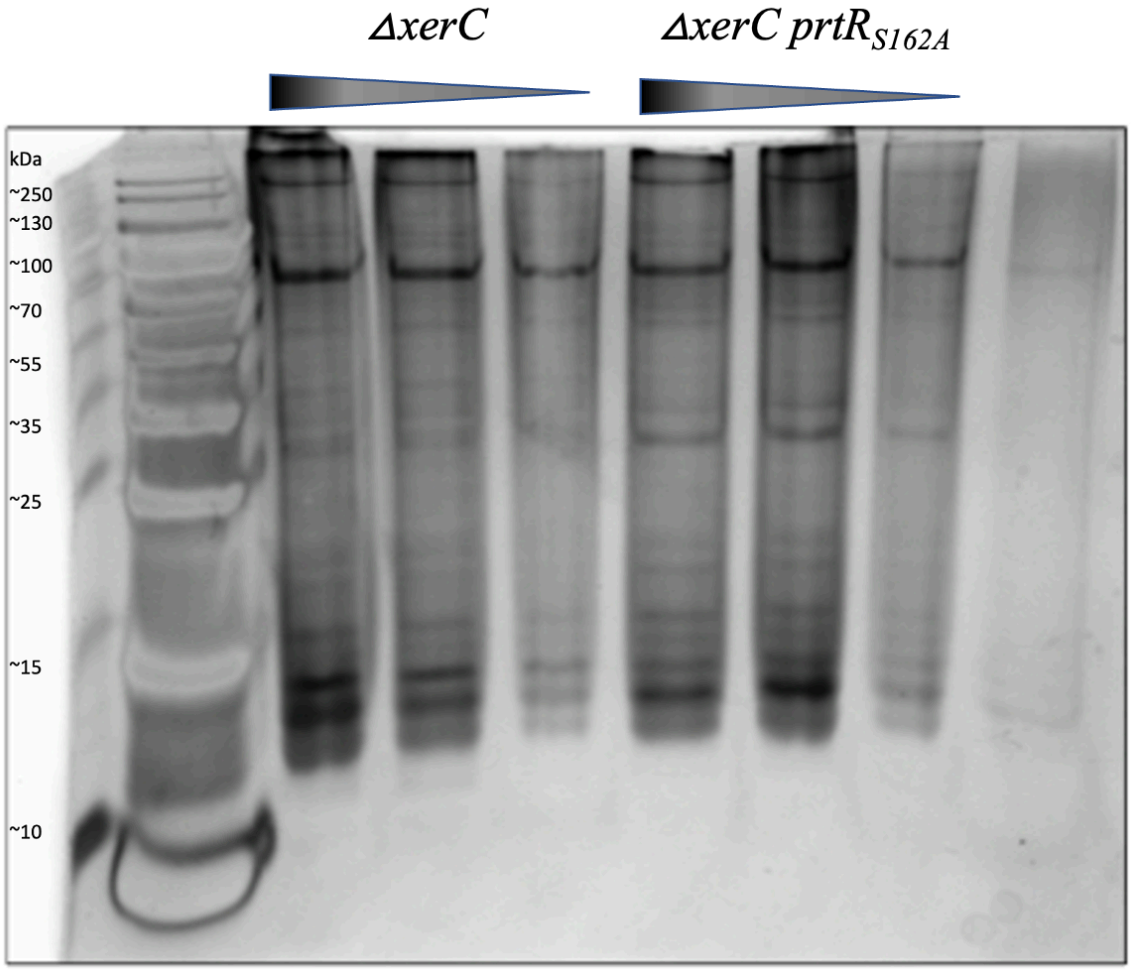

Figure S9. SDS-PAGE gel of purified lysates for pyocins of PA14 *ΔxerC* (MTC2266) and PA14 *ΔxerC prtR$_{S162A}$* (MTC2304). Gel was silver stained using Invitrogen SilverQuest Staining Kit.

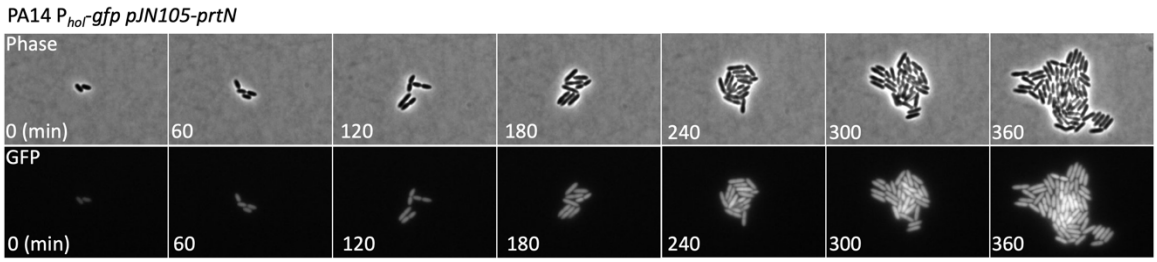

Figure S10. Time lapse microscopy of PA14 P$_{hol}$-*gfp pJN105-prtN* (HAM155) with inducible *prtN* expression. *prtN* was induced with 1% agarose both in culture prior to spotting on agarose pad, as well as in the agarose pad itself.

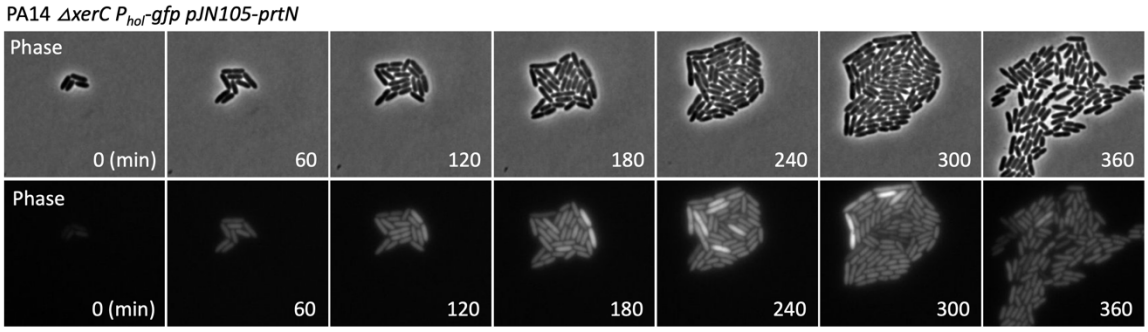

Figure S11. Time lapse microscopy of PA14 *ΔxerC* P$_{hol}$*-gfp pJN105-prtN* (HAM157) with inducible *prtN* expression. *prtN* was induced with 1% agarose both in culture prior to spotting on agarose pad, as well as in the agarose pad itself.

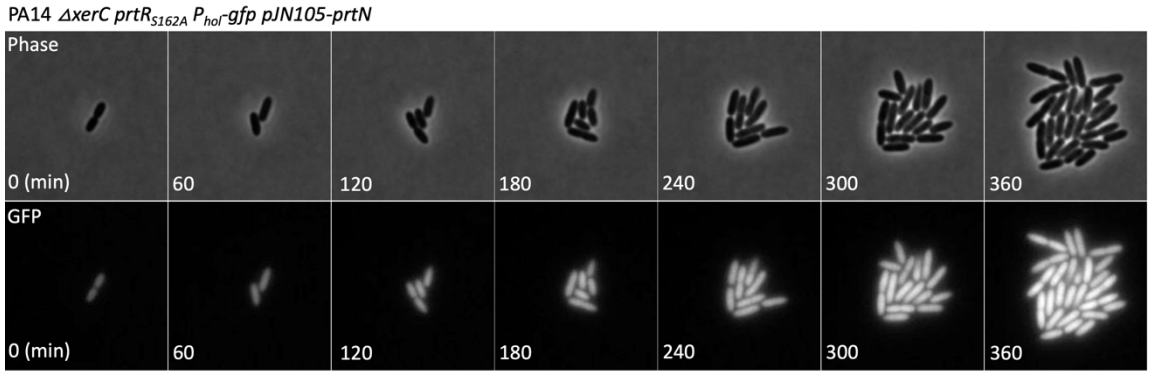

Figure S12. Time lapse microscopy of PA14 *ΔxerC prtR*$_{S162A}$ P$_{hol}$*-gfp pJN105-prtN* (HAM158) with inducible *prtN* expression. *prtN* was induced with 1% agarose both in culture prior to spotting on agarose pad, as well as in the agarose pad itself.

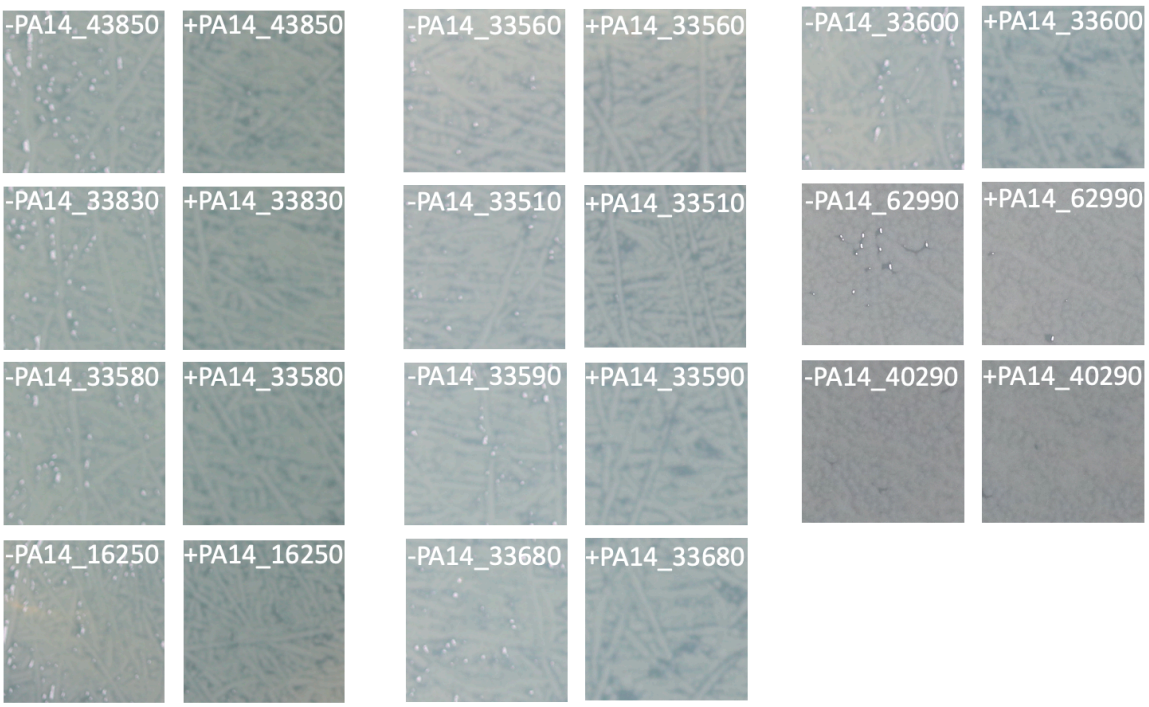

Figure S13. Images of spotting for *ΔxerC prtR*$_{S162A}$ with or without inducible pJN105 and the indicated PA14 gene.

Strain	Genotype or description	Source
MTC2286	SM10 *pCTX-1*-P$_{hol}$-*gfp*	[78]
MTC2287	SM10 *pCTX-1*-P$_{hol}$-*lux*	[78]
MTC2212	SM10 *pEGX2-ΔxerC*	[78]
MTC2407	SM10 *pEXG2-ΔalpB-E*	This Study
CSS1152	SM10 *pEXG2-ΔprtR*	This Study
HAM173	SM10 *pJN105-PA14_16250*	This Study
HAM174	SM10 *pJN105-PA14_23680*	This Study
HAM175	SM10 *pJN105-PA14_33510*	This Study
HAM176	SM10 *pJN105-PA14_33560*	This Study
HAM177	SM10 *pJN105-PA14_33580*	This Study
HAM178	SM10 *pJN105-PA14_33590*	This Study
HAM179	SM10 *pJN105-PA14_33600*	This Study
HAM180	SM10 *pJN105-PA14_33830*	This Study
HAM181	SM10 *pJN105-PA14_40290*	This Study

HAM182	SM10 *pJN105-PA14_43860*	This Study
HAM183	SM10 *pJN105-PA14_62970*	This Study
HAM184	SM10 *pJN105-PA14_62990*	This Study
MTC2399	SM10 *pJN105-PrtN*	This Study
Primer Name	**Sequence**	**Source**
33510_pJN105_Eco_F	ATGACTTCAGTGTTCGACCG	This study
33510_pJN105_Xba_R	TCAGCCGGCCGCC	This study
40290_pJN105_Eco_F	ATGCAGCACAAAAGATCCCG	This study
40290_pJN105_Xba_R	TCAGAGCGCCAGGCC	This study
33830_pJN105_Eco_F	ATGACCCATTCGCCCGTC	This study
33830_pJN105_Xba_R	CTTTACCCGCTGCCCGAG	This study
33600_pJN105_Eco_F	TGTCGAAAAAGTCCCGCTC	This study
33600_pJN105_Xba_R	TCATGGCTGTCCCTCCG	This study
16250_pJN105_Eco_F	TGAAGAAGGTTTCTACGCTTGA	This study
16250_pJN105_Xba_R	TTACAACGCGCTCGGGC	This study
33580_pJN105_Eco_F	TGAGCATCCACACCCGC	This study
33580_pJN105_Xba_R	GGCGCGGCGATG	This study
33590_pJN105_Eco_F	ATGAGCAAGGCCGCCGT	This study
33590_pJN105_Xba_R	TGCTTACCTCGTTTGTTCA	This study
33560_pJN105_Eco_F	ATGCTGTTCTCCCGTCGC	This study
33560_pJN105_Xba_R	GCGCCGGACTCCT	This study
43850_pJN105_Eco_F	ATGAGCGTGGAAACCCAAAAAGAG	This study
43850_pJN105_Xba_R	CGGGCTTTGTCGGGGCTAC	This study
23680_pJN105_Eco_F	ATGAGCAACGCTTTTTCCCTC	This study
23680_pJN105_Xba_R	CTTTTTTCGATCACCGCTGAC	This study
62990_pJN105_Eco_F	GGAGAGTGGCATGGCTGACG	This study
62990_pJN105_Xba_R	CAAGCCTGCTCGTCGATGGAA	This study

Supplemental Table S2. *E. coli* mating strains constructed, and primers used in the study in chapter 3.

Strain construction details for strains used in chapter 3

MTC2424

MTC2294 was mated with MTC2407 and selected on appropriate plates as indicated above.

CSS1180

MTC2266 was mated with CSS1152 and selected on appropriate plates as indicated above.

MTC2449

MTC2280 was mated with MTC2399 and selected on appropriate plates as indicated above.

HAM202

MTC2297 was mated with MTC2399 and selected on appropriate plates as indicated above.

HAM199

MTC2398 was mated with MTC2399 and selected on appropriate plates as indicated above.

HAM197

MTC2307 was mated with MTC2399 and selected on appropriate plates as indicated above.

MTC2486

MTC2304 was mated with MTC2286 and selected on appropriate plates as indicated above.

HAM157

MTC2252 was mated with MTC2399 and selected on appropriate plates as indicated above.

HAM158

MTC2486 was mated with MTC2399 and selected on appropriate plates as indicated above.

CSS1206

CSS1180 was mated with MTC2287 and selected on appropriate plates as indicated above.

CSS1285

CSS1206 was mated with MTC2399 and selected on appropriate plates as indicated above.

HAM198

MTC2304 was mated with MTC2399 and selected on appropriate plates as indicated above.

HAM185

MTC2304 was mated with HAM173 and selected on appropriate plates as indicated above.

HAM186

MTC2304 was mated with HAM174 and selected on appropriate plates as indicated above.

HAM187

MTC2304 was mated with HAM175 and selected on appropriate plates as indicated above.

HAM188

MTC2304 was mated with HAM176 and selected on appropriate plates as indicated above.

HAM189

MTC2304 was mated with HAM177 and selected on appropriate plates as indicated above.

HAM190

MTC2304 was mated with HAM178 and selected on appropriate plates as indicated above.

HAM191

MTC2304 was mated with HAM179 and selected on appropriate plates as indicated above.

HAM192

MTC2304 was mated with HAM180 and selected on appropriate plates as indicated above.

HAM193

MTC2304 was mated with HAM181 and selected on appropriate plates as indicated above.

HAM194

MTC2304 was mated with HAM182 and selected on appropriate plates as indicated above.

HAM195

MTC2304 was mated with HAM183 and selected on appropriate plates as indicated above.

HAM196

MTC2304 was mated with HAM184 and selected on appropriate plates as indicated above.

locus_tag	protein_id	product	logFC

PA14_RS13655	WP_003089636.1	MbtH family protein	-3.6348715
PA14_RS13720	WP_003139291.1	ferripyoverdine/pyocin S3 receptor FpvA	-3.5617977
PA14_RS16340	WP_003139897.1	protease LasA	-3.2608859
PA14_RS13795	WP_003089535.1	transcriptional repressor	-3.2105504
PA14_RS13555	WP_003113068.1	pyoverdine signaling pathway sigma factor PvdS	-3.1353358
PA14_RS13700	WP_003106912.1	PepSY domain-containing protein	-3.0547396
PA14_RS06505	WP_003092588.1	M4 family elastase LasB	-2.988546
PA14_RS13690	WP_003089624.1	hypothetical protein	-2.91009
PA14_RS13695	WP_003139248.1	hypothetical protein	-2.8954852
PA14_RS13680	WP_003113055.1	zinc ABC transporter substrate-binding protein	-2.6366086
PA14_RS14315	WP_003089304.1	monooxygenase PumA	-2.4835428
PA14_RS13670	WP_003106903.1	metal ABC transporter permease	-2.4692542
PA14_RS13675	WP_003106905.1	metal ABC transporter ATP-binding protein	-2.4243153
PA14_RS09600	WP_003091405.1	Hsp20 family protein	-2.3184575
PA14_RS13685	WP_003139246.1	hypothetical protein	-2.2510522
PA14_RS14425	WP_003089254.1	sodium:alanine symporter family protein	-2.240699
PA14_RS15545	WP_003139695.1	DUF1127 domain-containing protein	-2.2347177
PA14_RS15055	WP_003088871.1	DUF4142 domain-containing protein	-2.202863
PA14_RS13785	WP_003114509.1	L-ornithine N(5)-monooxygenase PvdA	-2.1832901

PA14_RS13665	WP_003111290.1	zinc ABC transporter substrate-binding protein	-2.1639683
PA14_RS21680	WP_003140848.1	chitin-binding protein CbpD	-2.0772374
PA14_RS22830	WP_003141191.1	type 4b pilus Flp major pilin	-2.0650461
PA14_RS17175	WP_003100751.1	YscE family type III secretion system co-chaperone PscE	-2.0268091
PA14_RS14195	WP_003139388.1	chitinase	-2.0149445

Supplemental Table 3. RNA sequencing hits for genes downregulated over a log fold change of 2 between ΔxerC prtR$_{S162A}$ and a ΔxerC.

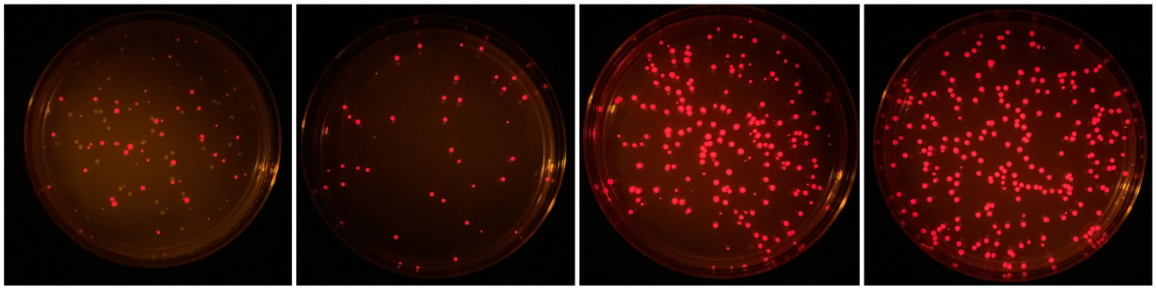

Experiment : *ΔxerC* vs 13S + Cipro								
	T:0		**T: 2 hours**		**T: 4 hours**		**T: 6 hours**	
	# of colonies	%	# of colonies	%	# of colonies	%	# of colonies	%
ΔxerC (RFP)	56	32.4%	57	100.0%	245	100.0%	320	100.0 %
13S	117	67.6%	0	0.0%	0	0.0%	0	0.0%
Total #	173	Total #	57	Total #	245	Total #	320	

Supplemental Figure 14. Competition between *ΔxerC* (MTC2454) and the 13S (MTC2191) in the presence of 0.03 μg/mL of ciprofloxacin. Strains were serially diluted and plated on LB plates, *ΔxerC* contains a constitutive mKate2 (RFP) reporter.

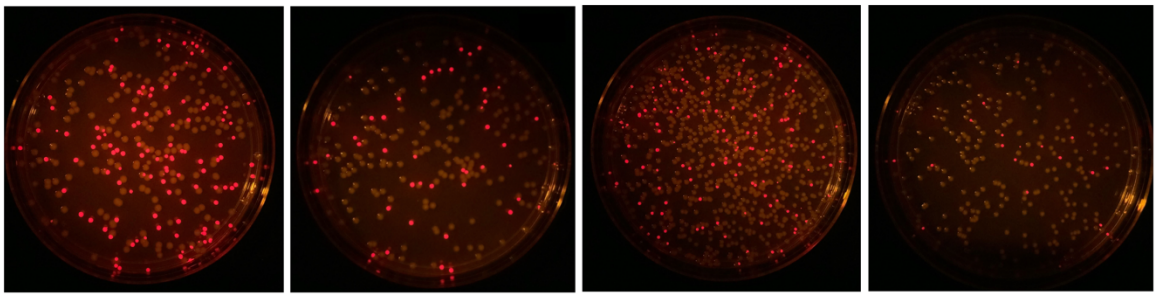

Experiment : Δ*xerC Δpyocin* vs 13S + Cipro								
	T:0		**T: 2 hours**		**T: 4 hours**		**T: 6 hours**	
	# of colonies	%	# of colonies	%	# of colonies	%	# of colonies	%
Δ*xerC Δpyocin*	122	38.2%	45	19.4%	139	17.5%	20	6.8%
13S	197	61.8%	187	80.6%	655	82.5%	274	93.2%
Total #	319	Total #	232	Total #	794	Total #	294	

Supplemental Figure 15. Competition between *ΔxerC Δpyocin* (MTC2455) and the 13S (2191) in the presence of 0.03 µg/mL of ciprofloxacin. Strains were serially diluted and plated on LB plates, *ΔxerC Δpyocins* contains a constitutive mKate2 (RFP) reporter.

Strain	**Relevant genotype or description**	**Source or Reference**
MTC1202	PA14 *attTn7*::P_{pBR322}-*mKate2*	This study
MTC2454	PA14 Δ*xerC attTn7*::P_{pBR322}-*mKate2*	This study
MTC2191	13S	[78]
MTC22	PAO1	This study
MTC2455	PA14 Δ*xerC Δpyocin attTn7*::P_{pBR322}-*mKate2*	This study
MTC2519	PA14 *ΔxerD*	This study
MTC1520	PA14 *ΔxerD* P_{holin}-*gfp*	This study
HAM122	PA14 *ΔxerC ΔxerD*	This study
HAM125	PA14 *ΔxerC ΔxerD* P_{holin}-*gfp*	This study
MTC2416	SM10 *pEXG2-ΔxerD*	This study
HAM132	SM10 *pEXG2-Δ51650*	This study
HAM133	SM10 *pEXG2-Δ60140*	This study
HAM138	PA14 *ΔxerC ΔxerD Δ51650* P_{holin}-*gfp*	This study
HAM144	PA14 *ΔxerC ΔxerD Δ60140* P_{holin}-*gfp*	This study
HAM154	PA14 *ΔxerC ΔxerD Δ51650 Δ60140*	This study

Supplemental Table 4. A list of strains used in chapter 4.

Primer Name	Sequence	Source
PA14_60140_pEXG2_Up_F	AGAAACAGACGATTTGTATGCACT	This study
PA14_60140_pEXG2_Up_R	GGCCAGGCTT CTCGGTGAGCTGCTGCG	This study
PA14_60140_pEXG2_Down_F	GCTCACCGAG AAGCCTGGCCCAAGG	This study
PA14_60140_pExG2_Down_R	TTTCTGTTTCTAAGGCCCTGAA	This study
pEXG2_PA14_51650_up_F	CGGCGCAGGAGGCCCA	This study
pEXG2_PA14_51650_up_R	ATCGGTATCG GTCATTCCACACCTCCTTCGGC A	This study
pEXG2_PA14_51650_Down_F	GTGGAATGAC CGATACCGATACTGAGGGGCC G	This study
pEXG2_PA14_51650_Down_R	GAGCAGGGGCGTGCGTGC	This study

Supplemental Table 5. A list of primers used in the study of chapter 4.

VITA

Christopher William Hamm

Candidate for the Degree of

Doctor of Philosophy

Dissertation: **MOLECULAR REGULATION OF BACTERIAL STRESS RESPONSES AND PYOCIN PRODUCTION**

Major Field: Microbiology, Cell & Molecular Biology

Biographical:

Education:

Completed the requirements for the Doctor of Philosophy in Microbiology & Molecular Genetics at Oklahoma State University, Stillwater, Oklahoma in May, 2023.

Completed the requirements for the Bachelor of Science in Biological Sciences at Oklahoma State University, Stillwater, Oklahoma in May, 2018.

Experience:

- Researcher in Dr. Matthew Cabeen's laboratory. Research has been concentrated on *Bacillus subtilis*' stress response using microfluidic fluorescence coupled microscopy, and pyocin regulation and mechanism of action in *Pseudomonas aeruginosa*.
- Worked in a diagnostic laboratory extracting and running COVID-19 patient samples via qPCR for the state of Oklahoma.
- Worked as a 911 Paramedic throughout doctorate at Oklahoma State University with Lifenet in Payne County, 2017-2023.